



UNIVERSIDADE ESTADUAL PAULISTA
FACULDADE DE ODONTOLOGIA DE ARARAQUARA



ROBERTO SALES E PESSOA

**INFLUÊNCIA DO TIPO DE CONEXÃO PROTÉTICA, DO PLATFORM-
SWITCHING E DO DESIGN DO IMPLANTE NO AMBIENTE
BIOMECÂNICO DE IMPLANTES IMEDIATOS COM CARGA IMEDIATA**

**ARARAQUARA
2010**



UNIVERSIDADE ESTADUAL PAULISTA
FACULDADE DE ODONTOLOGIA DE ARARAQUARA



ROBERTO SALES E PESSOA

INFLUÊNCIA DO TIPO DE CONEXÃO PROTÉTICA, DO PLATFORM-SWITCHING E DO DESIGN DO IMPLANTE NO AMBIENTE BIOMECÂNICO DE IMPLANTES IMEDIATOS COM CARGA IMEDIATA

Tese apresentada ao Programa de Pós-Graduação em Odontologia – Área de Periodontia, da Faculdade de Odontologia de Araraquara, Universidade Estadual Paulista para obtenção do título de Doutor em Odontologia.

Orientador:

Prof. Dr. Luis Geraldo Vaz

Co-orientadores:

Prof. Dr. Elcio Marcantonio Jr

Profa. Dra. Sônia A Goulart de Oliveira

ARARAQUARA

2010

Pessoa, Roberto Sales

Avaliação da influência do tipo de conexão protética, do platform-switching e do design do implante no ambiente biomecânico de implantes imediatos com carga imediata / Roberto Sales Pessoa.– Araraquara: [s.n.], 2010.

185 f. ; 30 cm.

Tese (Doutorado) – Universidade Estadual Paulista,
Faculdade de Odontologia

Orientador : Prof. Dr. Luis Geraldo Vaz

Co-orientador: Prof. Dr. Elcio Marcantonio Junior

Co-orientadora: Profa. Dra. Sônia A. Goulart de Oliveira

1. Implantes dentários 2. Análise de Elemento finito I. Título

Roberto Sales e Pessoa

**INFLUÊNCIA DO TIPO DE CONEXÃO PROTÉTICA, DO
PLATFORM-SWITCHING E DO DESIGN DO IMPLANTE NO
AMBIENTE BIOMECÂNICO DE IMPLANTES IMEDIATOS COM
CARGA IMEDIATA**

BANCA EXAMINADORA

Presidente e Orientador: Prof. Dr. Luis Geraldo Vaz

2º. Examinador: Prof. Dr. José Maurício dos Santos Reis Nunes

3º. Examinador: Prof. Dr. Rogério Margonar

4º. Examinador: Prof. Dr. Pedro Yoshito Noritomi

5º. Examinador: Prof. Dr. Flávio Domingues das Neves

Araraquara, 25 de Março de 2010

DADOS CURRICULARES

Roberto Sales e Pessoa

| | |
|-------------------|--|
| Nascimento | 19 de Agosto de 1978 em Jequié, Bahia, Brasil |
| Filiação | Nery Pessoa e Silva Lúcia de Sales Pessoa |
| 1997/2000 | Graduação em Odontologia na Faculdade de Odontologia da Universidade Federal de Uberlândia |
| 2001/2002 | Especialização em Periodontia na Associação Brasileira de Odontologia / Escola de Aperfeiçoamento Profissional |
| 2002/2004 | Pós-Graduação em Odontologia, Nível de Mestrado, na Faculdade de Odontologia da Universidade Federal de Uberlândia |
| 2006/2010 | Pós-Graduação em Periodontia, Nível de Doutorado, na Faculdade de Odontologia de Araraquara da Universidade Estadual Paulista “Júlio de Mesquita Filho”. |

DEDICATÓRIA

Dedico este trabalho a **Deus**, por ter estado sempre comigo e me dado a força e o discernimento necessários para superar todos os obstáculos.

À minha esposa **Giuliana Abdo Souza Vertemati Pessoa** pelo amor, companheirismo e compreensão, nos inúmeros momentos difíceis da minha ausência. Ao **Bani** pelo amor sincero e desinteressado. Ter me furtado à companhia de vocês foi um alto preço. Aos meus pais **Nery Pessoa e Silva e Lucia de Sales Pessoa** e meus irmãos **Marcelo de Sales Pessoa e Luciana Sales Pessoa**. Tudo que me tornei, devo à minha família. Eles são o alicerce, a base, o norte.

Ao amigo **Sérgio Ricardo de Oliveira** com quem aprendi algumas das melhores lições da minha vida.

AGRADECIMENTOS ESPECIAIS

Ao **Prof. Dr. Luis Geraldo Vaz**, pela bondade, compreensão e confiança que demonstrou desde o início do meu doutorado. Mais que orientador e orientado, nos tornamos amigos. Minha eterna gratidão.

À engenheira **Profa. Dra. Sônia Aparecida Goulart de Oliveira** pela generosidade e paciência com que me ensinou a dar os primeiros passos na Biomecânica. Seu carinho e dedicação tornaram possível a realização deste trabalho.

Ao **Prof. Dr. Elcio Marcantônio Jr**, pelo exemplo de profissionalismo, competência e seriedade na construção de uma carreira acadêmica de sucesso. Obrigado pelos conselhos e incentivos.

Ao **Dr. Siegfried Jaecques, Dra. Luiza Muraru, Prof. Dr. Jos Vander Sloten, Mrs. Rita Vanroelen e Mr. Stefan Goovaerts**, pelo carinho e generosidade com que me acolheram no BMGO-K.U.Leuven.

Ao **Prof. Dr. Rogério Margonar**, com quem compartilhei as primeiras idéias deste trabalho. Seu incentivo foi fundamental para meu ingresso no Programa de Pós-graduação de Araraquara.

Aos amigos **Romeu, Rubinho, Miltinho, Andrés, Wagner, Gabi, Ju Rico, Débora e Rubão** pelo companheirismo e amizade nos momentos difíceis e de descontração. A presença de vocês foi fundamental.

AGRADECIMENTOS

À Faculdade de Odontologia de Araraquara, Universidade Estadual Paulista (UNESP), na pessoa de seu Diretor **Prof. Dr. José Cláudio Martins Segalla**, e Vice-Diretora **Profa. Dra. Andreia Affonso Barreto Montandon**.

Ao Programa de Pós-Graduação em Periodontia da Faculdade de Odontologia de Araraquara - UNESP, na pessoa de seu Coordenador **Prof. Dr. Joni Augusto Cirelli**, e Vice-Coordenador **Prof. Dr. Mario Tanomaru Filho**, pela minha aceitação no quadro de alunos, e pelo apoio à realização desta pesquisa.

Aos professores do Programa de Pós-Graduação em Periodontia da Faculdade de Odontologia de Araraquara - UNESP, **Prof. Dr. Benedicto Egbert Corrêa de Toledo**, **Prof. Dr. Carlos Rossa Junior**, **Prof. Dr. Elcio Marcantonio Junior**, **Prof. Dr. Joni Augusto Cirelli**, **Prof. Dr. José Eduardo Cezar Sampaio**, **Prof. Dr. Ricardo Samih Georges Abi Rached**, **Profa. Dra. Rosemary Adriana Chiérici Marcantonio** e **Profa. Dra. Silvana Regina Perez Orrico**, pelo exemplo de competência e dedicação à ciência.

A todos os colegas do Programa de Pós-Graduação em Periodontia da Faculdade de Odontologia de Araraquara, em especial aos meus colegas de turma **Daniela Leal Zandim**, **Daniela Spirandeli Salgado**, **Débora Aline Silva Gomes**, **Fábio Renato Manzolli Leite**, **Gabriela Giro**, **Rafael Sartori**, **Rafael Silveira Faeda**, **Rafaela Fernanda Melo**, pelo privilégio do convívio com pessoas tão competentes e capazes.

A todos os funcionários da Disciplina de Periodontia, **Cláudia, D. Maria do Rosário, D. Teresa, Maria José (Zezé), Regina Lúcia, Thelma, Sueli e Toninho**, pela amizade, carinho, e eficiência.

À **FAPESP** (Fundação de Amparo à Pesquisa do Estado de São Paulo, Auxílio à Pesquisa, Projeto 2006/06844-2), ao **CNPq** (Conselho Nacional de Desenvolvimento Científico e Tecnológico, Bolsa de Doutorado, Processo 141365/2006-4), e a **CAPES** (Coordenação de Aperfeiçoamento de Pessoal de Nível Superior, Bolsa de Doutorado-Sanduíche, Processo 4482-07-7) agradeço pelo suporte financeiro dado a mim e a esta pesquisa.

Às empresas de implantes **Neodent** e **SIN – Sistema de Implante** pelo suporte material dado à realização deste estudo.

A todos que de alguma forma colaboraram para a execução deste trabalho.

SUMÁRIO

| | |
|------------------------------|-----|
| PREFÁCIO | 08 |
| LISTA DE ABREVIATURAS | 09 |
| RESUMO | 10 |
| ABSTRACT | 11 |
| 1 INTRODUÇÃO | 12 |
| 2 PROPOSIÇÃO | 15 |
| 2.1 Geral | 15 |
| 2.2 Específica | 15 |
| 3 CAPÍTULO 1 | 16 |
| 4 CAPÍTULO 2 | 66 |
| 5 CAPÍTULO 3 | 100 |
| 6 CAPÍTULO 4 | 131 |
| 7 DISCUSSÃO | 167 |
| 8 CONCLUSÕES | 176 |
| 9 REFERÊNCIAS | 177 |

PREFÁCIO

Esta tese é constituída de quatro trabalhos, incluídos nos capítulos de 1 a 4.

O primeiro é um capítulo aceito para publicação no livro intitulado “Biomechanics of dental implants: Handbook of Researchers” que está sendo organizado pelo Prof. Murat Cehreli da Ankara University, Turquia. Este livro de capa dura será publicado pela Nova Science Publishers de Nova York e tem por objetivo ser um guia para cientistas e estudantes que se propõem a estudar a biomecânica dos implantes dentais. Neste sentido, coube a nós redigir sobre a análise em elementos finitos e sua aplicabilidade na avaliação dos aspectos relevantes para a previsibilidade dos implantes em seus diversos protocolos de uso. À medida que o capítulo do livro enfoca detalhadamente a metodologia utilizada na presente tese, este substituirá a seção de Material e Método.

Os demais capítulos (2, 3 e 4) são artigos científicos decorrentes do trabalho de pesquisa desenvolvido durante o curso de doutorado nesta instituição e na Division of Biomechanics and Engineering Design – BMGO da Katholieke Universiteit Leuven. O BMGO, chefiado pelo Prof. Dr. Jos Vander Sloten, é considerado um dos mais respeitados laboratórios de biomecânica do mundo. Os artigos produzidos foram publicados (ou estão em processo de publicação) em periódicos de renome internacional.

Uma introdução, discussão e conclusão gerais foram também incluídas para dar coesão ao texto da tese.

LISTA DE SÍMBOLOS E ABREVIATURAS

2D: bidimensional

3D: tridimensional

ANOVA: Análise de Variância

DICOM: Digitalização de Imagens e Comunicação em Medicina

CAD: desenho desenvolvido com o auxílio do computador (Computer Aided Design)

CT: tomografia computadorizada

EQV: equivalente

FE: elementos finitos

FEA: análise em elementos finitos

FEM: método de elementos finitos

HA: hidroxiapatita

HPC: ambiente computacional de alta performance

μ : coeficiente de fricção

μ CT: micro-tomografia computadorizada

$\mu\epsilon$: micro-deformações

μ m: micrometro

MPa: MegaPascal

N: Newton

STL: linguagem triangular padrão (stereolithography)

SGA: análise por extensometria

Pessoa RS. Influência do tipo de conexão protética, do platform-switching e do design do implante no ambiente biomecânico de implantes imediatos com carga imediata [Tese de Doutorado]. Araraquara: Faculdade de Odontologia da UNESP; 2010.

RESUMO

O objetivo do presente trabalho de pesquisa foi avaliar a influencia do tipo de conexão protética, do platform-switching, e do design do implante no ambiente biomecânico de implantes imediatos com carga imediata. Para tanto, um modelo de alvéolo de extração de um incisivo central superior foi construído baseado em tomografia computadorizada. Implantes inseridos no alvéolo de extração foram avaliados por meio de análises em elementos finitos. Uma Análise de Variância ($\alpha=0.05$) foi utilizada para interpretar os dados do pico de deformação equivalente no osso, do pico de tensões equivalentes no parafuso do abutment, do deslocamento relativo osso-implante e do gap do abutment. A maior influência do tipo de conexão protética e do platform-switching foi observado na tensão do parafuso e no gap do abutment. Por sua vez, o design do implante afetou consideravelmente as deformações no osso e o deslocamento relativo entre o osso e o implante. Não obstante, evitar a sobrecarga do implante e garantir uma alta estabilidade inicial são os fatores mais importantes na previsibilidade de implantes imediatos com carga imediata.

Palavras-chave: tipo de conexão, platform-switching, design do implante, implante dentário, carga imediata, implante imediato, análise de elemento finito.

Pessoa RS. Influence of connection type, platform-switching, and implant design on the biomechanical environment of immediately placed and loaded implants [Tese de Doutorado]. Araraquara: Faculdade de Odontologia da UNESP; 2010.

ABSTRACT

The aim of the present research work was to evaluate the influence of different connection type, platform switching and implant designs on the biomechanical environment of immediately placed implants. A CT-based model of an upper central incisor extraction socket was constructed. The immediately placed implants were evaluated by finite element analysis. An Analysis of Variance was used to interpret the data for the peak equivalent strain in the bone, peak Von Mises stress in the abutment screw, bone-to-implant relative displacement and abutment gap. The largest influence of the connection type and platform-switching was seen on the peak equivalent stress in the abutment screw and implant-abutment gap. On contrary, the implant design considerably affects the biomechanical environment of immediately placed implants. However, avoiding implant overloading and ensuring a high implant initial stability are the most important factors for the predictability of implants in this protocol.

Keywords: connection type, platform-switching, implant design, immediate implant loading, immediate implant placement, finite element analysis.

1 INTRODUÇÃO

Implantes com carga imediata e precoce têm sido amplamente utilizados na tentativa de minimizar o tempo de espera pela reabilitação de elementos dentais perdidos.¹ Do ponto de vista clínico, o carregamento imediato de implantes oferece muitos benefícios, pois a estética e a função são imediatamente restauradas. Em algumas situações, este protocolo é associado à instalação imediata de implantes em alvéolos de extração, reduzindo o número de procedimentos cirúrgicos e otimizando os resultados estéticos.² Neste sentido, o protocolo de implante imediato com carga imediata tem sido apresentado como uma alternativa mais alinhada às expectativas dos pacientes.

Entretanto, independe do implante ser colocado em função posteriormente a um período de reparação sem cargas, ou imediatamente após a instalação, a previsibilidade e o sucesso ao longo prazo do tratamento é altamente influenciado pelo ambiente biomecânico ao qual o implante está exposto. O íntimo contato na interface permite que cargas aplicadas sobre as próteses implanto-suportadas sejam transmitidas diretamente ao osso adjacente. A concentração de micro-deformações ($\mu\epsilon$) pode exceder os limites de tolerância do osso, causar o acúmulo de micro-danos, e induzir a reabsorção óssea.^{3,4} Sob certas circunstâncias, este carregamento oclusal excessivo pode causar a falência da ossointegração e a perda do implante.^{6,7}

No caso dos implantes em fase de reparação, relacionados aos protocolos com carga imediata, o requerimento principal é controlar a movimentação relativa na interface entre o implante e o osso, que pode induzir

a formação de tecido conjuntivo fibroso em detrimento à desejável reparação óssea.^{8,9,10} Um complicador nos casos de carga imediata é a existência de uma delicada interação entre a reabsorção óssea nas regiões de contato osso-implante e a formação óssea nas regiões livres de contato, nos primeiros períodos após a inserção do implante.¹¹ Sendo a capacidade biomecânica do osso em formação muito menor que a do tecido ósseo funcionalmente adaptado, é crucial atingir uma alta estabilidade primária intra-óssea e um ambiente biomecânico favorável. Outra dificuldade, considerando implantes instalados em alvéolos de extração, é o inevitável defeito ósseo na região marginal.¹² Este defeito aumenta consideravelmente a proporção coroa/implante e, teoricamente, leva a maiores tendências ao deslocamento do implante.¹³

Muitos fatores são reconhecidos por influenciar o ambiente biomecânico ao qual os implantes estão expostos, como a qualidade óssea na área de implantação, a natureza da interface osso-implante, as propriedades dos materiais de implantes e próteses, o tipo de rugosidade superficial dos implantes e as condições oclusais (i.e., magnitude, direção e frequência das cargas). Desta maneira, do ponto de vista da Biomecânica, um fator chave para a previsibilidade dos protocolos de implantes é o desenvolvimento de designs de implantes e próteses capazes de promover algum grau de estabilidade, sob as cargas mastigatórias regulares. Entretanto, o complexo desenho dos implantes, sua relação com os tecidos de suporte e a estrutura protética reabilitadora impedem o uso de fórmulas simples na análise do efeito de cargas externas e sua relação com as tensões internas e deformações. Nestes tipos de avaliação, a análise em elementos finitos (FEA) tem proporcionado dados

valiosos, a um custo operacional relativamente baixo e um tempo reduzido. Esta técnica envolve a solução de problemas mecânicos complexos por meio da divisão de uma geometria complexa em domínios menores e mais simples denominados elementos.¹⁴ Estes elementos são interpolados por pontos nodais, os quais permitem a determinação de deslocamentos, tensões e deformações resultantes de forças externas, não apenas em cada elemento, mas também no conjunto da estrutura analisada. Além disso, este método é capaz de fornecer informações desconhecidas dos estudos clínicos e de proporcionar grande versatilidade na variação de situações: geometrias, propriedades mecânicas e forças aplicadas.^{15,16} Neste sentido, FEA tem sido aplicada à área de implantes dentais para prognosticar o padrão de distribuição de tensões, deformações e deslocamentos não apenas na comparação de vários designs de implantes, mas também remodelando diferentes cenários clínicos e desenhos de próteses.¹⁷⁻²²

Na literatura recente, é possível encontrar um número relativamente grande de estudos demonstrando os efeitos de diversos fatores biomecânicos sobre a previsibilidade de implantes ossoeintegrados. Porém, uma quantidade limitada de informações está disponível sobre as variáveis que determinam os resultados de implantes instalados em alvéolos de extração.²⁰⁻²³

2 PROPOSIÇÃO

2.1 Geral

O objetivo geral do presente estudo foi analisar o ambiente biomecânico de implantes instalados em alvéolos de extração e submetidos à carga imediata, por meio do método de elementos finitos.

2.2 Específica

- Avaliar a influência de diferentes tipos de conexão protética;
- Avaliar a influência da utilização de um intermediário protético de diâmetro menor que o da plataforma do implante (configuração em platform-switching);
- Avaliar a influência de diferentes design de implante.

3 CAPÍTULO 1

Este capítulo é constituído pelo capítulo de livro que discute a aplicabilidade do método de elementos finitos na análise biomecânica de implantes dentais:

Pessoa RS, Jaecques SVN. Finite element analysis in dental implant Biomechanics. In: Cehreli M, Akca K. Biomechanics of dental implants: Handbook of Researchers. 1st ed, New York: Nova Science Publishers; 2010.

FINITE ELEMENT ANALYSIS IN DENTAL IMPLANT BIOMECHANICS

Roberto S. Pessoa, DDS, MS, PhD

Department of Diagnostic and Surgery, Division of Periodontics, UNESP –
São Paulo State University, Araraquara, Brazil

Address:

UNESP - Faculdade de Odontologia
Departamento de Diagnóstico e Cirurgia
Rua Humaitá, 1680, Sala 218 - Cep: 14802-550
Araraquara, São Paulo – Brasil
Phone: (55 34) 3210-6446
rp@inpes.com.br

Siegfried V. N. Jaecques, MS, PhD

Leuven Medical Technology Centre (L-MTC) and Division of Biomechanics and
Engineering Design (BMGO), Catholic University of Leuven (K.U.Leuven),
Leuven, Belgium

Celestijnenlaan 300C PB 2419

3001 Heverlee

Siegfried.Jaecques@mech.kuleuven.be

+32 16 327096

ABSTRACT

A key factor for the predictability and long-term success of implant treatment is the development of implants and prosthesis designs providing sufficient biomechanical stability, under masticatory standard loading. However, the intricate design of the implants and their relationship with the supporting tissues and prosthetic restoration prevent the use of simple analytical formulas for the evaluation of the effect of external loading on the internal stresses and displacements. In these analysis types, the finite element method has provided valuable data, for a relatively low operational cost and time investment. The finite element analysis (FEA) is a technique by which a physical prototype can

be evaluated through a detailed mathematical model. FEA uses a computer to solve a large set of mathematical equations, simulating the physical properties of the evaluated structure. The method has two essential characteristics: the finite elements and the interpolation function. The finite elements are subdivisions of the model, sufficiently small to justify an analytical approximation in each of these elements and also in the combination of its effects. These elements are interconnected by union points called nodal points or nodes. The interpolation functions allow, once the displacement in each node is determined, to interpolate displacements and calculate the stresses and strains in any point of the structure. In implantology, FEA has been applied to predict the biomechanical behavior of various implant designs, clinical scenarios and prosthesis designs. Although it is an incontestably useful tool, FEA results should be interpreted with some care. The assumptions made during the process of developing a finite element model, principally regarding the material properties and the interface conditions, limit the validity of the absolute values of the stress/strain and displacement calculated in a model if a rigorous experimental validation was not accomplished. On the other hand, the association of the FEA with a statistical analysis has been demonstrated as capable of accurately interpreting the relative influence that each input parameters (i.e. loading magnitude, clinical situation, implant design, prosthesis design) has on the encountered results. Hence, especially considering the recent changes in osseointegrated implant usage clinical protocols, FEA of the stresses/strains and displacements generated in the supporting structures and the various elements involved in an implant-supported rehabilitation can contribute to more accurate treatment decisions, diminishing the risks of failure.

INTRODUCTION

The replacement of lost teeth by dental implants has proven to be a reliable treatment modality in a variety of clinical scenarios. However, regardless of the rehabilitation protocol, the predictability and long-term success of implant treatment are greatly influenced by the biomechanical environment. The intimate bone-implant contact at the interface allows the direct transmission of the loads applied over the implant-supported prostheses to the surrounding bone. The stress concentration can exceed bone's tolerance level, cause microdamage accumulation and induce bone resorption (Duyck et al. 2001, Hoshaw et al. 1994, Misch et al. 2005). Under certain conditions, this excessive occlusal loading may cause the failure of successfully osseointegrated implants (Isidor 1996, 1997). In the immediate loading protocols, the overall requirement is to control interfacial movement between the implant and the surrounding bone. Micromovements that exceed 150 μm can induce fibrous connective tissue formation instead of the desirable bone regeneration (Søballe et al. 1992, Brunski 1992, Geris et al. 2004). Hence, adverse forces over the implant-supported prosthetic device could not only cause abutment screw loosening and mechanical failures, but could also impair osseointegration.

Several factors are recognized to influence the biomechanical environment which the implants are exposed to, such as: bone quality in the insertion area, the nature of the bone-implant interface, the materials' properties of the implants and prosthesis, the surface roughness of the implant material, the occlusal condition (i.e., magnitude, direction and frequency of the loading), and the design of the implant (Bozkaya et al. 2004, De Smet et al. 2007, Vandamme et al. 2007, Misch et al. 2005, Duyck et al. 2006). Thus, from a biomechanical

point of view, a key factor for the predictability of implant protocols is the development of implants and prosthesis designs capable of providing some degree of stability, under masticatory standard loading (Hansson 1999). However, the elaborate design of the implants and their relationship with the supporting tissues and prosthetic restoration prevent the use of simple analytical formulas for the evaluation of the effect of external loading on the internal stresses and displacements. In these analysis types, the finite element method (FEM) has provided valuable data, for a relatively low operational cost and time investment (Geng et al. 2001, Van Staden et al. 2006, Wakabayashi et al. 2008). This technique implies the solution of a complex mechanical problem, by dividing an intricate geometry into smaller and simpler geometric domains called elements (Zienkiewicz & Taylor 1989). These elements are interpolated by nodes, which allow the determination of displacement, stress and strain resulting from external force, not only in each element, but also in the whole analyzed structure. In Implantology, finite element analysis (FEA) has been applied to predict the biomechanical behavior of various implant designs, clinical scenarios and prosthesis designs (Hansson 1999, Lin et al. 2007, Ding et al. 2008, Lin et al. 2008; Pessoa et al. 2009 a,b).

However, the success of a FEA study depends on the proper simulation of geometries, interface characteristics, material properties, loading and support conditions of the implant and surrounding bone, as well as on the correct interpretation of the obtained results. In this way, the present chapter aims to discuss the methodology, applications and limitations of finite element techniques in implant dentistry.

FEA Basic Concepts

The finite element analysis (FEA) is a technique by which a physical prototype can be evaluated through a detailed mathematical model. This method uses a computer to solve a large set of mathematical equations, which simulate the physical properties of the evaluated structure (Zienkiewicz & Taylor 2004).

The FEA is essentially a discretization process, in which an infinity-dimensional problem is transformed into a finite-dimensional problem, with a finite number of unknown quantities. The method consists in dividing the domain over which the problem is studied into many smaller interrelated regions, so called elements. Thus, the finite elements are subdivisions of a model, sufficiently small to justify an analytical approximation in each of these elements and also in the combination of its effects. These elements are interconnected through union points (inside and/or at the border) called nodal points or nodes (figure 1). The interpolation functions allow, once the displacement in each node is determined, to interpolate displacements and to calculate the stress and strains in any point of the structure. The set of elements used in the discretization is called a mesh (Zienkiewicz & Taylor 1989). The type, arrangement and total number of elements, as well as the interpolation function, are important factors affecting the accuracy of the results.

Although FEA is an indisputably valuable and efficient tool for the analysis of diverse Biomechanical problems, it is important to understand the limitations of the method. FEA uses approximated mathematical models to represent the behavior of physical systems. In addition, the elaboration of a finite element

model for an implant evaluation involves the acquisition of the implant system and bone geometries, the assignment of appropriate materials properties and interface conditions, and the determination of proper boundary conditions, loading magnitude and direction. Simplifications in any of these stages will have a direct effect on the model's precision. Thus, to validate a finite element model, it is recommended to confront its previsions with data derived from other analysis types, in particular, from experimental measurements.

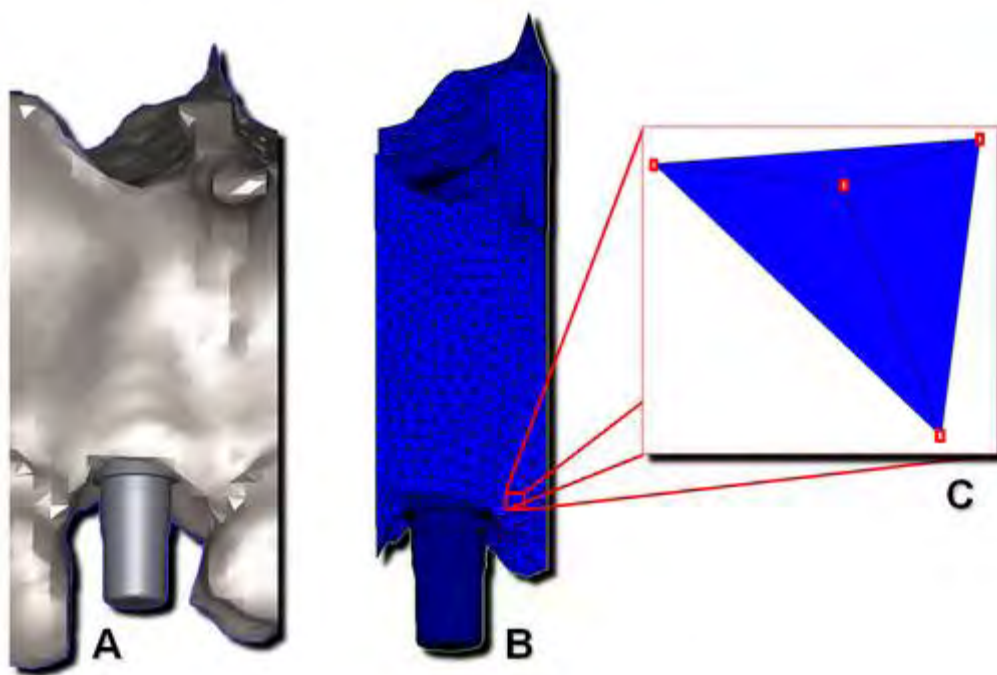


Figure 1: A – CAD solid model. B – Finite element model. C – Tetrahedral element used in the discretization of the model. Note the nodes at the element vertices.

Individualized Finite Element Modeling

In one of the first publications using FEA in implant dentistry, Atmaram and colleagues (1979) evaluated five different materials and three different geometries of implants. The authors reported that the optimal combination of

implant material and geometry may reduce the stress in the implant system and surrounding tissues threefold, compared with an arbitrary design. From those initial studies on, new implant designs and materials have been developed and the indications for dental implants have been amplified. Likewise, once the importance of the Biomechanics on the predictability and long term success of implant treatment had been confirmed, more researchers have become interested in this assessment modality.

However, the finite element modeling of valid and precise three-dimensional (3D) maxillary bones and implant systems is difficult to accomplish using traditional modeling techniques. Early studies frequently assumed two-dimensional (2D) representation of implants and jawbone structures. In addition, some studies even failed to recognize the difference between cortical and trabecular bone, and failed to accurately describe the implant's geometry. At that time, the authors claimed that, in a comparative analysis, complex reality could be simplified, assuming that proportions and relative effects would reflect the actual clinical situation with sufficient accuracy. As those studies were merely concentrated on the comparison of different conditions, the relative values were supposed to still lead to a better qualitative understanding of the biomechanics around implants. Furthermore, 3D models would lead to a huge number of nodes and, thus to unacceptably high computational costs, considering the limited performance of the hardware available at the time. Hence, little attention was paid to the extent to which the modeling method significantly influences the results. Considering these limitations, and although those pioneer studies were extremely important for the development of FEA in the implantology field, 2D FEA can no longer be accepted as a clinically useful

guidance to the implant treatment. As a matter of fact, the in vivo stress and strain state is a three-dimensional problem and the meticulous representation of the object to be modeled greatly influences the accuracy of a FEA.

On the other hand, the evaluation of the local mechanical loading stimulus determinant in the processes of tissue differentiation and bone formation/resorption around a given implant involves a detailed knowledge of the stress and strain state in the peri-implant bone (Jaecques et al. 2004). The finite element (FE) model used to address this aim necessarily should incorporate the site-specific bone anatomy, bone density distribution, implant position and in vivo measured implant loads (Van Oosterwyck et al. 2001). In addition, the assumptions made during the process of developing the numerical model, especially regarding the assignment of material properties and interfaces conditions, entail a rigorous experimental validation. However, once a relationship between the numerical results and the real in vivo biomechanical environment of an implant is established, it is possible to determine the specific conditions that accelerate or consolidate osseointegration, as well as the aspects related to implant failure. This information may be further applied in the optimization of implant designs as a function of the biomechanical parameters beneficial to the peri-implant bone. In this way, especially considering the recent changes in osseointegrated implant usage clinical protocols, individualized FEA can contribute to more accurate treatment decisions, diminishing the risks of implant failure.

Bone Geometry

One major difficulty in simulating the mechanical behavior of dental implants is the modeling of human bone tissue. The substantial complexity of the mechanical characteristics of bone and its interaction with implant systems has led to major and often incorrect simplifications made in early FEA. However, for an accurate individualized FE model, the correct bone and implant geometry as well as the correct position of the implant with respect to the bone must be incorporated in the model. A state of the art method to perform such a task involves X-ray computer tomography (CT) images and computer image processing technique. CT images have become a valuable tool to create anatomical, patient-specific finite element models of bony parts, either or not in combination with implants (Jaecques et al. 2004).

Once a set of digital CT images of the jawbone are obtained, an accurate 3D geometric model of jawbone and surrounding tissue can be readily established using image processing and reverse engineering approaches. Figure 2 shows the acquisition of CT images of an extraction socket of a dry maxilla, provided by the Department of Anatomy of the Faculty of Odontology at Araraquara (São Paulo State University, Brazil), taken by a Picker UltraZ CT scanner with a gantry tilt of 0°, at 120 kV acceleration voltage and 1mA current. The projection data were exported using the DICOM (Digital Imaging and Communication in Medicine) file format. The data set had a voxel size of 0.391 x 0.391 x 1.000 mm and consisted of contiguous slices with respect to the Z-axis. The higher the quality of the CT images, the better is the geometric representation of the bone derived from it. In some studies, because of the high resolution needed to

visualize the bone geometry and the bone adaptive response to the loading regime, micro computer tomography (μ CT) instead of conventional CT was used to create individualized, animal-specific FE models (Jaecques et al. 2004, Duyck et al. 2001, De Smet et al. 2007, Vandamme et al. 2007).

In the present example, bone segmentation and reconstruction of the bone geometry were accomplished by thresholding within an image-processing software (MIMICS®, Materialise, Haasrode, Belgium) (Figure 3). Subsequently, in order to obtain the FE model, a computer-aided design (CAD) approach was followed. This means that, a geometrical model (CAD model), consisting of analytical surfaces and solids, was first created. If the interest in the study is on the biomechanical environment in the vicinity of the implant, only the relevant part of the bone must be reconstructed. A reconstruction of the entire maxilla, for instance, would have led to a larger FE model, with unnecessary higher time processing.

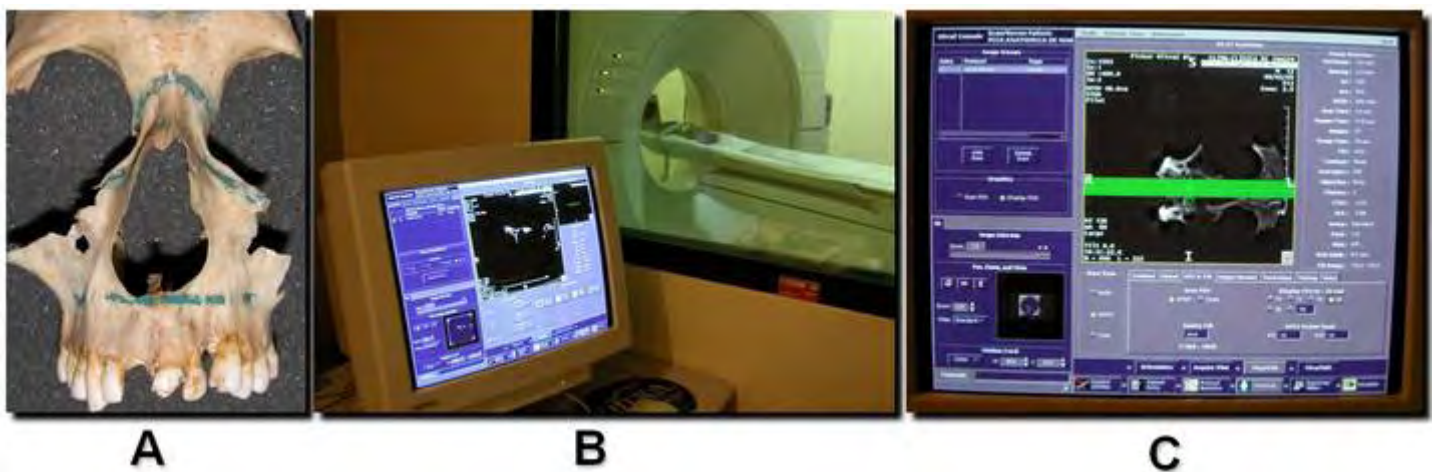


Figure 2: A – Dry maxilla. B, C – Acquisition of CT images of an extraction socket of the dry maxilla.

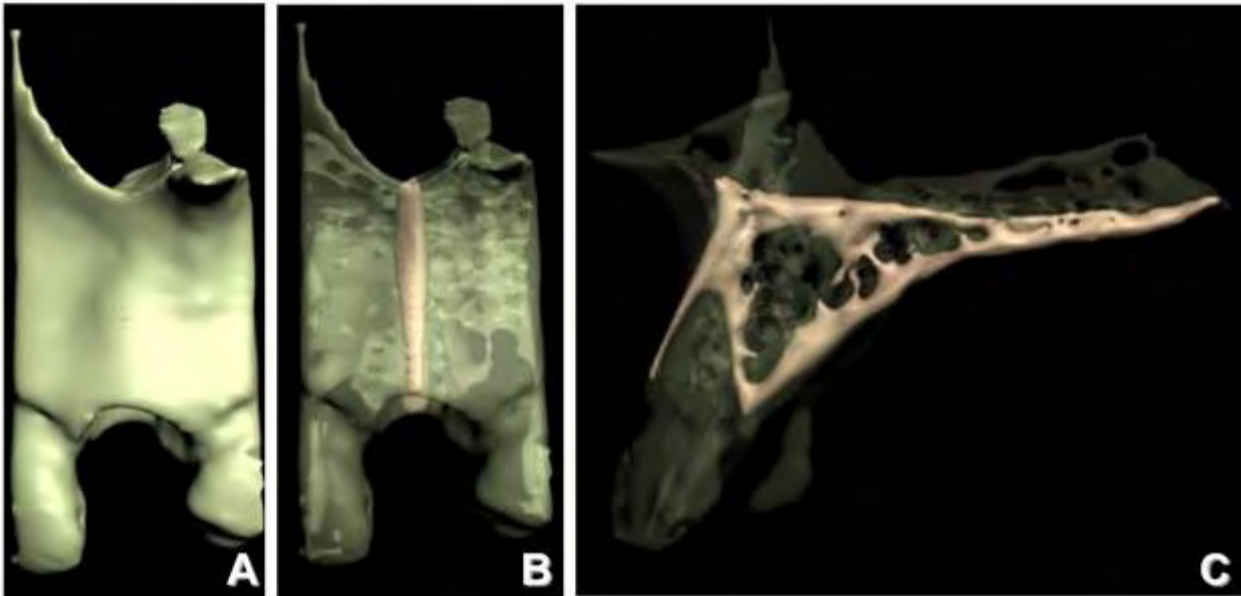


Figure 3: Extraction socket solid model. A – Buccopalatal view. B – Buccopalatal view, evidencing the internal cortical bone structure. C – Lateral view, evidencing the internal cortical bone structure.

An analytical surface was fitted to the outer surface of the segmented bone. Based on this analytical surface, the bone solid model (volumetric model) was designed in a CAD system (Unigraphics). This CAD model was then imported to MSC.Patran® 2005r2 (MSC.Software, Gouda, the Netherlands) and meshed (figure 4). Tetrahedral elements were used for both bone and implant system to ensure smooth contact at the interfaces, which would not have been possible when using hexahedral elements (Marks & Gardner 1993). The volumetric meshes of bone and implant were generated based on the surfaces' standard triangulated language (STL) descriptions.

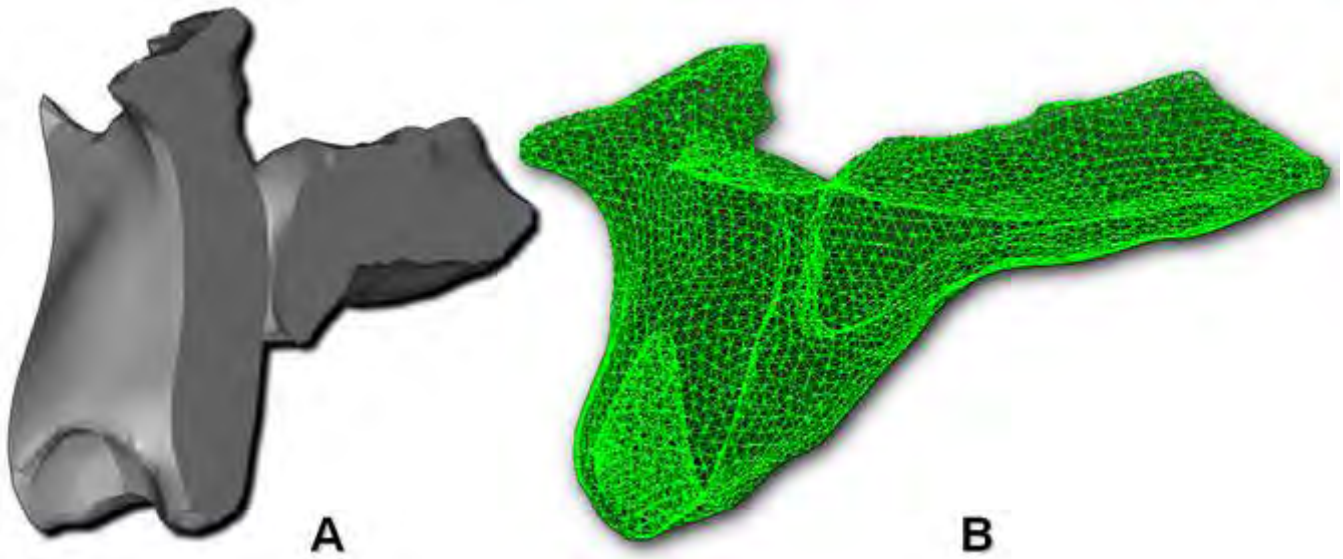


Figure 4: A – Extraction socket solid model. B – Extraction socket mesh.

Implant System Geometry and Positioning

Creating an accurate analytical model of a dental implant involves the modeling of all the possible aspects that may exert an influence within the region to be investigated. In producing realistic and reliable solutions, the modeling of the whole implant design is desirable (i.e. implant shape, length and diameter, thread design, implant-abutment connection design, abutment design and abutment screw design). Modeling assumptions and software limitations might lead to a number of inaccuracies within the obtained results. Figure 5 shows 3 examples of detailed implant system CADs (\varnothing 4.5 x 13 mm SIN SW® [SIN Sistema de Implante, São Paulo, Brazil], \varnothing 4.1 x 12 mm RN synOcta® ITI Standard [Institut Straumann AG, Basel, Switzerland] and \varnothing 4.3 x 13 mm Nobel Replace™ [Nobel Biocare AB, Göteborg, Sweden]) made by reverse engineering and exported as CAD models. The implant system CAD

models were then separately meshed in MSC.Patran® 2005r2 (MSC.Software, Gouda, the Netherlands). Different degrees of mesh refinement were used for feature recognizing (i.e., at threads). In addition, as the results of FEA to some extent depend upon the size of the elements, the mesh was refined at locations with large stress gradients. The smaller elements used in this instance were about 50 µm.

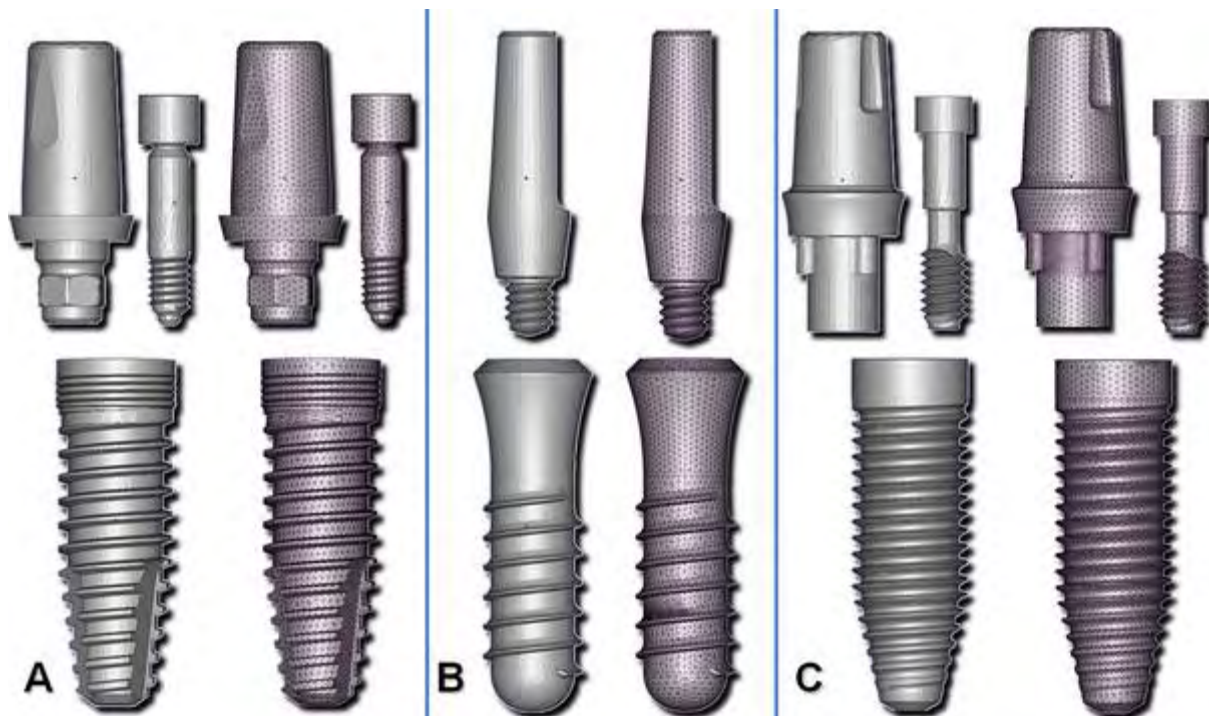


Figure 5: Implant, abutment and abutment screw solid models (left) and meshes (right).

A – SIN SW®. B - ITI® Standard. C - Nobel Replace™.

This process allows the construction of high quality structured meshes in a relatively simple and effective way (figure 5). Figure 6A shows a STL triangulation of a 3i® implant (3i, Palm Beach Gardens, USA) exported by SolidWorks® (Solidworks Corporation, Concord, MA, USA). The STL triangulation was then worked in Patran® and the resultant mesh is presented

in figure 6B. Although a considerable improvement in STL tessellation can be noted in 6B implant mesh, an even higher quality could be reached when the mesh was constructed in Patran® based on the implant CAD models (figure 6C). Furthermore, as can be clearly noted in figure 6A, STL triangulations cannot be directly used to generate FE meshes. In FEA, the elements must have a specific shape and a proper quality factor to achieve accurate predictions (Bechet et al. 2002).

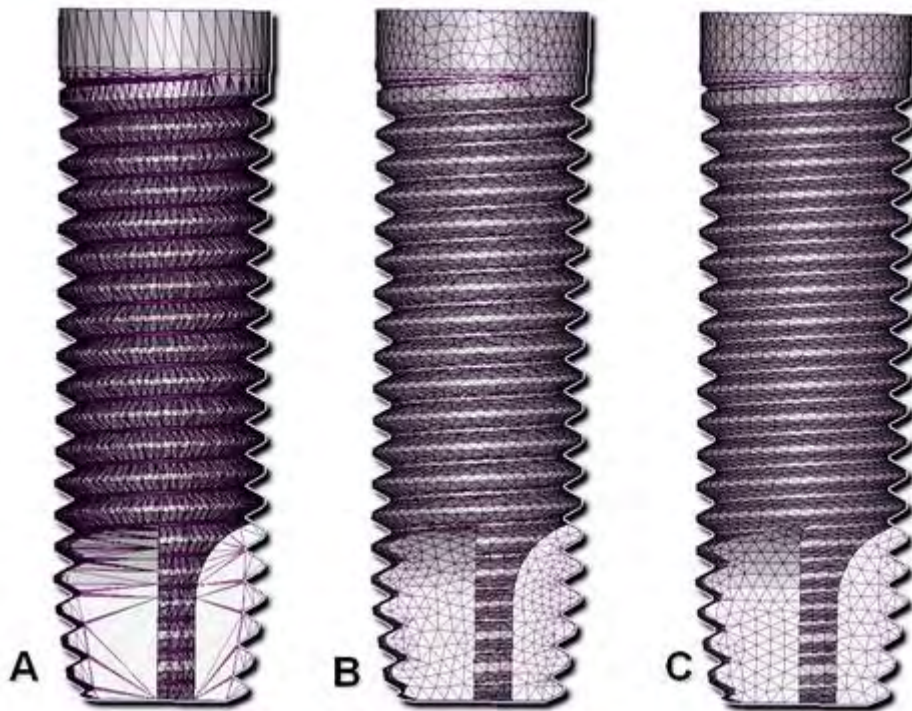


Figure 6: Different implant (3i®) mesh qualities. A – STL triangulation exported by SolidWorks®. B - Tetrahedral mesh constructed in Patran® based on the STL triangulation (A). C – Tetrahedral mesh constructed in Patran® based on the implant CAD model. Note the higher quality of 6C implant mesh.

Moreover, no simplifications should be made regarding the implant external and internal threads (i.e., the spiral characteristic of the threads was maintained). There is a large body of biomechanical research, however, in which to simplify the modeling, the threads of the implant and the abutment were not represented in their spiral characteristics, but as symmetric rings. Huang and colleagues (2008), comparing spiral and nonspiral threaded implants by FEA, found differences in stress values and distribution between the evaluated models. The author argued that a nonspiral threaded implant does not represent actual implant design and, consequently, the information obtained by concentric circle threads should be interpreted with some care.

After having created the bone solid model, the implant solid model must be correctly positioned with respect to the bone structures. In Figure 7, the implant was positioned 1 mm deep inside the extraction socket, in a central position, to a palatal direction. The contra-lateral teeth, as well as the socket anatomy, were used as a reference. Another option, when the CT images already contain a previously placed implant, is to align the implant solid model with implant contours extracted from the CT images (Jaecques et al. 2004). A first approximation of the correct position is performed in Unigraphics. The final—more accurate—position of the implant is determined by means of a matching algorithm. This may be accomplished on the STL files within 3Matic® software (Materialise, Haasrode, Belgium) (Muraru et al. 2009).

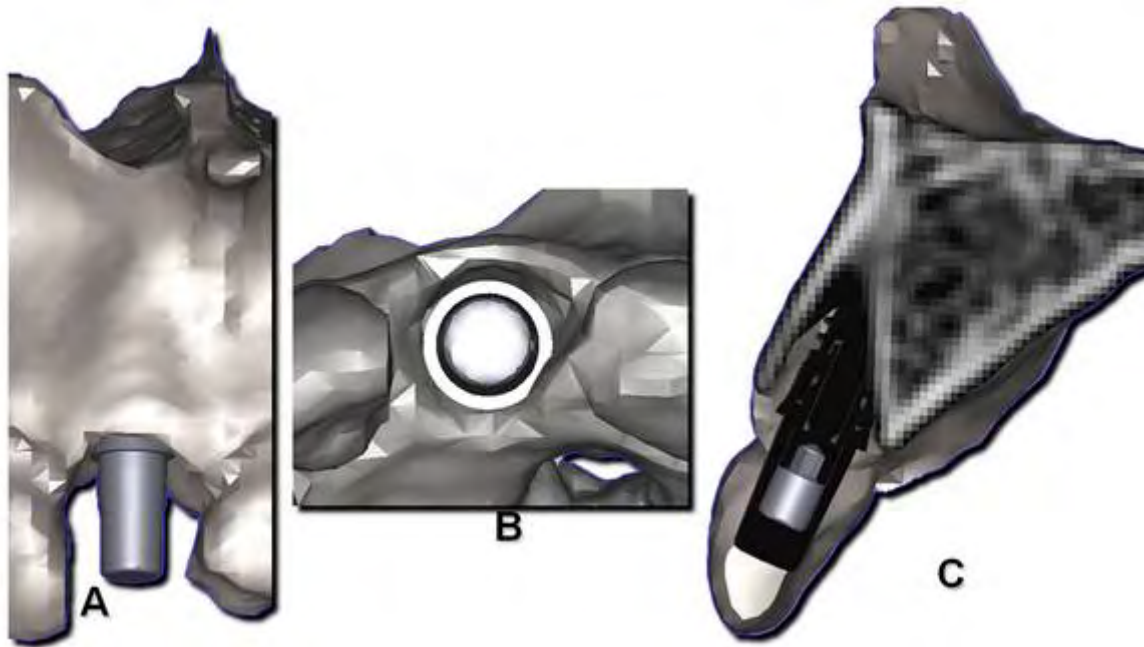


Figure 7: 3D CT-based model of an upper central incisor extraction socket and an implant model positioned inside of the alveolus. A – Frontal view. B – Occusal view. C – Proximal view.

After having obtained the correct position of the implant, the implant insertion hole in the bone solid model may be obtained by means of a Boolean subtraction. The abutment and abutment screw must be subsequently aligned to the implant, following the instructions by the implant producer.

Materials Properties of Bone and Implant Components

The quality and quantity of bone surrounding an implant greatly influences the load transfer from implant to the jawbone. Hence, it is important for the correct evaluation of the biomechanical environment around a given implant to implement in the FE model the local tissue heterogeneity in a patient-dependent manner. However, in the example given in figure 4, during meshing of the bone

solid model, the entire volume that is contained within the outer bone surface is meshed. This means that the mesh consists of tetrahedral elements located in either cortical or trabecular bone. To discriminate between both tissues, different elastic properties can be assigned, based on the grey values in the CT images (Jaecques et al. 2004, Pessoa et al. 2009 a,b). In this way, the information in the CT images may be used not only to extract the patient's bone geometry and but also to assign patient-specific bone mechanical properties (figure 8).

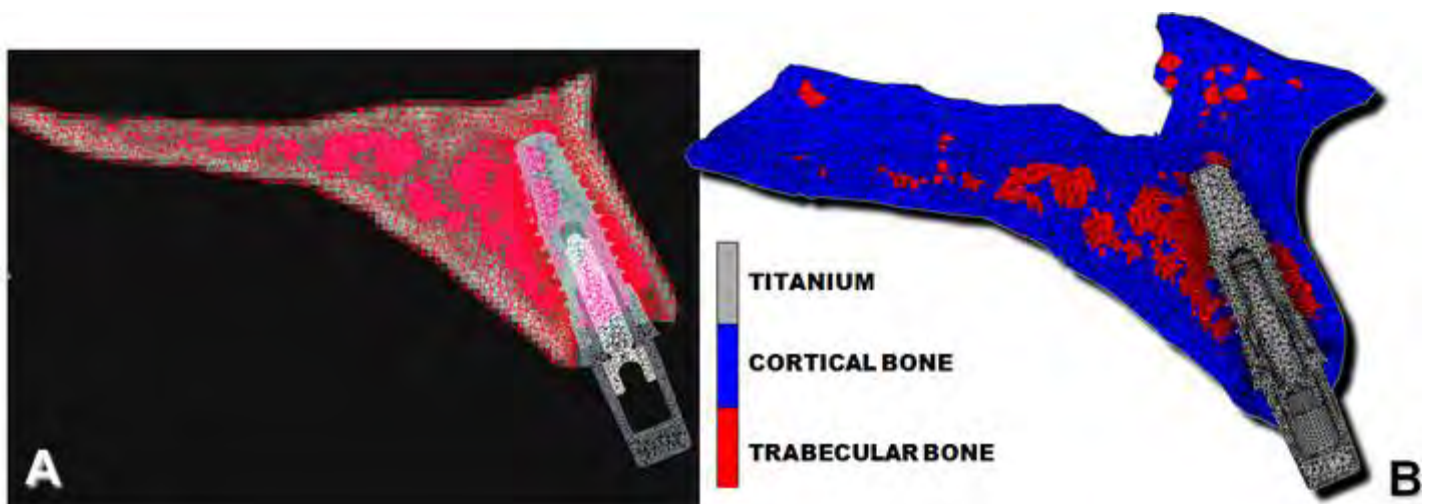


Figure 8: Assignment of CT based properties to the bone: buccopalatal medial plane view. A – Bone and implant system solid meshes superposed to the CT image. B – 3D FE model with the assigned material properties. Note the coincidence between the grey values in CT scan (A) and the elements assigned as cortical bone (B). Also note that the CT is a 2D slice, while the 3D FE model is shown as a sectional view starting in the plane of the CT slice and showing also the bone behind this plane.

Nevertheless, trabecular bone is an extremely porous structure, especially in this region of the maxilla. It consists of interconnected plates and rods of bone surrounded by marrow. At a microscopic level, the tissue elastic properties of each bone trabecula could be assigned. But in this case, once again the mesh density and, afterward, the computational costs would be unacceptable (unless high performance computing (HPC) resources such as a computing cluster are available). In the presented FE bone model the mechanical behavior of trabecular bone should be studied at the macroscopic level, by considering it as a continuum. Therefore, the stresses and strains calculated for trabecular bone must be interpreted in a qualitative rather than a quantitative way. On the other hand, the stresses and strains that were calculated in the cortical bone can also be interpreted quantitatively.

The living cortical as well as trabecular bone tissues exhibit a certain degree of anisotropy, to some extent they are viscoelastic and contain voids (Katz 1971). However, as data on measurements of anisotropic properties from the human mandible and maxilla are still lacking today, even some of the more recent FEA studies considered the cortical and trabecular jawbones as isotropic, homogeneous, and linearly elastic (Lin et al. 2007, Lin et al. 2008, Huang et al. 2008, Pessoa et al. 2009a,b). The mechanical parameters necessary for the characterization of the mechanical behavior of the elastic materials are the Young's modulus and Poisson ratio. The values of these parameters for the materials used in different FEA may be found in the relevant literature (Geng et al. 2001, Van Staden et al. 2006). Further investigations on the measurement of anisotropic properties and its influence on the stress pattern around oral implants are required.

On the other hand, the mechanical properties of an implant are very different to the original tissue. In general, dental implants are made from titanium and bio-ceramic materials, such as hydroxyapatite (HA). These materials present the advantage of high compatibility with hard tissue and living bone (Hedia & Mahmoud 2004). Titanium has reasonable stiffness and strength, while HA has low stiffness, low strength and high ability to reach full integration with living bone. The majority of the previous and current FEA used titanium implants and components in their simulations. A high number of material properties have been adopted for titanium in these investigations, based on different material testing (Geng et al. 2001, Van Staden et al. 2006).

Interface Conditions

Linear static models have been employed extensively in previous FEA studies. These analyses usually assumed that all modeled volumes were bonded as one unit. However, the validity of a linear static analysis may be questionable when the investigation aims to explore more realistic situations that are generally encountered in the dental implant field. Some actual implant clinical situations will give rise to nonlinearities, principally related to the changing of interrelations between the simulated constituents of a FE model (Wakabayashi et al. 2008). Moreover, frictional contact mode provides a greater fidelity with respect to the relative inter-components micro-motion within the implant system, and, therefore, a more reasonable representation of the real implant condition (Merz et al. 2000). This configuration allows minor displacements between all components of the model without interpenetration.

Under these conditions, the contact zones transfer pressure and tangential forces (i.e. friction), but not tension. Some FE analyses have shown remarkable differences in the values and even in the distribution of stresses between “fixed bond” and “non-linear contact” interface conditions (Brunski 1992, Van Oosterwyck et al. 1998, Huang et al. 2008). Figure 9 presents a comparison between these two conditions of bone to implant interface, by a 3D FEA. The same interface condition (contact) was assumed for the implant system components in both situations. The results presented in figure 9 corroborates that not only the stress and strain levels but also the stress and strain distribution are highly affected by the interface state. Van Oosterwyck et al. (1998) argued that through the bonded interface the force was dissipated evenly in both the compressive site and the tension site. However, on the contact interfaces, tensions are not transferred and force is only passed on through the compressive site, which results in excessive stresses. Additionally, note that the condition of the bone to implant interface also influences the strain distribution and level even inside of the implant system (figure 9).

Conventionally, the osseointegrated bone to implant interface is treated as fully bonded. This assumption is supported by experimental investigations in which removal of rough implants frequently resulted in fractures in bone distant from the implant surface (Gotfredsen et al. 2000), suggesting the existence of an implant-bone “bond”. On the other hand, frictional contact elements are used to simulate a nonintegrated bone to implant interface (i.e. in immediately loaded protocols), which allows minor displacements between the implant and the bone. The occurrence of relative motion between implant and bone introduces a

source of non-linearity in the FEA, since the contact conditions will change during load application.

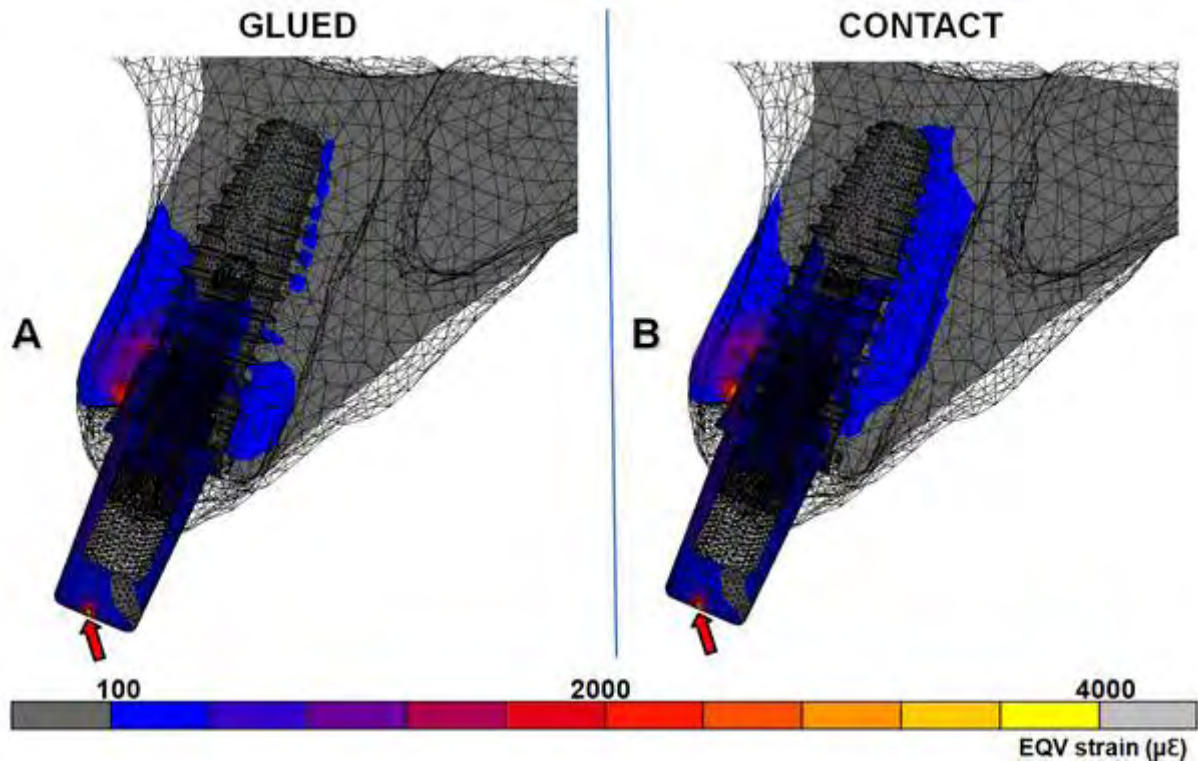


Figure 9: Equivalent strain ($\mu\epsilon$) distribution for 100N loaded implant in a superior central incisor region, in a median buccopalatal plane. The bone to implant interfaces were assumed as fixed bond ("glued") (A) and frictional contact (B). The arrows indicate the loading direction for clarity.

The friction coefficient (μ) to be used in such simulations depends on many factors including mechanical properties and the roughness of the contact interface, exposure to interfacial contaminants (Williams 2000) and in some cases the normal load (Adams et al. 2003). A $\mu = 0.3$ was measured for interfaces between a smooth metal surface and bone, while a $\mu = 0.45$, for interfaces between a rough metal surface and bone (Rancourt et al. 1990).

Frequently, the frictional coefficient between bone and implant is assumed as being $\mu = 0.3$. In this direction, Huang et al. 2008 investigated the effects of different frictional coefficients ($\mu = 0.3, 0.45$ and 1) on the stress and displacement of an immediately loaded implant simulation. The authors demonstrated that enlarging the value of μ shows no significant influence for increasing or decreasing the tensile and compressive stresses of bone. Nevertheless, increasing μ from 0.3 to 1 , the interfacial sliding between implant and bone was mainly reduced from 20% to $30\text{--}60\%$, depending on the implant design (Huang et al, 2008).

Moreover, when an implant is surgically placed into the jawbone, the implant is mechanically screwed into a drilled hole of a smaller diameter. Large stresses will occur due to the torque applied in the process of implant insertion. As the implant stability and stress state around an immediately loaded implant may be influenced by such conditions, this should be also considered in a FE simulation of immediately loaded implants. However, this phenomenon has not been researched adequately yet. The implementation of such implant insertion stresses in a FEA is still unclear and should therefore be a matter of further investigations.

In addition, some earlier FEAs have undertaken linear solutions, underestimating the friction and torque between implant components. The solution of such linear FEA is simple, with a very low computational cost. However, perfect bonding between implant, abutment and abutment screw is not the actual scenario for dental implants. Non-linear contact analysis was proven to be the most effective interface condition for realistically simulating the relative micro-motions occurring between different components within the

implant system (Merz et al. 2000, Pessoa et al. 2009a,b). For lateral or oblique loading conditions, specific parts can separate, or new parts that were initially not in contact can come into contact (figure 10). Consequently, higher stress levels may be expected to occur in an implant-abutment connection simulated with contact interfaces, compared to a glued connection. In this regard, the pattern and magnitude of deformation will be influenced by the implant connection design (Merz et al. 2000, Pessoa et al. 2009a).

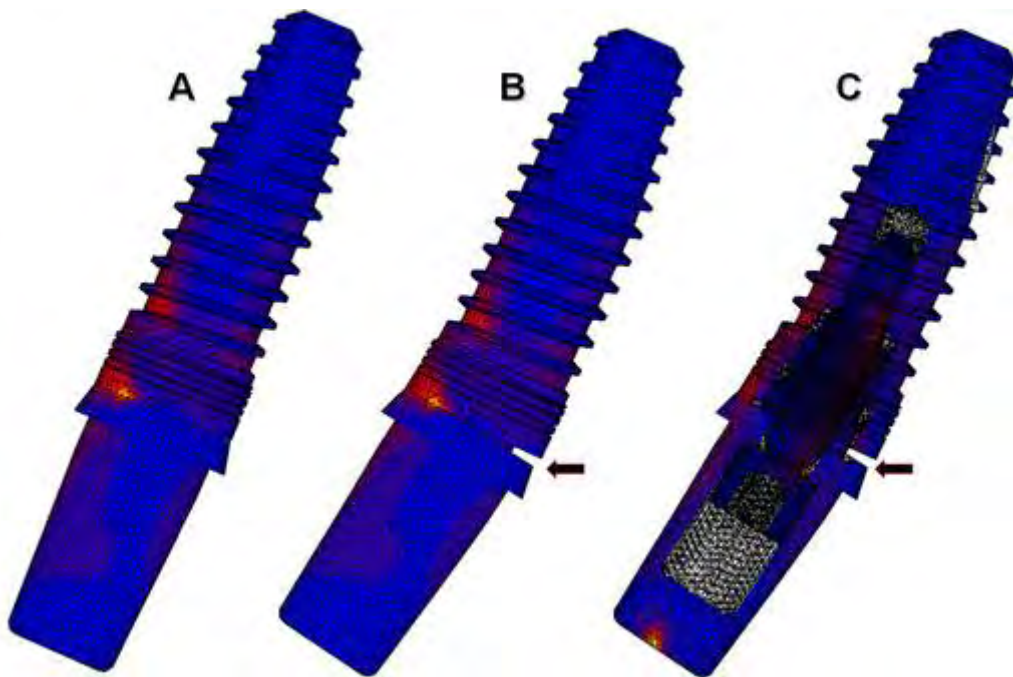


Figure 10: A – Stress distribution on implant-abutment surface, lateral view. B – The deformation is 10-fold magnified (note the abutment displacement; arrow indicates where contact is lost and non-linearity is introduced). C - The deformation is 10-fold, medial slice.

Therefore, for correct simulation of an implant-abutment connection, frictional contact should be defined between the implant components. For the friction coefficients, Abkowitz et al. (1955) reported a value of 0.5 for dry

titanium to titanium friction and Steinemann et al. (1993) found values of 0.43 to 0.53 for titanium in sodium chloride solution. Accordingly, between implant, abutment and abutment screw regions in contact, a frictional coefficient of 0.5 was generally assumed in non-linear simulations of implant-abutment connection (Merz et al. 2000, Lin et al. 2007, Pessoa et al. 2009 a,b).

Furthermore, besides the implant-abutment connection design, preload applied to the abutment screw was also considered to be a factor influencing the abutment stability (Schwarz 2000, Merz et al. 2000). The tightening process causes interference in the abutment screw, which in turn causes the threads of the abutment screw and the implant to engage with a positive force. This resulting tensile load in the abutment screw is known as the preload (Bozkaya & Müftü 2005). The achieved preload is influenced by the geometry of the screw, the contact between the screw head and abutment screw bore, the screw threads and the screw bore internal to the implant, friction between the various implant parts, and the material properties of the screws (Lang et al. 2002, Burguete et al. 1994, Sakaguchi & Borgersen 1995). The implant-abutment joint efficiency, and therefore the strain state in the implant connection region, is considered a function of the design characteristics of the implant-abutment connection as well as, to some extent, of the preload stress achieved in the abutment screw when the suggested tightening torque is applied. Iplikçioğlu et al. (2003) compared the type and magnitude of strain on the implant collar assessed by FEA and strain gauge analysis (SGA). The authors found the same quality of strains on the implant collar, for lateral loading. However, FEA showed almost 2-fold higher strain than in vitro SGA. They argued that this finding may be dependent on several factors in FEA, including assumptions

made during the construction of the mathematical model, the contact phenomenon, number and type of elements, and number of nodes used for calculation. Another reason for these differences may be lack of preload application in the Iplikçioğlu et al. (2003) FE model. The absence of preload may not have any effect during vertical loading, but will result in more separation at the screw joint under lateral loading. Considering that this clamping force has a considerable effect on the maintenance of abutment complex stability, a decreased amount of strain and separation is likely to be observed when preload is incorporated in FEA (Iplikçioğlu et al. 2003).

In this way, preload in the abutment screw is desirable to be included for a realistic FEA evaluation of the implant-abutment connection. Merz et al (2000) included, in a non-linear FEA study, a torque value of 53.2 Ncm for the taper joint and 358.6 Ncm for the butt joint, which was determined by preload testing and calculations. The determined axial preload was introduced into the model with the help of a layer of temperature sensitive elements between the implant body and the cone or butt joint. These were submitted to a negative temperature difference, which resulted in a contraction such that the required tension was generated. Superior stress-relieving mechanics was indicated for the taper joint connection compared to the butt joint (Merz et al. 2000).

Loading and Boundary Condition

In order to successfully replicate, by means of FEA, the clinical situation that an implant might encounter in the oral environment, it is important to understand and correctly reproduce the natural forces that are exerted against

the implants. These forces are mainly the result of the masticatory muscles action, and are related to the amount, frequency and duration of the masticatory function.

Forces acting on dental implants possess both magnitude and direction, and are referred to as vector quantities (figure 11B). For accurate predictions on the implant–jawbone behavior, it is essential to determine realistic in vivo loading magnitudes and directions. However, at each specific bite point, bite forces can be generated in a wide range of directions. Moreover, although bite forces are generally supposed as acting downward, toward the apex of the implant, therefore tending to compress the implant into the alveolar bone, tensile forces and, principally, bending moments, may also be present depending on where the bite force is applied relative to the implant-supported prosthesis. This fact is even more important when the investigation aims to simulate multiple-implant models, because of the geometric factors involving the restorations which are linking the implants, such as the existence of distal cantilevers (Mericske-Stern et al. 1996, Fontijn-Tekamp et al. 1998). Nevertheless, although for implants used in single-tooth replacement simulations, in vivo forces ought to replicate the forces exerted on natural teeth, factors such as the width of the crown occlusal table, the height of the abutment above the bone level, and the angulation of the implant with respect to the occlusal plane will affect the value of the moment on the single-tooth implant.

A significant amount of investigations have assumed the direction of the load applied to the implant to be horizontal, vertical and oblique. Figure 11B shows vertical and horizontal components of load applied on the top of an abutment, at the central region. The resultant force simulates a palato-buccal

static point oblique loading, with 45 degrees of inclination in relation to the implant longitudinal axis. The rationale for use of an oblique loading condition in this case was based on the finding that vertical (axial) forces directed to the implant system are relatively low and well tolerated in comparison to oblique forces, which generate bending moments, principally in the superior central incisor region. The selected location for loading was assumed to simulate the contact point with the antagonist tooth (figure 11B).

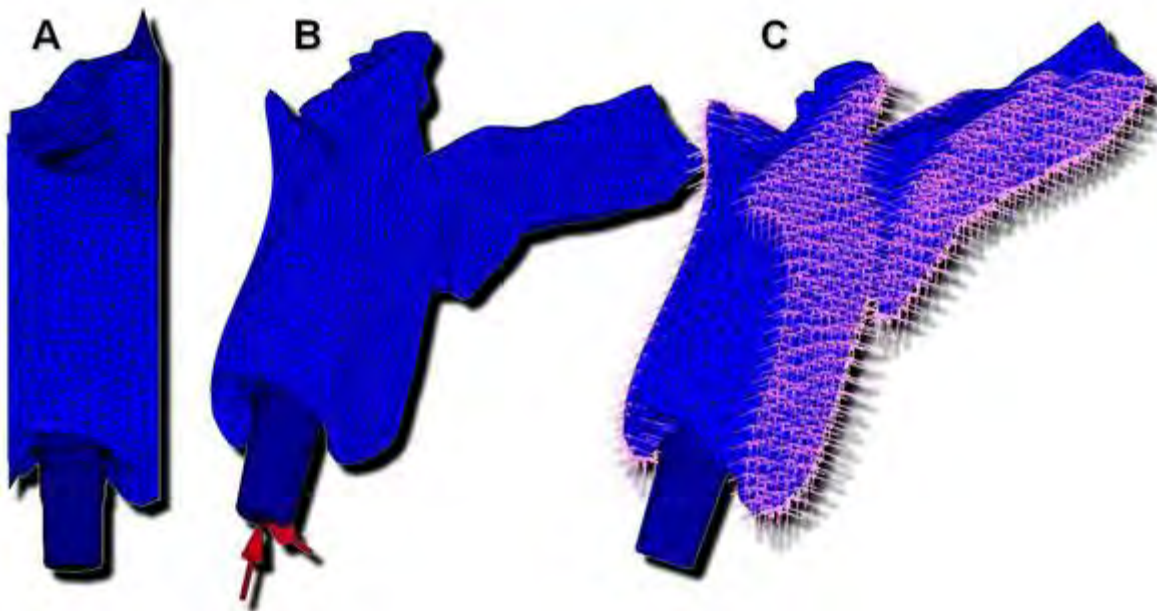


Figure 11: A – FE model of a superior central incisor extraction socket and the positioned implant. B – Loading applied on the abutment central region. C – Displacement constrain in all directions, at the nodes on mesial and distal borders.

Many investigators have tried to gain insight into implant loading magnitudes by performing tests using experimental, analytic, and computer-based simulations of various implant-supported prosthesis types (Duyck et al.

2000, Mericske-Stern et al. 1996, Morneburg & Proshchel 2002, Fontijn-Tekamp et al. 1998). Bite forces ranging from 50 to 400 N in the molar regions and 25 to 170 N in the incisor areas have been reported. These variations are influenced by patient's gender, muscle mass, exercise, diet, bite location, parafunction, number of teeth and implants, type of implant-supported prosthesis, physical status and age (Fontijn-Tekamp et al. 1998, Morneburg & Proshchel 2002, Duyck et al. 2000).

Ideally the entire jawbone structure should be evaluated for its contribution to the force exerted unto the dental implant. However, since the simulation of the whole mandibular and maxillary bone is very elaborate, smaller models have been proposed for parameter studies (Lin et al. 2007, Lin et al. 2008, Huang et al. 2008, Pessoa et al. 2009a,b). As already discussed above, if the interest in the study is on the biomechanical peri-implant environment, the modeling of no more than the relevant segment of the bone is required. This procedure allows saving computing and modeling time. In addition, Teixeira et al. (1998) demonstrated, by a 3D FEA, that modeling the mandible at a distance greater than 4.2 mm mesially or distally from the implant did not result in any significant improvement in accuracy. Hence, besides the application of a proper implant loading, it is also essential for a reasonable FE modeling the determination of restrictions to the model displacement compatible with the anatomic segment to be simulated. In figure 11C, the model of a central incisor extraction socket was fully constrained in all directions at the nodes on mesial and distal borders, preventing the rotation of the maxillary section.

Obviously, if necessary, expanding the domain of the model could reduce the effect of inaccurate modeling of the boundary condition (Zhou et al. 1999).

Convergence Study

In a FEA, the results are an approximation rather than an exact solution. Under considerations of computational resource cost and limitations, the target to reach is the establishment of a compromise between the complexity of the model and the accuracy that is considered satisfactory.

Although in a comparative FEA study, to have similar element size meshes would be enough to eliminate the effect of different mesh density on the stress/strain values and distribution, the mesh refinement is a major factor in the achievement of an accurate model (Hart et al. 1992). In addition, an accurate FE model would allow comparison with in vivo available data and further validation of the model. Therefore, following FEA best practice, a convergence test of the FE models should be performed to verify the mesh quality, ensuring that the numerical results are mesh-independent.

This requires comparison of the numerical results yielded by some different element size models, which have a difference in excess of 10% between the numbers of nodes of the meshes (figure 12), thus ensuring that numerical convergence will be achieved without further mesh refinement. Figure 13 exemplifies a convergence study, in which the convergence criterion was considered as being less than 5% change of the peak von Mises stress (EQV Stress) at the bone-implant edge. In this region the highest stress levels were encountered in the first test analysis. These peaks were found to be in the same coordinates for all 5 mesh element sizes tested. Obviously, the time of processing was also considered as an exclusion criterion in the study. Based on

the result of the convergence study, the optimal global element size for the bone mesh was 0.75 mm (figure 13).

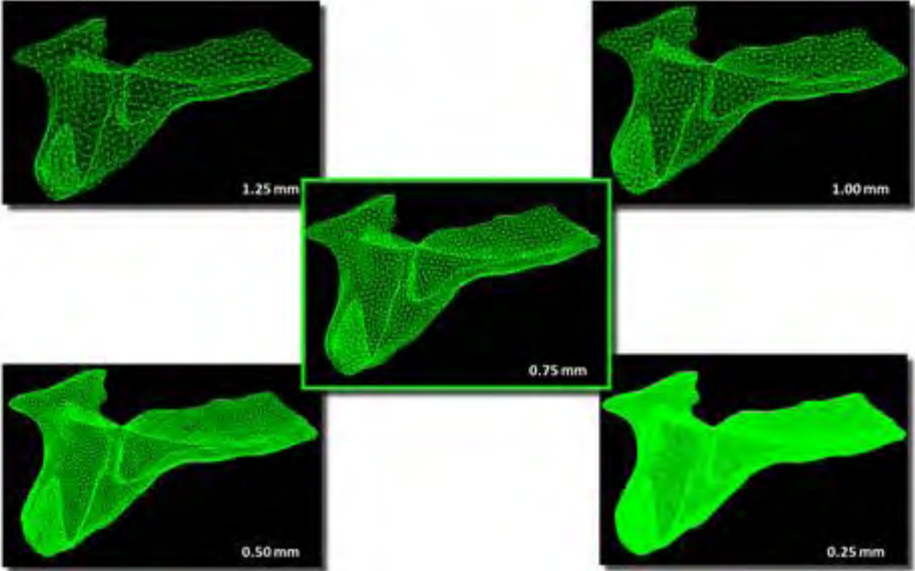


Figure 12: Different element size mesh models of a superior central incision extraction socket.

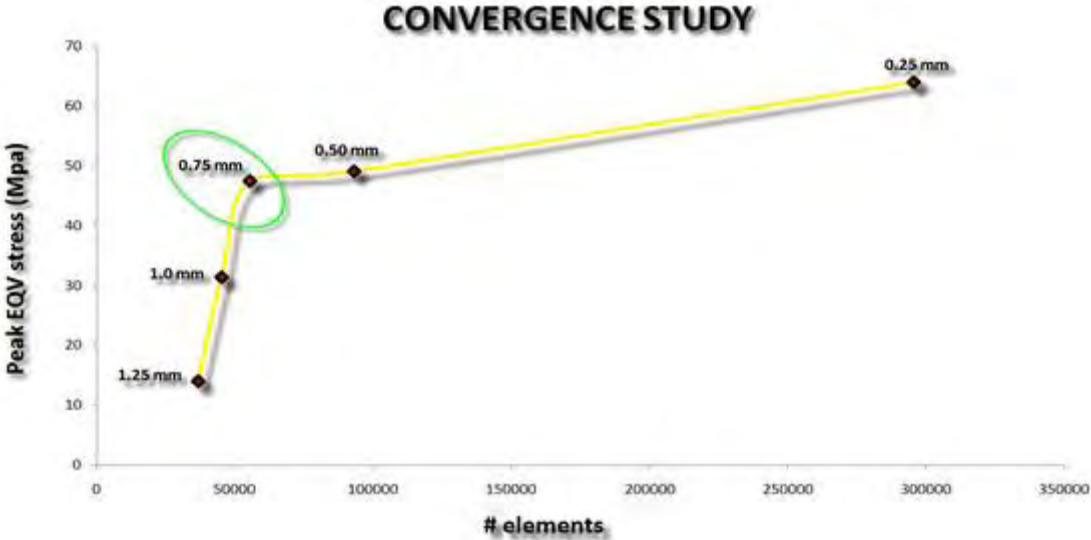


Figure 13: Influence of element size (1.25 mm, 1.0 mm, 0.75 mm, 0.50 mm and 0.25 mm) on bone mesh density and peak EQV stress in a bone model.

Reference Values for FEA Results

A FEA study can be used to gain insight into the biomechanics of oral implants and to verify some of the hypotheses that relate mechanical loading to peri-implant bone responses (Duyck et al. 2001, Jaecques et al. 2004, Geris et al. 2004, De Smet et al. 2007). This can be achieved by a combination of the FEA and animal experiments. An individualized FE model, which incorporates specific bone geometry, implant position relative to the bone geometry and peri-implant bone quality may be created, in order to calculate the bone stresses and strains resulting from a loading experiment, and then relate them to the observed bone response of a given implant. In summary, animal experiments provide insights and measurements, which can then be interpreted within the context of FEA. FE simulations permit investigation of possible explanations that require *in vivo* validation and will suggest further experimental investigations. From this approach, important parameters for osteogenic, as well as for bone-resorptive mechanical stimulus can be identified.

On the other hand, even generic FE models, which intend to focus only on the relative influence of some implant parameter rather than to the absolute *in vivo* results, may be evaluated in respect to its coherence with biological available data (Mellal et al. 2004). Hence, it is possible to determine whether numerical models are consistent in their predictive capacity and whether the provided information could be extrapolated, or at least be useful, to the clinical context. Some criteria for adaptive bone modeling (bone gain and bone loss) have been proposed in relevant Biomechanical literature, and might be used as reference for FEA results.

Although, precise determination of the loading level that separates mechanical loading into acceptable, osteogenic or failure-inducing levels is difficult and until now unresolved, some authors focused on the bone strain amplitudes as the mechanical stimulus determinant to bone adaptive process. It has been shown that above a certain strain threshold (1,500 $\mu\epsilon$), bone formation is initiated in cortical bone and that with increasing strain, bone responds with increasing formation activity (Rubin & Lanyon 1985, Turner et al. 1994, Pilliar et al. 1991, De Smet et al. 2007). Underloading of the bone (< 100 $\mu\epsilon$) may lead to disuse atrophy and eventually to bone loss (Vaillancourt et al. 1996, Frost 1992). A possible threshold for pathological bone overload was considered by Frost (1992) as 4,000 $\mu\epsilon$. Also Duyck et al. (2001), by FEA based on CT-images, estimated 4,200 $\mu\epsilon$ as the value associated with overload-induced resorption.

Figures 14 and 15 show the strain distribution obtained by a FE model of an immediately placed and loaded implant. The model scale was set to range between 100-4,000 $\mu\epsilon$ to facilitate the visualization of the strain state in bone. Nevertheless, although the possible zones of bone underloading (< 100 $\mu\epsilon$, bone loss by disuse), normal load (100 – 1,500 $\mu\epsilon$, bone maintaining), mild overload (2,000 – 4,000 $\mu\epsilon$, bone gain) and pathologic overload (> 4000 $\mu\epsilon$, bone loss by microdamage accumulation) can be easily identified, this does not necessarily imply the bone remodeling in such areas. Rather than only strain amplitude, also loading frequency and number of loading cycles are parameters capable to greatly influence the cortical bone adaptive response (De Smet et al. 2007, Forwood & Turner 1994, Hsieh & Turner 2001, Robling et al. 2002, Rubin & McLeod 1984).

Furthermore, the loading applied in the presented simulation was static and bone responds to dynamic rather than to static loads (Duyck et al. 2001, Lanyon et al. 1984, Robling et al. 2001, Turner 1998). In this way, it must be clear that the modeling of bone adaptive processes was not one of the aims in the given FEA example. In addition, the peaks of strain appeared locally in a minor part of the marginal bone, where indeed some localized bone resorption is likely to occur (figure 15).

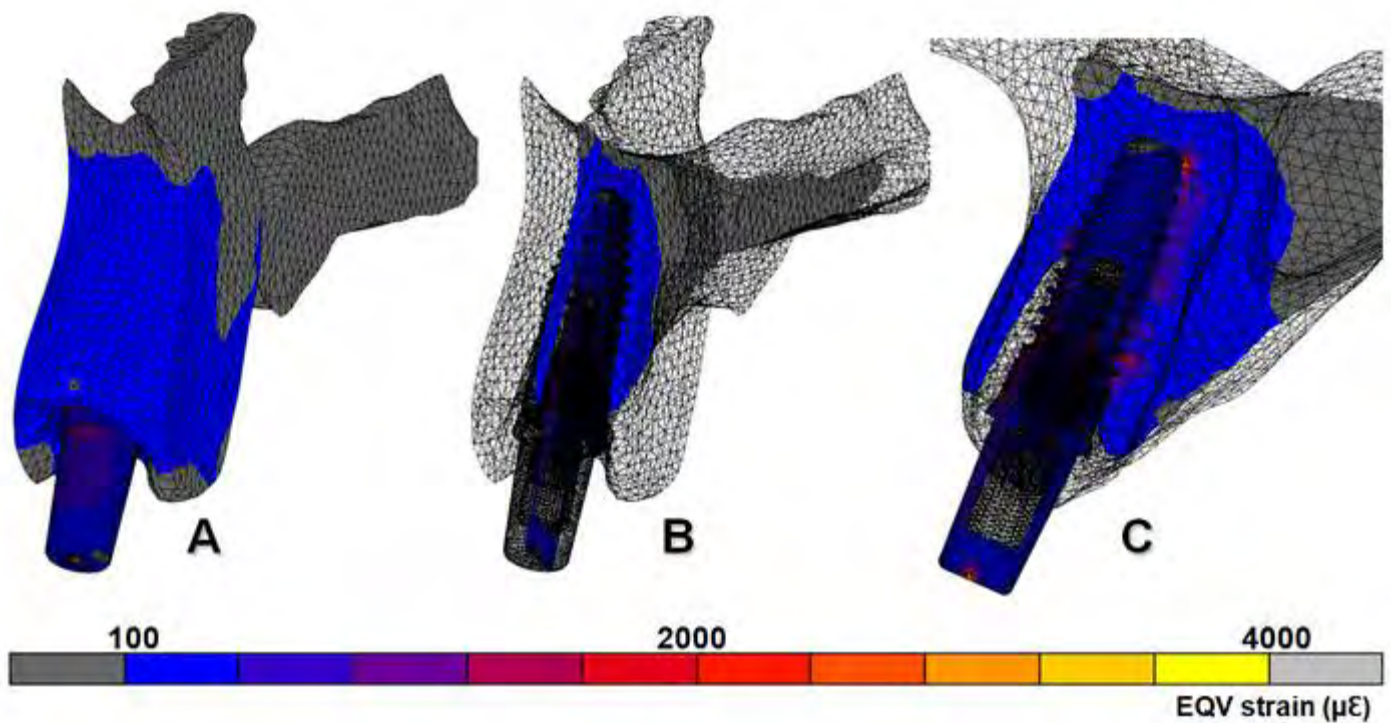


Figure 14: A – Strain distribution, latero-frontal view. B – bucco-palatal medial slice, lateral-frontal view. C – bucco-palatal medial slice, lateral view.

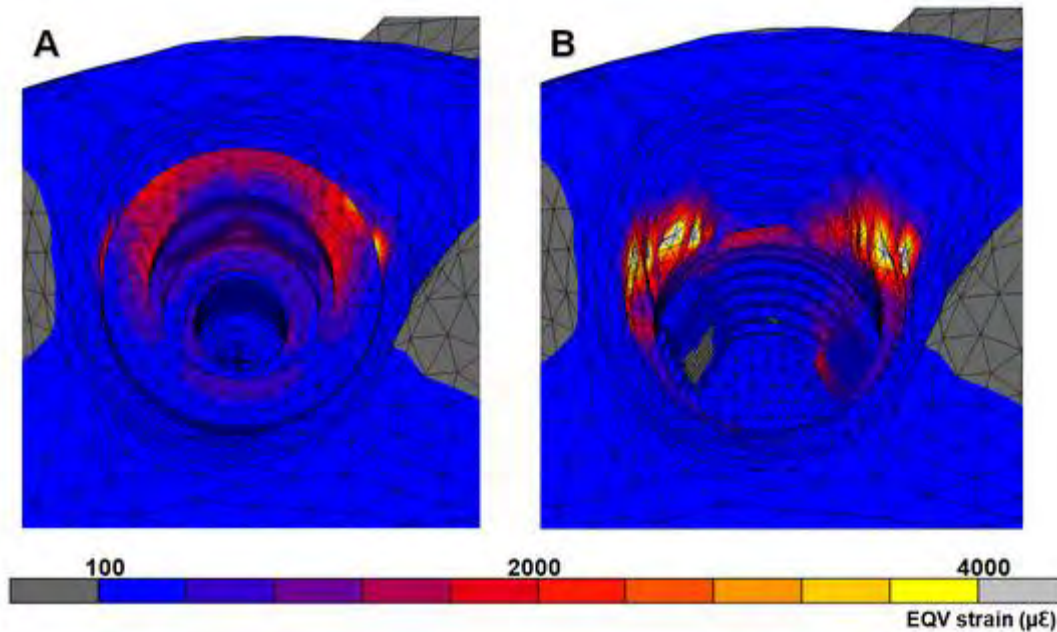


Figure 15: Occlusal view of the strain distribution in the alveolus. A – Implant positioned inside the alveolus. B – Strain distribution in bone (Note that the implant was removed for clarity).

Likewise, principal stresses have been also used as a local risk indicator of physiological bone failure and of the activation of bone resorption at the bone-implant interface. Assuming ultimate bone strength as a physiological limit, local overloading at cortical bone arises in compression when the maximum compressive principal stress exceeds 170-190 MPa and in tension when the maximum tensile principal stress exceeds 100-130 MPa (Reilly & Burstein 1975, Martin et al. 1998). Ultimate compressive strength for cancellous bone was calculated as 5–6MPa (Birnbaum et al. 2001). Nevertheless, the strength of cortical bone varies between different patients, diverse anatomical locations and is also dependent upon the strain rate (Carter & Hayes 1977).

On the other hand, a number of FEA studies have been using the von Mises stress to provide a global measure of load transfer mechanisms at the peri-implant region. However, considering the fact that bone responds differently to different types of stress (Reilly & Burstein 1975), the Von Mises stress is not the most appropriate alternative to describe the stress state in the bone. It has been demonstrated that, cortical bone is strongest when loaded in compression, 30% weaker when subjected to tensile forces, and 65% weaker when loaded in shear (Cowin 1989).

On contrary, the implant, abutment and abutment-screw may be correctly evaluated by means of von Mises stress (figure 16 – Neodent® Implant System, Curitiba, Brazil). The maximum admissible stress value for the titanium is about 900 MPa.

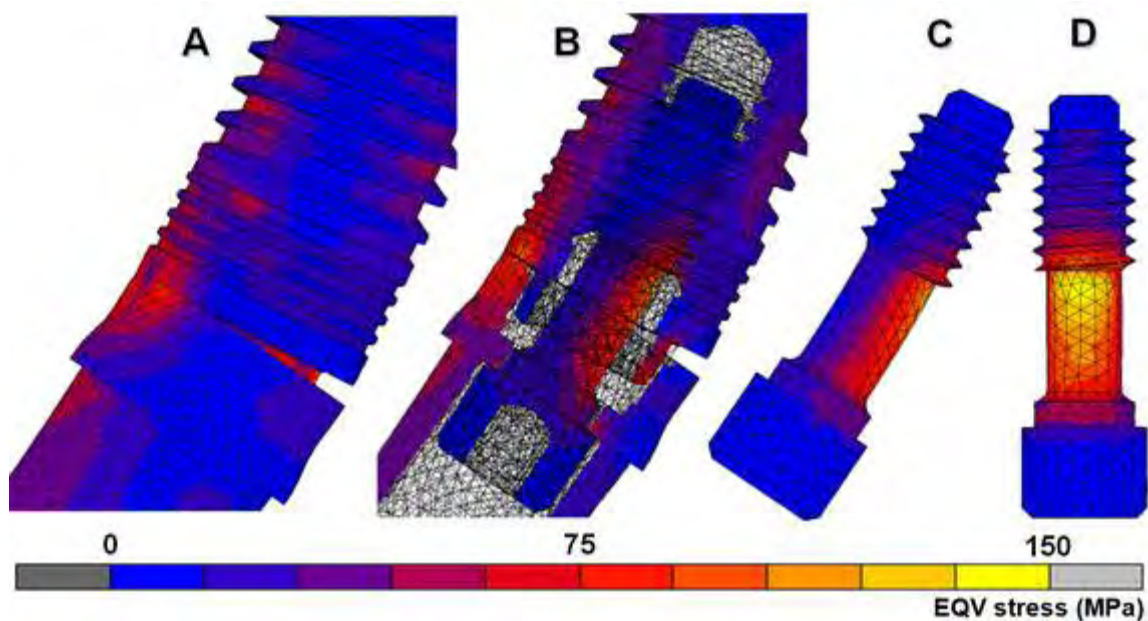


Figure 16: von Mises (EQV) stress evaluation of implant components (Neodent®).

The deformation is 50-fold magnified. A – Implant-abutment surface, lateral view. B

– Implant-abutment connection, medial slice. C – Abutment screw, lateral view. D –

Abutment screw, frontal view.

Regarding the immediately loading protocols, some recent FEA studies used the bone to implant relative displacement as a parameter for the evaluation of diverse implant aspects (Huang et al. 2008, Pessoa et al. 2009 a,b). In fact, one of the most critical elements for the promotion of a safe biomechanical environment for an uneventful bone tissue formation around an immediately loaded implant is a stiff bone-implant interface, allowing low implant micro-movement in bone. Vandamme et al. (2007) demonstrated that an implant displacement between 30 and 90 μm positively influenced osseointegration compared with no implant displacement. On the other hand, micromovement beyond 150 μm can induce fibro connective tissue formation, preventing immediately loaded implant osseointegration (Geris et al. 2004). In addition, Duyck et al. (2006) reported a negative influence of 30 μm micro-motion on osseointegration of cylindrical smooth-surfaced implants. The authors suggested that a good force transfer from the implant towards the surrounding tissues is mandatory and is dictated not only by the mechanical loading, as such, but also by the implant geometry and roughness. However, the above mentioned data were retrieved from studies in a bone chamber, in well-controlled mechanical conditions, protected from external influences (Duyck et al. 2004). Although implant installation in fresh extraction sockets mimics the bone chamber environment, at least in its neck part, direct extrapolation of the results of this in vivo animal study to the clinical context is not possible.

Statistical Analysis in FEAs

Although it is an incontestably useful tool to obtain information that is difficult to acquire from laboratory experiments or clinical studies, the results obtained by FEA should be interpreted with some care. The assumptions made during the process of developing a FE model, principally regarding the material properties and the interface conditions, limit the validity of the absolute values of the stress/strain and displacement calculated in a model in which a rigorous experimental validation was not accomplished. In addition, few attempts have been made to evaluate model sensitivities to variations of input parameters (i.e. clinical situation, implant design, implant-abutment connection type, prosthesis design, implant position, bone quality, loading condition) or possible interactions between these parameters. On the contrary, most of the FEA studies have focused on only one or two parameters.

Table 1 exemplifies a possible inaccuracy that would occur on the interpretation of the results for the peak equivalent strain (EQV strain) obtained by FE simulations of implants with different implant-abutment connection types, immediately loaded into extraction socket (Pessoa et al. 2009a). If the connection type had been the only included parameter in the study, the conclusions would wrongly be that the Morse-taper connection presented the highest peak EQV strain in the bone for the immediately placed protocol. However, by modeling some other clinical situations and loading magnitudes, and applying an Analysis of Variance (ANOVA) on the results, Pessoa et al. (2009a) conclude that the connection type does not have a significant influence on the variation of EQV strain in the immediately placed situation (table 2).

Loading magnitude and the clinical situation are the main factors affecting the equivalent bone strain in this protocol.

In this way, the association of the FEA with a statistical analysis has been demonstrated as capable of accurately interpreting the relative influence that each of the input parameters have on the encountered results of implant FEAs (Dar et al. 2002, Lin et al. 2007, Ding et al. 2008, Lin et al. 2008; Pessoa et al. 2009 a,b).

Table 1: Results for the peak equivalent strain (EQV strain) in the bone (Pessoa et al. 2009a). The results for the 100N loading models are highlighted in yellow. Note that, considering these models, the Morse-taper connection presented the highest EQV strain in the bone.

| Connection types | Clinical situations | Loading | Bone EQV strain ($\mu\epsilon$) |
|---------------------|---------------------|---------|-----------------------------------|
| Morse-taper | immediately placed | 50N | 4,997.8 |
| | osseointegrated | 50N | 892.9 |
| | immediately placed | 100N | 6,060.3 |
| | osseointegrated | 100N | 1,817.0 |
| | immediately placed | 200N | 9,910.1 |
| | osseointegrated | 200N | 3,924.4 |
| Internal hex | immediately placed | 50N | 3,762.4 |
| | osseointegrated | 50N | 1,103.1 |
| | immediately placed | 100N | 5,053.4 |
| | osseointegrated | 100N | 2,593.5 |
| | immediately placed | 200N | 9,048.2 |
| | osseointegrated | 200N | 5,079.4 |
| External hex | immediately placed | 50N | 4,013.7 |
| | osseointegrated | 50N | 1,119.0 |
| | immediately placed | 100N | 5,444.6 |
| | osseointegrated | 100N | 2,232.8 |
| | immediately placed | 200N | 10,209.8 |
| | osseointegrated | 200N | 4,329.9 |

*Table 2: Analysis of Variance for the peak equivalent strain in the bone. $P < 0.05$, * statistically significant (Pessoa et al. 2009a). DF: degrees of freedom; SS: sum of squares; MS: mean square. Note that the connection type does not have a significant contribution to the results (highlighted in yellow).*

| Parameter | DF | SS | MS | P-Value | Contribution (%) |
|--|----|-------------|-------------|----------|------------------|
| Connection Type | 2 | 83004.42 | 41502.21 | 0.6799 | 0.06 |
| Clinical Situation | 1 | 69652650.49 | 69652650.49 | <0.0001* | 49.94 |
| Connection Type X Clinical Situation | 2 | 2301719.20 | 1150859.60 | 0.0210* | 1.65 |
| Loading Magnitude | 2 | 63012208.21 | 31506104.10 | <0.0001* | 45.18 |
| Connection Type X Loading Magnitude | 4 | 340997.31 | 85249.33 | 0.5503 | 0.24 |
| Clinical Situation X Loading Magnitude | 2 | 4068982.43 | 2034491.22 | 0.0077* | 2.92 |

Nevertheless, when applying the FE method to explore every possible combination of values for each investigated parameter, the total number of simulations required might be very high. In addition, the using of advanced engineering techniques, such as CT imaging, CAD systems and reasonable interface conditions, such as contact, to construct FE models capable to simulate the detailed mechanical characteristics of implant systems, may lead to complex models and relatively high processing time. Hence, instead of having a full factorial scheme, which must include all possible combination of parameters, Dar et al. (2002) suggested combining FEA with the statistical Taguchi method, which utilizes an orthogonal array to reduce significantly the

total number of required simulations and contains a well-chosen subset of all possible test condition combinations (Dar et al. 2002). This procedure allows achieving a balanced comparison of the levels of any factor. Therefore, the Taguchi method can be combined with non-linear FEA to explore the sensitivity of a model to different input parameters and thereby reduce the experimental effort required to investigate multiple factors in FEA studies.

Conclusion

An in-depth understanding of the biomechanical environment of dental implants can be gained through the use of FEA. This increase in knowledge of stress/strain distributions and magnitudes within implant systems and surrounding jawbone may give support for the optimization of the implant design and protocols of implant usage, as a function of the parameters beneficial to peri-implant bone, thereby diminishing the risks of implant failure. Therefore, it is of great importance that the clinician and researchers gain understanding on the methodology, applications and limitations of FEA in implant dentistry and become more confident to interpret the results of FEA studies.

References

1. Abkowitz, S; Burke, JJ; Hiltz, RH. *Titanium in Industry*. New York: Van Nostrand Co Inc; 1955.
2. Adams, GG; Muftu, S; Mohd Azar, N. A scale-dependent model for multi-asperity model for contact and friction. *Journal of Tribology*, 2003 125, 700–708.
3. Atmaram, GH; Mohammed, H; Schoen, FJ. Stress analysis of single tooth implants. I. Effects of elastic parameters and geometry of implant. *Biomaterials, Medical Devices and Artificial Organs*, 1979 7, 99–104.
4. Bechet, E; Cuilliere, JC; Trochu, F. Generation of a finite element mesh from stereolithography (STL) files. *Computer-Aided Design*, 2002 34, 1-17.
5. Birnbaum, K; Sindelar, R; Gartner, JR; Wirtz, DC. Material properties of trabecular bone structures. *Surgical and Radiological Anatomy*, 2001 23, 399–407.
6. Bozkaya, D. & Müftü, S. (2005). Mechanics of the taper integrated screwed-in (TIS) abutments used in dental implants. *Journal of Biomechanics*, 38, 87–97.
7. Bozkaya, D; Müftü, S; Müftü, A. Evaluation of load transfer characteristics of five different implants in compact bone at different load levels by finite elements analysis. *Journal of Prosthetic Dentistry*, 2004 92, 523-530.
8. Brunski, JB. Biomechanical factors affecting the bone-dental implant interface. *Clinical Materials*, 1992 10, 153–201.
9. Burguete, RL; Johns, RB; King, T; Patterson, EA. Tightening characteristics for screwed joints in osseointegrated dental implants. *Journal of Prosthetic Dentistry*, 1994 71, 592-599.
10. Carter, D.R. & Hayes, W.C. (1977). The compressive behavior of bone as a two-phase porous structure. *Journal of Bone and Joint Surgery*, 59-A, 954–962.
11. Cowin, SC. Bone mechanics. Boca Raton, FL: CRC Press; 1989.

12. Dar, FH; Meakina, JR; Aspden, RM. Statistical methods in finite element analysis. *Journal of Biomechanics*, 2002 35, 1155–1161.
13. De Smet, E; Jaecques, SVN; Jansen, JJ; Walboomers, F; Vander Sloten, J; Naert, IE. Effect of constant strain rate, composed by varying amplitude and frequency, of early loading on peri-implant bone (re)modelling. *Journal of Clinical Periodontology*, 2007 34, 618–624.
14. Ding, X; Liao, S-H; Zhu, X-H; Zhang, X-H; Zhang, L. Effect of Diameter and Length on Stress Distribution of the Alveolar Crest around Immediate Loading Implants. *Clinical Implant Dentistry and Related Research*, 2008 DOI 10.1111/j.1708-8208.2008.00124.x
15. Duyck, J; De Cooman, M; Puers, R; Van Oosterwyck, H; Vander Sloten, J; Naert, I. A repeated sampling bone chamber methodology for the evaluation of tissue differentiation and bone adaptation around titanium implants under controlled mechanical conditions. *Journal of Biomechanics*, 2004 37, 1819–1822.
16. Duyck, J; Ronald, HJ; Van Oosterwyck, H; Naert, I; Vander Sloten, J; Ellingsen, JE. The influence of static and dynamic loading on marginal bone reactions around osseointegrated implants: an animal experimental study. *Clinical Oral Implants Research*, 2001 12, 207-218.
17. Duyck, J; Van Oosterwyck, H; Vander Sloten, J; De Cooman, M; Puers, R; Naert, I. Magnitude and distribution of occlusal forces on oral implants supporting fixed prostheses: An in vivo study. *Clinical Oral Implants Research*, 2000 11; 465–475.
18. Duyck, J; Vandamme, K; Geris, L; Van Oosterwyck, H; De Cooman, M; Vander Sloten, J; Puers, R; Naert I. The influence of micro-motion on the tissue

differentiation around immediately loaded cylindrical turned titanium implants. *Archives of Oral Biology*, 2006 51, 1–9.

19. Fontijn-Tekamp, FA; Slagter, AP; van't Hof, MA; et al. Bite forces with mandibular implant-retained overdentures. *Journal of Dental Research*, 1998 77, 1832–1839.

20. Forwood, M. R. & Turner, C. H. (1994). The response of rat tibiae to incremental bouts of mechanical loading: a quantum concept for bone formation. *Bone*, 1994 15, 603–609.

21. Frost, HM. Perspectives: bone's mechanical usage windows. *Bone Mineral*, 1992 19, 257–271.

22. Geng, JP; Tan, KB; Liu, GR. Application of finite element analysis in implant dentistry: a review of the literature. *Journal of Prosthetic Dentistry*, 2001 85, 585-98.

23. Geris, L; Andreykiv, A; Van Oosterwyck, H; Vander Sloten, J; van Keulen, F; Duyck, J; Naert, I. Numerical simulation of tissue differentiation around loaded titanium implants in a bone chamber. *Journal of Biomechanics*, 2004 37, 763–769.

24. Gotfredsen, K; Berglundh, T; Lindhe, J. Anchorage of titanium implants with different surface characteristics: An experimental study in rabbits. *Clinical Implant Dentistry Related Research*, 2000 2, 120–128.

25. Hart, RT; Hennebel, VV; Thongpreda, N; van Buskirk, WC; Anderson, RC. Three-dimensional finite element study of the biomechanics of the mandible. *Journal of Biomechanics*, 1992 25, 261–286.

26. Hedia, H. S. & Mahmoud, N. A. (2004). Design optimization of functionally graded dental implant. *Biomedical Materials and Engineering*, 14, 133–143.

27. Hoshaw, SJ; Brunski, JB; Cochran, GVB. Mechanical loading of Brånemark implants affects interfacial bone modeling and remodeling. *International Journal of Oral Maxillofacial Implants*, 1994 9, 345–360.
28. Hsieh, Y. F. & Turner, C. H. (2001) Effects of loading frequency on mechanically induced bone formation. *Journal of Bone and Mineral Research*, 16, 918–924.
29. Huang, HL; Hsu, JT; Fuh, LJ; Tu, MG; Ko, CC; Shen, YW. Bone stress and interfacial sliding analysis of implant designs on an immediately loaded maxillary implant: A non-linear finite element study. *Journal of Dentistry*, 2008 36, 409-417.
30. Iplikçioğlu, H; Akça, K; Çehreli, CM; Sahin, S. Comparison of Non-linear Finite Element Stress Analysis with In Vitro Strain Gauge Measurements on a Morse Taper Implant. *International Journal of Oral and Maxillofacial Implants*, 2003 18, 258–265.
31. Isidor, F. Loss of osseointegration caused by occlusal load of oral implants. A clinical and radiographic study in monkeys. *Clinical Oral Implants Research*, 1996 7, 143–152.
32. Isidor, F. Histological evaluation of periimplant bone at implants subjected to occlusal overload or plaque accumulation. *Clinical Oral Implants Research*, 1997 8, 1–9.
33. Jaecques, SVN; Van Oosterwyck, H; Muraru, L; Van Cleynenbreugel, T; De Smet, E; Wevers, M; Naert, I; Vander Sloten, J. Individualised, micro CT-based finite element modelling as a tool for biomechanical analysis related to tissue engineering of bone. *Biomaterials*, 2004 25, 1683–1696.
34. Katz, JL. Hard tissue as a composite material. 1. Bounds on the elastic behaviour. *Journal of Biomechanics*, 1971 4, 455–473.

35. Lang, LA; Wang, RF; May, KB. The influence of abutment screw tightening on screw joint configuration. *Journal of Prosthetic Dentistry*, 2002 87, 74-9.
36. Lanyon, L. E. & Rubin, C. T. (1984). Static vs dynamic loads as an influence on bone remodelling. *Journal of Biomechanics*, 17, 897–905.
37. Lin, C-L; Chang, S-H; Chang, W-J; Kuo, Y-C. Factorial analysis of variables influencing mechanical characteristics of a single tooth implant placed in the maxilla using finite element analysis and the statistics-based Taguchi method. *European Journal of Oral Science*, 2007 115, 408–416.
38. Lin, C-L; Wang, J-C; Chang, W-J. Biomechanical interactions in tooth–implant-supported fixed partial dentures with variations in the number of splinted teeth and connector type: a finite element analysis. *Clinical Oral Implants Research*, 2008 19, 107–117.
39. Marks, L. W. & Gardner, T. N. (1993). The use of strain energy as a convergence criterion in the finite element modelling of bone and the effect of model geometry on stress convergence. *Journal of Biomedical Engineering*, 15, 474-476.
40. Martin, R. B., Burr, D. B., Sharkey, N. A. (1998). *Skeletal tissue mechanics*. New York: Springer, 127-78.
41. Mericske-Stern, R; Piotti, M; Sirtes, G. 3-D in vivo force measurements on mandibular implants supporting overdentures. A comparative study. *Clinical Oral Implants Research*, 1996 7, 387–396.
42. Mellal, A; Wiskott, HWA; Botsis, J; Scherrer, SS; Belser, UC. Stimulating effect of implant loading on surrounding bone. Comparison of three numerical models and validation by in vivo data. *Clinical Oral Implants Research*, 2004 15, 239–248.

43. Merz, BR; Hunenbart, S; Belser, UC. Mechanics of the implant-abutment connection: An 8-degree taper compared to a butt joint connection. *International Journal of Oral Maxillofacial Implants*, 2000 15; 519–526.
44. Misch, CE; Suzuki, JB; Misch-Dietsh, FM; Bidez, MW. A positive correlation between occlusal trauma and peri-implant bone loss: literature support. *Implant Dentistry*, 2005 14, 108-16.
45. Morneburg, T. R. & Proschel, P. A. (2002). Measurement of masticatory forces and implant loads: a methodologic clinical study. *International Journal of Prosthodontics*, 15, 20-27.
46. Muraru, L; Van Lierde, C; Naert, I; Vander Sloten, J; Jaecques, SVN. Three-dimensional finite element models based on in vivo microfocus computed tomography: Elimination of metal artefacts in a small laboratory animal model by registration with artefact-free reference images. *Advances in Engineering Software*, 2009 40, 1207–1210.
47. Pessoa, RS; Muraru, L; Marcantonio Jr, E; Vaz, LG; Vander Sloten, J; Duyck, J; Jaecques, SVN. Influence of implant connection type on the biomechanical environment of immediately placed implants – CT-based nonlinear, 3D finite element analysis. *Clinical Implant Dentistry and Related Research*, 2009(a) DOI 10.1111/j.1708-8208.2009.00155.x.
48. Pessoa, RS; Vaz, LG; Marcantonio Jr, E; Vander Sloten, J; Duyck, J; Jaecques, SVN. Biomechanical evaluation of platform switching in different implant protocols – CT based 3D finite element analysis. *International Journal of Oral Maxillofacial Implants*, 2009(b) accepted for publication.

49. Pilliar, RM; Deporter, DA; Watson, PA; Valiquette, N. Dental implant design– effect on bone remodelling. *Journal of Biomechanics and Materials Research*, 1991 25, 467–483.
50. Rancourt, D; Shirazi-Adl, A; Drouin, G; Paiement, G. Friction properties of the interface between porous-surfaced metals and tibial cancellous bone. *Journal of Biomedical Materials Research*, 1990 24, 1503–1519.
51. Reilly, D. T. & Burstein, A. H. (1975). The elastic and ultimate properties of compact bone tissue. *Journal of Biomechanics*, 8, 393–405.
52. Robling, AG; Duijvelaar, KM; Geever, JV; Ohashi, N; Turner, CH. Modulation of appositional and longitudinal bone growth the rat ulna by applied static and dynamic force. *Bone*, 2001 29, 105–113.
53. Robling, AG; Hinant, FM; Burr, DB; Turner, CH. Improved bone structure and strength after long-term mechanical loading is greatest if loading is separated into short bouts. *Journal of Bone and Mineral Research*, 2002 17, 1545–1554.
54. Rubin, C. & Lanyon, L. (1985). Regulation of bone mass by mechanical strain magnitude. *Calcified Tissue International*, 37, 411–417.
55. Rubin, C. T. & McLeod, K. J. (1984). Promotion of bony ingrowth by frequency-specific, low-amplitude mechanical strain. *Clinical Orthopaedics and Related Research*, 298, 165–174.
56. Sakaguchi, R. L. & Borgersen, S. E. (1995). Nonlinear contact analysis of preload in dental implant screws. *International Journal of Oral Maxillofacial Implants*, 10, 295-302.
57. Schwarz, MS. Mechanical complications of dental implants. *Clinical Oral Implants Research*, 2000 11(Suppl.), 156–158.

58. Søballe, K; Brockstedt-Rasmussen, H; Hansen, ES; Bünger, C. Hydroxyapatite coating modifies implant membrane formation. Controlled micromotion studied in dogs. *Acta Orthopaedica Scandinavica*, 1992 63, 128–140.
59. Steinemann, SG; Mäusli, PA; Szmukler-Moncler, S; Semlitzsch, M; Pohler, O; Hintermann, HE; Perren, SM. Betatitanium alloy for surgical implants. In: Froes, F. H. & Caplan, I. (1993). *Titanium '92. Science and Technology*. The Minerals, Metals & Materials Society, 2689–2696.
60. Teixeira, ER; Sato, Y; Akagawa, Y; Shindoi, N. A comparative evaluation of mandibular finite element models with different lengths and elements for implant biomechanics. *Journal of Oral Rehabilitation*, 1998 25, 299-303.
61. Turner, CH. Three rules for bone adaptation to mechanical stimuli. *Bone*, 1998 23, 399–407.
62. Turner, CH; Forwood, MR; Rho, JY; Yoshikawa, T. Mechanical loading thresholds for lamellar and woven bone formation. *Journal Bone and Mineral Research*, 1994 9, 87–97.
63. Vaillancourt, H; Pilliar, RM; McCammond, D. Factors affecting crestal bone loss with dental implants partially covered with a porous coating: a finite element analysis. *International Journal Oral Maxillofacial Implants*, 1996 11, 351–359.
64. Van Oosterwyck, H; Duyck, J; Vander Sloten, J; van der Perre, G; de Cooman, M; Lievens, S; Puers, R; Naert, I. The influence of bone mechanical properties and implant fixation upon bone loading around oral implants. *Clinical Oral Implants Research*, 1998 9, 407–418.
65. Van Oosterwyck, H; Duyck, J; Vander Sloten, J; Van der Perre, G; De Cooman, M; Puers, R; Naert, I. Patient-dependent FE modeling as a tool for biomechanical optimization of oral reconstruction. In: Middleton, J; Jones, ML;

Shrive, NG; Pande, GN; *Computer Methods in Biomechanics and Biomedical Engineering*. Amsterdam: Gordon and Breach Science Publishers; 2001 3, 559–564.

66. Van Staden, RC; Guan, H; Loo, YC. Application of the finite element method in dental implant research. *Computer Methods Biomechanics Biomedical Engineering*, 2006 9, 257-270.

67. Vandamme, K; Naert, I; Geris, L; Vander Sloten, J; Puers, R; Duyck, J. The effect of micromotion on the tissue response around immediately loaded roughened titanium implants in the rabbit. *European Journal of Oral Science*, 2007 115, 21–29.

68. Wakabayashi, N; Ona, M; Suzuki, T; Igarashi, Y. Nonlinear finite element analyses: Advances and challenges in dental applications. *Journal of Dentistry*, 2008 26, 463-471.

69. Williams, JA. *Engineering Tribology*. Oxford: Oxford University Press; 2000.

70. Zienkiewicz, O. C. & Taylor, R. L. (2004) *El método de los elementos finitos*. Barcelona, CIMNE.

71. Zienkiewicz, O. C. & Taylor, R. L. (1989) *The Finite Element Method*. New York, McGraw-Hill.

72. Zhou, X; Zhao, Z; Zhao, M; Fan, Y. The boundary design of the mandibular model by means of the three-dimensional finite element method. *West China Journal Stomatology*, 1999 17, 1-6.

4 CAPÍTULO 2

Este capítulo é constituído pelo artigo que avalia a influência de diferentes tipos de conexão protética no ambiente biomecânico de implantes imediatos com carga imediata:

Pessoa RS, Muraru L, Marcantonio Jr E, Vaz LG, Vander Sloten J, Duyck J, Jaecques S. Influence of implant connection type on the biomechanical environment of immediately placed implants – CT-based nonlinear, 3D finite element analysis. Clin Implant Dent Relat Res 2009; DOI 10.1111/j.1708-8208.2009.00155.x.

Influence of implant connection type on the biomechanical environment of immediately placed implants – CT-based nonlinear 3D finite element analysis

Roberto S. Pessoa, DDS, MS

Department of Diagnostic and Surgery, Division of Periodontics, UNESP – São Paulo State University, Araraquara, Brazil

Address:

UNESP - Faculdade de Odontologia
Rua Humaitá, 1680, Sala 409 - Quarto Andar, Cep: 14802-550
Araraquara, São Paulo – Brasil
Mobile: (55 34) 8845-6569
Fax: (55 16) 33016406
rspessoa@uol.com.br

Luiza Muraru, MS

Division of Biomechanics and Engineering Design, K.U.Leuven, Leuven, Belgium

Elcio Marcantonio Júnior, DDS, MS, PhD

Department of Diagnostic and Surgery, Division of Periodontics, UNESP – São Paulo State University, Araraquara, Brazil

Luis Geraldo Vaz, MS, PhD

Department of Dental Materials and Prosthesis, Division of Dental Materials, UNESP – São Paulo State University, Araraquara, Brazil

Jos Vander Sloten, MS, PhD

Division of Biomechanics and Engineering Design, K.U.Leuven, Leuven, Belgium

Joke Duyck, DDS, PhD

Department of Dentistry, Oral Pathology and Maxillo-Facial Surgery, BIOMAT Research Cluster, K.U.Leuven, Leuven, Belgium

Siegfried V. N. Jaecques, MS, PhD

Department of Dentistry, Oral Pathology and Maxillo-Facial Surgery, BIOMAT Research Cluster, K.U.Leuven, Leuven, Belgium

Running title: Influence of implant-abutment connection on the biomechanical behavior of implants.

Keywords: immediate implant loading, immediate implant placement, finite element analysis.

ABSTRACT

Objective: The purpose of the present study was to evaluate the biomechanical environment of immediately placed implants, before and after osseointegration, by comparing three different implant-abutment connection types. **Materials and Methods:** A CT-based finite element model of an upper central incisor extraction socket was constructed containing implants with either external hex, internal hex or Morse-taper connection. Frictional contact elements were used in the bone, implant, abutment and abutment screw interfaces in the immediately placed simulations. In osseointegrated simulations, the repair of bone alveolar defect and a glued bone-to-implant interface were assumed. By ANOVA, the influence was assessed of connection type, clinical situation and loading magnitude on the peak equivalent strain in the bone, peak Von Mises stress in the abutment screw, bone-to-implant relative displacement and abutment gap. **Results:** The loading magnitudes had a significant contribution, regardless of the assessed variable. However, the critical clinical situation of an immediately placed implant itself was the main factor affecting the peak EQV strain in the bone and bone-to-implant displacement. The largest influence of the connection type in this protocol was seen on the peak equivalent stress in the abutment screw. On the other hand, a higher influence of the various connection types on bone stress/strain could be noted in osseointegrated simulations. **Conclusion:** The implant-abutment connection design did not significantly influence the biomechanical environment of immediately placed implants. Avoiding implant overloading and ensuring a sufficient initial intraosseous stability, are the most relevant parameters for the promotion of a safe biomechanical environment in this protocol.

INTRODUCTION

In the last decade, promising results have been observed when non submerged dental implants were subjected to immediate functional loads.¹⁻³ Immediate loading of implants offers several clinical benefits because both function and esthetics are immediately restored. In some situations, this protocol has been associated to the immediate implant placement into fresh extraction sockets. This procedure reduces the treatment time and cost, decreases the number of surgical procedures and optimizes the esthetic results.^{4,5}

However, regardless of whether an implant is put in function after an undisturbed healing or immediately after placement, the predictability and long-term success of implant treatment are greatly influenced by the biomechanical environment. The intimate bone-implant contact at the interface allows the direct transmission of the loads applied over the implant prosthetic device to the surrounding bone. The stress concentration can exceed bone's tolerance level, cause microdamage accumulation and induce bone resorption.⁶⁻⁸ Under certain conditions, this excessive occlusal loading may cause implant failure, even in osseointegrated implants.^{9,10} In addition, the bone supporting level is one of the most important factors for the maintenance of peri-implant esthetic harmony because the bone level determines the peri-implant soft tissue position. Even if not progressive, marginal bone resorption in the buccal or proximal aspects of the implant can lead to recession or absence of papilla, respectively.^{11,12} In the immediate loading protocol, the overall requirement is to control interfacial movement between the implant and the surrounding bone. Micromovements

that exceed 150 μm can induce fibrous connective tissue formation instead of the desirable bone regeneration.¹³⁻¹⁶

Some studies have demonstrated that the initial breakdown of the implant–tissue interface generally begins at the crestal region in successfully osseointegrated implants.^{6,7,9,10} Also, the majority of the mechanical failures occur in the implant neck.¹⁷⁻²¹ Therefore, efforts have been made to evaluate the effects of different implant-abutment connections on the stress/strain distributions and magnitudes in the bone and in implant components. Merz and coworkers²⁰ compared, by experimental and finite element methods, the stresses induced by off-axis loads on tapered and butt-joint connections. They concluded that the tapered interface distributed the stresses more evenly when compared to the butt-joint connection. In another finite element study, Hansson²² observed that a morse-taper implant-abutment at the level of the marginal bone substantially decreased peak bone stresses. Moreover, it improved the distribution of stress in the supporting bone. On the other hand, the shear stress was found to be located at the very top of the marginal bone, for a ‘flat to flat’ implant–abutment interface. With a conical interface, the peak bone–implant interface shear stress had a more apical location, which could reduce marginal bone resorption.^{22,23}

There are already some experimental, numerical and clinical studies²⁴⁻²⁶ evaluating the influence of implant-abutment connection on osseointegrated implants. Nevertheless, there is limited information on many different outcome variables of immediately placed implants.²⁷ As well, no FEA studies were encountered on the biomechanical environment of dental implants placed into a fresh extraction socket. The evaluation of the stress/strain and displacement of

the prosthesis-implant-bone complex in this clinical situation could contribute to the insight into the impact of abutment connection design.

Therefore, the purpose of the present study is to evaluate the biomechanical environment of dental implants placed into extraction sockets, before and after osseointegration. The influence of external hex, internal hex and Morse-taper connections on the strain in peri-implant bone and on the stability of implants and abutments will be compared.

MATERIALS AND METHODS

The CT (computer tomography) images of a dry maxilla, provided by the Department of Anatomy of the Faculty of Odontology at Araraquara (São Paulo State University, Brazil) were taken by a Picker UltraZ CT scanner with a gantry tilt of 0°, at 120 kV acceleration voltage and 1mA current. The projection data were exported using the DICOM (Digital Imaging and Communication in Medicine) file format. The data set had a voxel size of 0.391 x 0.391 x 1.000 mm and consisted of contiguous slices with respect to the Z-axis.

Bone segmentation and reconstruction of an upper central incisor extraction socket geometry were accomplished by thresholding within an image-processing software (Mimics 9.11, Materialise, Haasrode, Belgium). As the interest in this study was on the biomechanical environment in the vicinity of the implant, only the relevant part of the maxilla was reconstructed. A reconstruction of the entire maxilla would have led to a larger finite element model, with unacceptably high computational costs. The CAD (computer-aided design) solid models of conical 13 mm implants, with a 4.3 mm diameter

shoulder, abutments and abutment screws were provided by the implant producer (Neodent, Curitiba, Brazil). Morse-taper abutment and abutment screw are one single piece.

Firstly, one implant model was imported in Mimics and positioned 1 mm deep inside the extraction socket, in a central position, to a palatal direction. The contra-lateral teeth and the socket anatomy were used as a guide (figure 1).²⁷

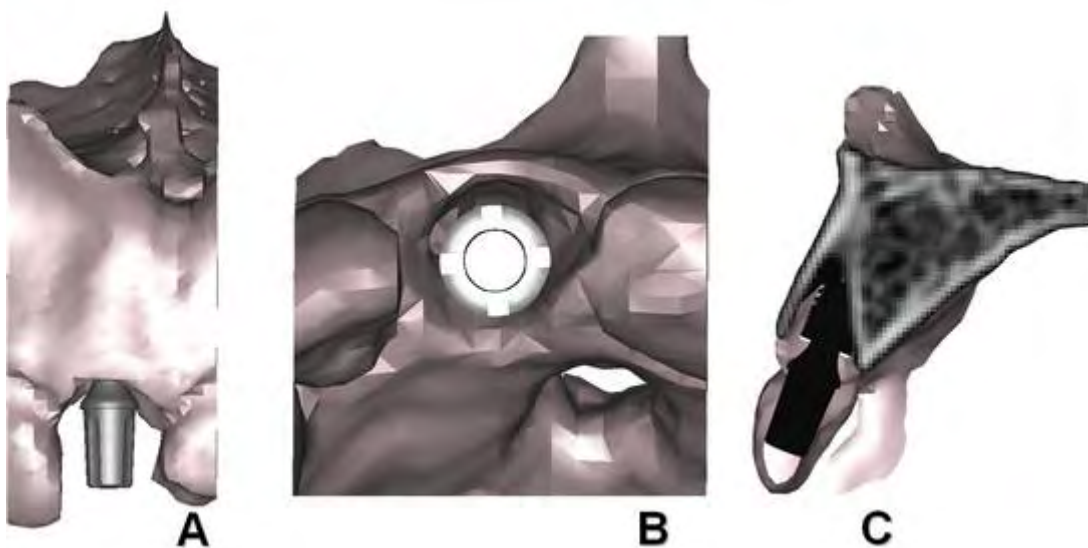


Figure 1: Implant positioned inside the extraction socket. A: vestibulo-palatal view. B: occlusal view. C: proximal view.

After having obtained the correct position of the implant, its inner part was removed and each implant-abutment connection was added. An external hex, an internal hex and a Morse-taper implant with the very same external design and position were created. This procedure allowed having the same bone mesh and bone-implant interface for the three different implant-abutment connections. The implant insertion hole in the extraction socket solid model was obtained by means of Boolean subtraction.

The abutment and abutment screw models were then imported and aligned to the implant in their correct positions, following the instructions from the implant producer. No simplifications were made regarding the implant external and internal threads (i.e., the spiral characteristic of the threads was maintained). However, the threads of the abutment screw CADs were edited to match perfectly the internal threads of the implants, to improve the contact status in this region. Second-order effects resulting from tightening of the abutment and the pre-load in the abutment screw were not considered in the present study.

Bone, implants, abutments and abutment screw models were meshed separately in MSC.Patran 2005r2 (figure 2) (MSC.Software, Gouda, The Netherlands).

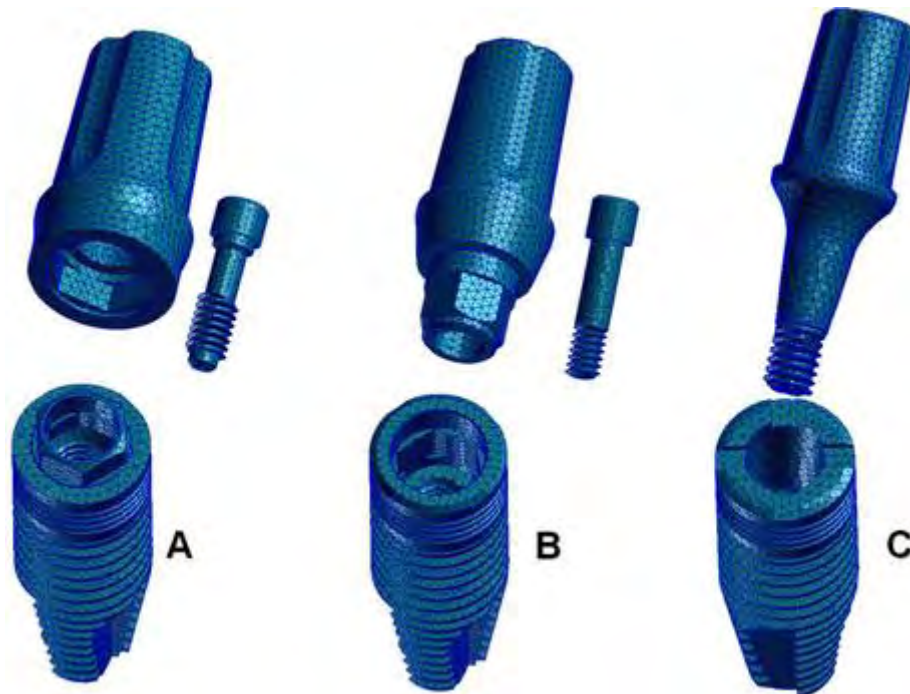


Figure 2: Implants, abutments and abutment screws meshes. A: external hex. B: Internal hex. C: Morse-taper. Note that Morse-taper abutment and abutment screw are one single piece.

A convergence study of the FE models was performed to verify the mesh quality. The convergence criterion was set to be less than 5% change of the peak von Mises stress (EQV Stress) at the bone-implant edge.²⁸ In this region the highest stress levels were encountered in the first test analysis. These peaks were found to be in the same coordinates for all 5 mesh element sizes tested. The time of processing was also considered as an exclusion criterion in the study. Based on the result of the convergence study, the optimal global element size for bone mesh was 0.75 mm. Figure 3 shows the result for the convergence study. Tetrahedral meshes were constructed with different degrees of refinement for feature recognizing (i.e., at threads). The smaller elements used were about 50 μm . Total number of elements and nodes in the models were an average of 110000 and 15000, respectively.

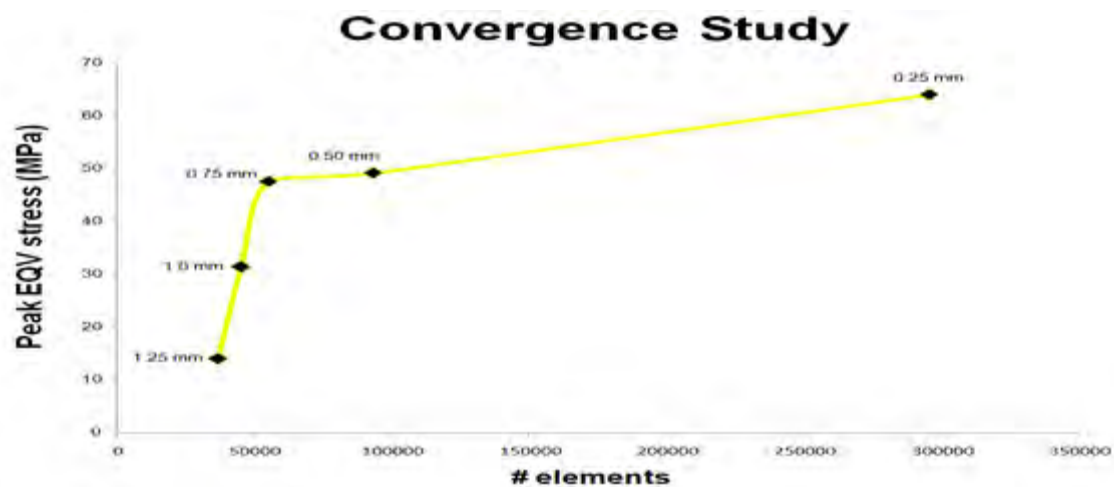


Figure 3: Influence of element size (1.25 mm, 1.0 mm, 0.75 mm, 0.50 mm and 0.25 mm) on bone mesh density and peak EQV stress in bone model.

During meshing of the bone solid model, the entire volume that is contained within the outer bone surface was meshed. This means that the mesh consists of tetrahedral elements located in either cortical or trabecular bone. To discriminate between both tissues, different elastic properties were assigned, based on the grey values in the CT images.²⁹

The values of the Young's modulus and Poisson ratio for the materials used in the present study were adopted from the relevant literature³⁰ and are summarized in table 1.

Table 1: Mechanical properties of bone, implant and prosthetic materials.

| Properties | Materials | | |
|----------------------------------|------------------|----------------------|------------------------|
| | Titanium | Cortical Bone | Trabecular Bone |
| Young's modulus (E) – MPa | 110000 | 13700 | 1370 |
| Poisson ratio (ν) | 0.33 | 0.30 | 0.30 |

For simulating the immediately placed implant, non-linear frictional contact elements (Coulomb frictional interface) were used. A friction coefficient μ of 0.3 was assumed between the bone and the implant.^{28,31} Between implant, abutment and abutment screw regions in contact, a frictional coefficient of 0.5 was assumed.^{20,32} Frictional contact configuration allows minor displacements between all components of the model without interpenetration. Under these conditions, the contact zones transfer pressure and tangential forces (i.e. friction), but no tension.

For simulating the stage after socket healing and implant osseointegration, the bone-implant interface was assumed to be a bonded contact. In this

configuration, no relative motion could occur at the bone-implant interface. In addition, a hard tissue bridge was modeled at the alveolar ridge region. The interface conditions for implant system components remained the same.

Models were fully constrained in all directions at the nodes on mesial and distal borders. A palato-buccal static load was applied as a point load centrally on the top of the abutment. The load inclination was 40 degrees in relation to the alveolus longitudinal axis. Loading magnitudes of 50 N, 100N and 200N were adopted for both the immediately placed and osseointegrated simulations.³³⁻³⁵ The analysis and post-processing were performed for each model by means of the MSC.MARC/Mentat 2005r3 software (MSC.Software, Gouda, NL).

The data for peak equivalent strain (EQV strain) in the bone, bone to implant relative displacement, peak Von Mises stress (EQV stress) in the abutment screw, and abutment gap were assessed and analyzed using a general linear model Analysis of Variance (ANOVA, SAS/STAT statistical software, version 9.1, SAS Institute, Cary, NC, USA). This procedure allowed calculating the percentage contribution of each of the evaluated parameters (connection type, clinical situation and loading magnitude) and their interactions on the assessed results.³⁶

RESULTS

The EQV strain for the 100N loading models was used to display the strain state in bone, for immediately placed simulations (figure 4 a-f) and for osseointegrated simulations (figure 5 a-f). The scale was set to range between

100-4000 $\mu\epsilon$.³⁷ In figures 4 a-c and 5 a-c, the implants were kept in order to make it easier to verify the influence of the strain transmission through the implant connection to the bone.

Data for EQV strain in the bone, bone to implant relative displacement, EQV stress in the abutment screw and abutment gap are listed in table 2. The EQV strains were also assessed in the implant median buccopalatal and mesiodistal paths in bone, 250 μm from the implant surface, for both 50N loading immediately placed and osseointegrated simulations (figures 6 and 7). In addition, shear stress was assessed along the path in the implant median marginal buccal bone for the osseointegrated simulation (figure 8).

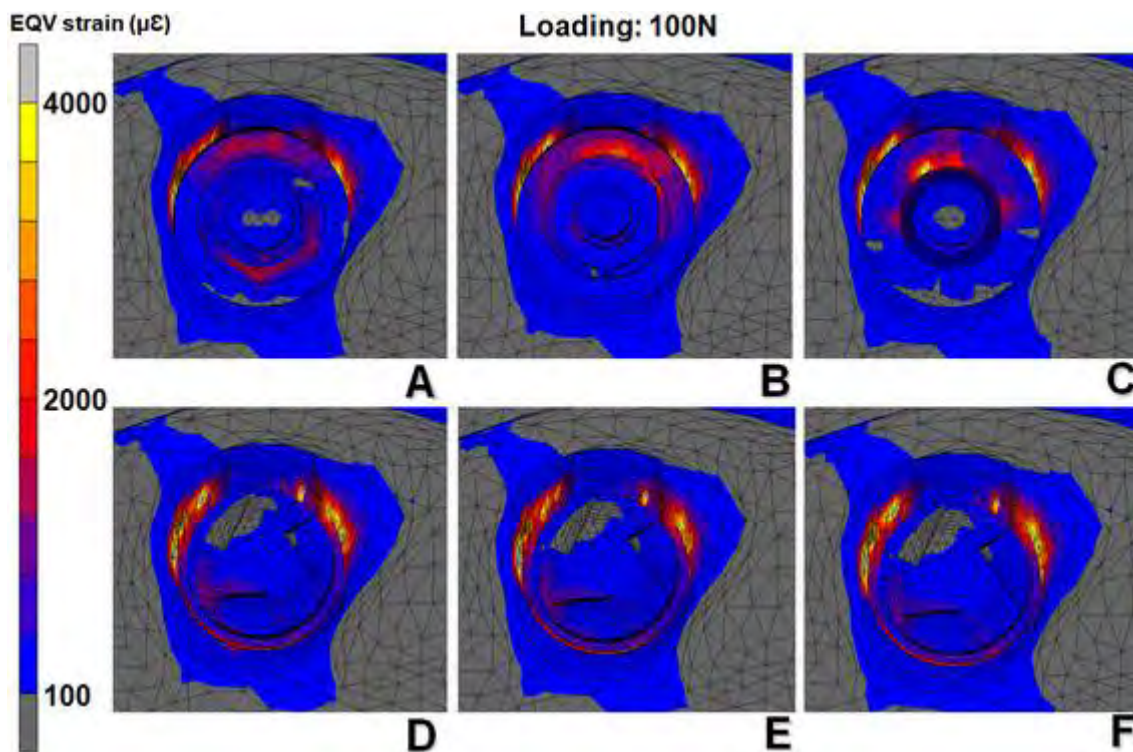


Figure 4: Occlusal view of EQV strain ($\mu\epsilon$) distribution for external hex (A and D), internal hex (B and E) and Morse-taper (C and F) in the immediately placed simulations. Note that the implants were removed for clarity in figures D-F.

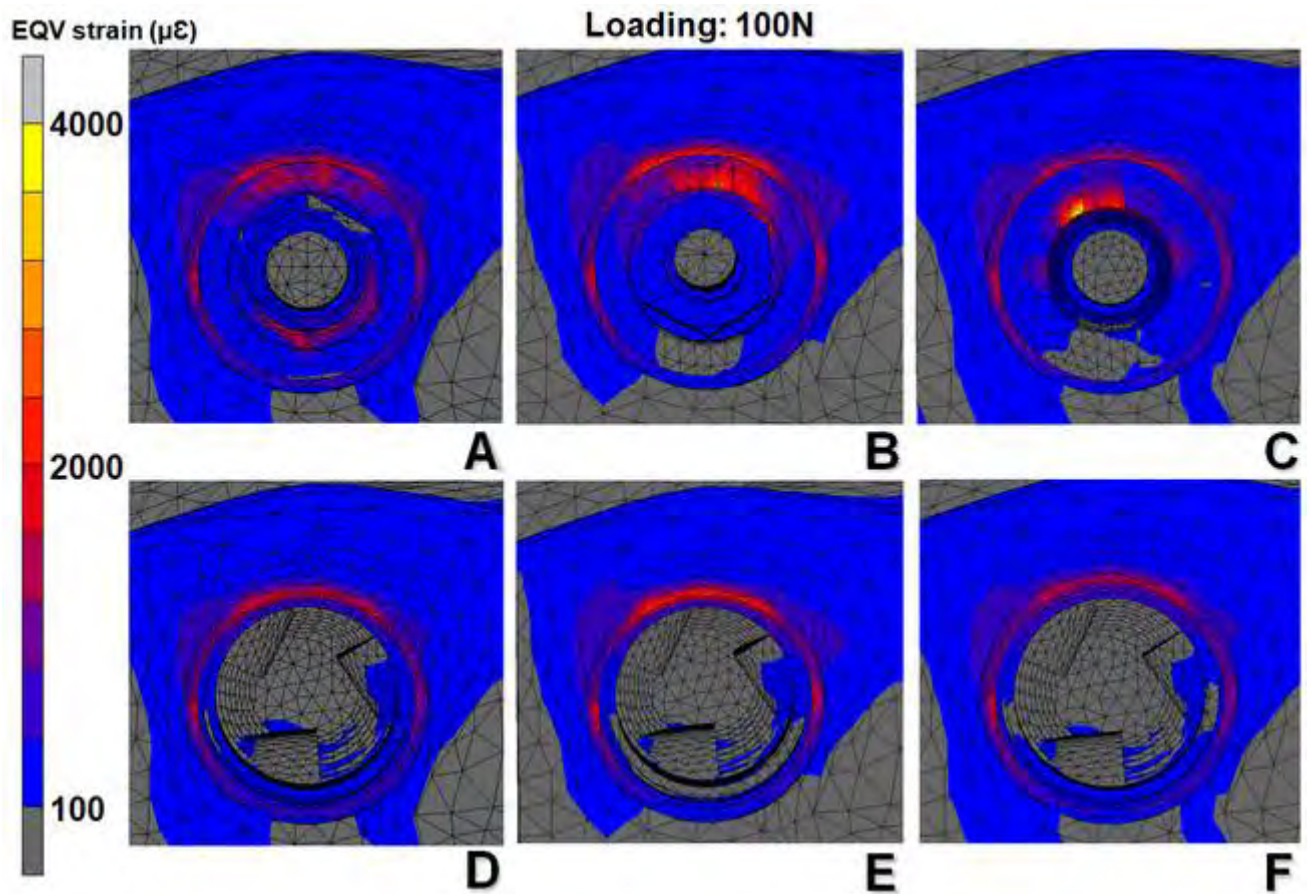


Figure 5: Occlusal view of EQV strain ($\mu\epsilon$) distribution for external hex (A and D), internal hex (B and E) and Morse-taper (C and F) in the osseointegrated simulation. Note that the implants were removed for clarity in figures D-F.

The ANOVA results on the percentage contribution of the connection type, clinical situation, loading magnitude and their interactions on the EQV strain in the bone, bone to implant relative displacement, EQV stress in the abutment screw and abutment gap are shown in Tables 3-6, respectively.

Regardless of connection types, the highest strain concentration was seen at the buccal aspect of peri-implant bone. Some high strains were also found at the outside of the ridge in both immediately placed and osseointegrated simulations. In immediately placed simulations, higher strain levels were seen for the Morse-taper connection, though in a more evenly distributed way, compared to internal hex and external hex connections. External hex presented intermediate strain values, which were concentrated mostly in the buccal aspect of the bone. The lowest strain levels were seen for internal hex. For this connection type the strains were more evenly distributed than for external hex. In a different way, for the osseointegrated simulation, external hex and internal hex showed similar strain levels while Morse-taper presented considerably lower strain values. Also in this clinical situation, the strain distribution was most even for the Morse-taper, followed by internal hex and external hex, respectively. Strain distribution and values assessed in the bone paths followed almost the same pattern for all three connections. A greater influence of connection designs could be noted only for the marginal regions in the osseointegrated simulations. In this region, the peak shear stress was much higher for the external hex followed by the internal hex. These peak shear stresses for external and internal hex were located at the very top of the marginal cortical bone. In a different way, for the Morse-taper connection, the shear stress was evenly distributed.

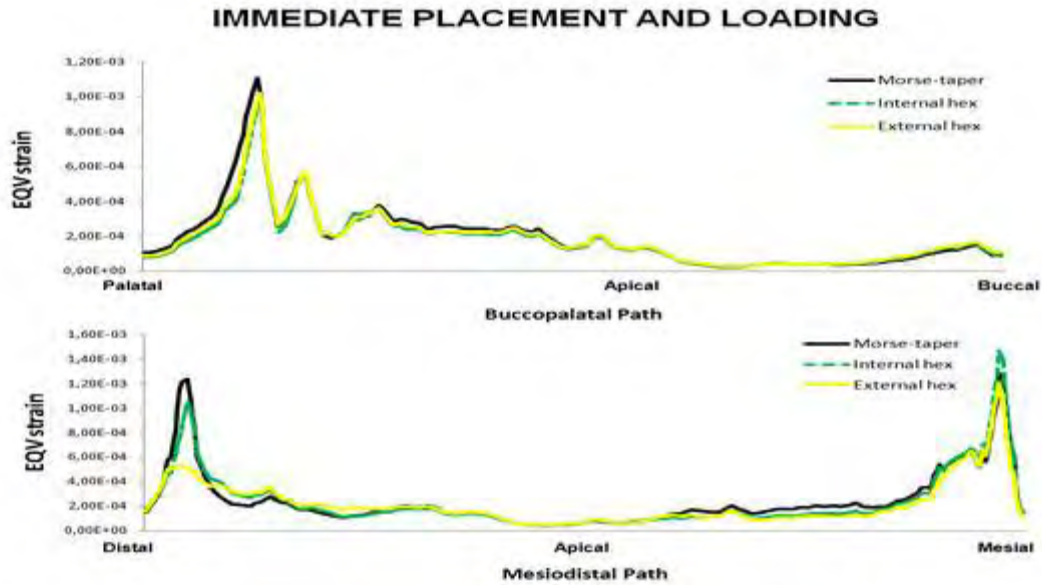


Figure 6: EQV strains [-] assessed along a path in bone, 250 μm from implant–bone interface in the implant median buccopalatal and mesiodistal planes for 50N loading immediately placed simulations.

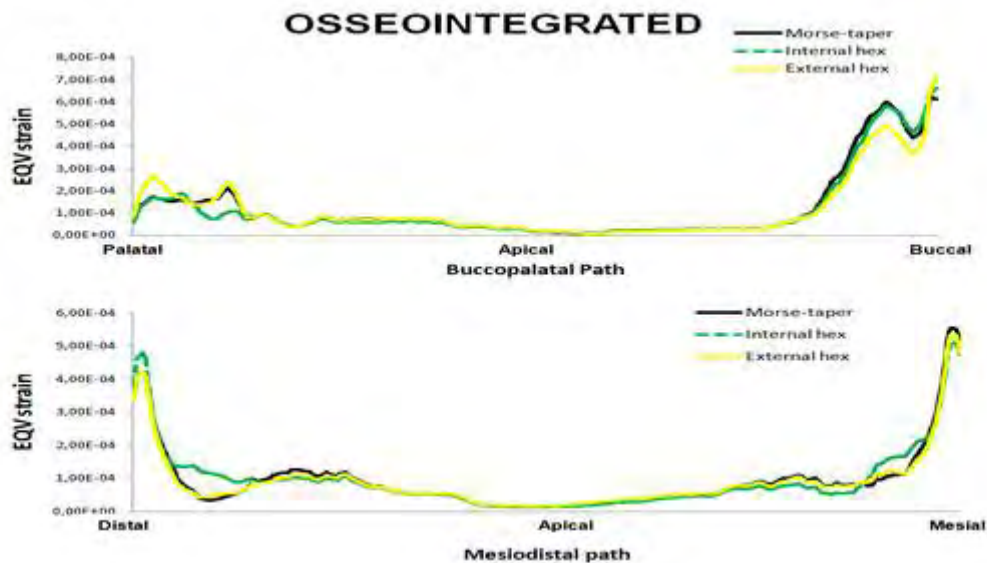


Figure 7: EQV strains [-] assessed along a path in bone, 250 μm from implant–bone interface in the implant median buccopalatal and mesiodistal planes for 50N loading osseointegrated simulations.

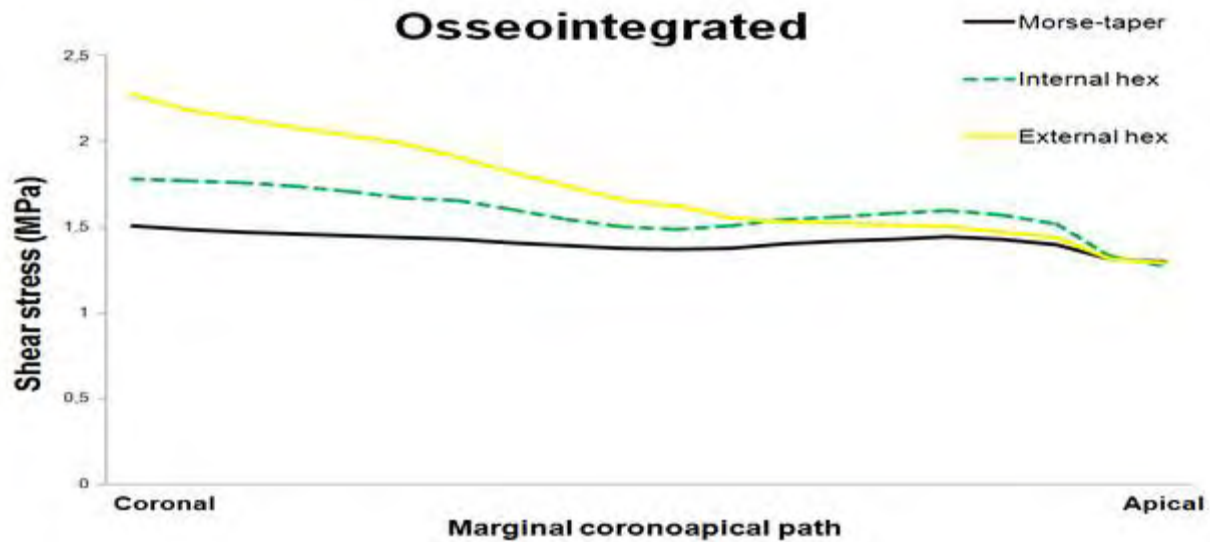


Figure 8: Shear stress (MPa) assessed along a path in marginal bone, 250 μm from implant–bone interface in the implant median buccopalatal plane, for 50 N loading osseointegrated simulations.

Regarding the bone to implant relative displacement in immediately placed simulations, the differences between the connection types were minor. The von Mises stress (EQV stress) distribution in implant components is shown in a bucco-palatal mesial plane in figure 9 a-c. The stress is mostly concentrated in the abutment conical part in the Morse-taper connection. Minor EQV stress values were found in the implant and in the abutment screw. On the contrary, for external hex connection the major stress was concentrated in the abutment screw and in the implant region that remained in contact with the abutment. The same trend was seen for internal hex. However, comparing both connections, the external hex presented considerably higher stress concentration in the abutment screw than the internal hex.

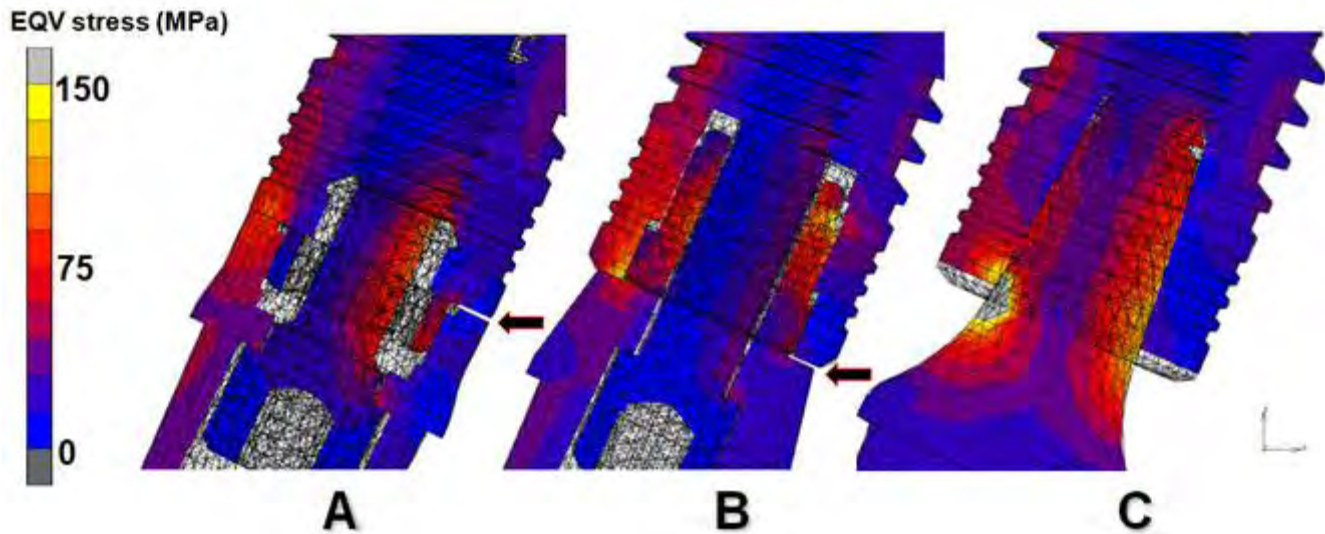


Figure 9: EQV stress (MPa) distribution inside implant connections (A: external hex, B: internal hex, C: Morse-taper). The deformation is 10-fold magnified for visualization. Note abutment gap due to the loading, for external hex and internal hex (black arrows).

Abutment stability was evaluated by means of the abutment vertical gap³⁸ in both immediately placed and osseointegrated simulations. However, it is important to emphasize that the gap reported in the present study is due to the movement and deformation of the abutment as a direct consequence of the loading applied. It is related to the capability of the connection to provide stability. No pre-existing misfit between implant and abutment, as is normally observed for internal hex and external hex connections,³⁸ was included in the model. The Morse-taper abutment showed the smallest gap. Internal hex was more stable and presented a smaller gap compared to external hex. Comparing the clinical situations, abutment instability was higher in immediately placed simulations.

The percentage contributions of each parameter evaluated are presented in tables 3-6. Regardless of the assessed result, the loading magnitudes have a significantly high contribution. The clinical situation has a greater contribution on the peak EQV strain in the bone and bone to implant displacement. The largest influence of the connection type was seen on the peak EQV stress in the abutment screw.

Table 2: Results for the peak equivalent strain (EQV strain) in the bone, peak equivalent stress (EQV stress) in the abutment screw, bone to implant relative displacement (displac.) and abutment gap, for all simulated models.

| Connection types | Clinical situations | Loading | Bone EQV strain ($\mu\epsilon$) | Bone_implant displac. (μm) | Screw EQV Stress (MPa) | Gap (μm) |
|-------------------------|----------------------------|----------------|---|---|-------------------------------|---------------------------------------|
| Morse-taper | immediately placed | 50N | 4,997.8 | 5.1 | 57.3 | 4.5 |
| | osseointegrated | 50N | 892.9 | ----- | 44.2 | 4.0 |
| | immediately placed | 100N | 6,060.3 | 11.7 | 110.4 | 9.1 |
| | osseointegrated | 100N | 1,817.0 | ----- | 89.1 | 8.1 |
| | immediately placed | 200N | 9,910.1 | 24.4 | 225.0 | 18.4 |
| | osseointegrated | 200N | 3,924.4 | ----- | 157.5 | 16.1 |
| Internal hex | immediately placed | 50N | 3,762.4 | 5.3 | 76.5 | 6.0 |
| | osseointegrated | 50N | 1,103.1 | ----- | 71.4 | 5.5 |
| | immediately placed | 100N | 5,053.4 | 11.1 | 144.8 | 13.3 |
| | osseointegrated | 100N | 2,593.5 | ----- | 128.6 | 11.6 |
| | immediately placed | 200N | 9,048.2 | 23.3 | 350.7 | 27.3 |
| | osseointegrated | 200N | 5,079.4 | ----- | 221.3 | 24.0 |
| External hex | immediately placed | 50N | 4,013.7 | 5.5 | 124.4 | 8.0 |
| | osseointegrated | 50N | 1,119.0 | ----- | 112.3 | 8.2 |
| | immediately placed | 100N | 5,444.6 | 11.7 | 251.9 | 15.5 |
| | osseointegrated | 100N | 2,232.8 | ----- | 224.1 | 15.5 |
| | immediately placed | 200N | 10,209.8 | 24.0 | 495.0 | 31.2 |
| | osseointegrated | 200N | 4,329.9 | ----- | 418.8 | 30.1 |

*Table 3: Analysis of Variance for the peak equivalent strain in the bone. $P < 0.05$, * statistically significant. DF: degrees of freedom; SS: sum of squares; MS: mean square.*

| Parameter | DF | SS | MS | P-Value | Contribution (%) |
|--|----|-------------|-------------|----------|------------------|
| Connection Type | 2 | 83004.42 | 41502.21 | 0.6799 | 0.06 |
| Clinical Situation | 1 | 69652650.49 | 69652650.49 | <0.0001* | 49.94 |
| Connection Type X Clinical Situation | 2 | 2301719.20 | 1150859.60 | 0.0210* | 1.65 |
| Loading Magnitude | 2 | 63012208.21 | 31506104.10 | <0.0001* | 45.18 |
| Connection Type X Loading Magnitude | 4 | 340997.31 | 85249.33 | 0.5503 | 0.24 |
| Clinical Situation X Loading Magnitude | 2 | 4068982.43 | 2034491.22 | 0.0077* | 2.92 |

Table 4: Analysis of Variance for the relative displacement between implant and bone.

Saturated experimental design, no p-values reported. DF: degrees of freedom; SS: sum of squares; MS: mean square.

| Parameter | DF | SS | MS | Contribution (%) |
|-------------------------------------|----|--------|--------|------------------|
| Connection Type | 2 | 0.50 | 0.25 | 0.10 |
| Loading Magnitude | 2 | 538.16 | 269.08 | 99.83 |
| Connection Type X Loading Magnitude | 4 | 0.44 | 0.11 | 0.08 |

*Table 5: Analysis of Variance for the peak equivalent stress in the abutment screw. $P < 0.05$, * statistically significant. DF: degrees of freedom; SS: sum of squares; MS: mean square.*

| Parameter | DF | SS | MS | P-Value | Contribution (%) |
|--|----|--------|--------|----------|------------------|
| Connection Type | 2 | 172.88 | 86.44 | <0.0001* | 29.16 |
| Clinical Situation | 1 | 14.58 | 14.58 | 0.0031* | 2.46 |
| Connection Type X Clinical Situation | 2 | 1.25 | 0.63 | 0.2841 | 0.21 |
| Loading Magnitude | 2 | 401.33 | 200.66 | <0.0001* | 67.69 |
| Connection Type X Loading Magnitude | 4 | 0.38 | 0.10 | 0.8864 | 0.06 |
| Clinical Situation X Loading Magnitude | 2 | 2.48 | 1.24 | 0.1338 | 0.42 |

*Table 6: Analysis of Variance for the abutment gap. $P < 0.05$, * statistically significant. DF: degrees of freedom; SS: sum of squares; MS: mean square.*

| Parameter | DF | SS | MS | P-Value | Contribution (%) |
|--|-----------|-----------|-----------|----------------|-------------------------|
| Connection Type | 2 | 69.35 | 34.68 | 0.4758 | 6.95 |
| Clinical Situation | 1 | 76.88 | 76.88 | 0.2308 | 7.70 |
| Connection Type X Clinical Situation | 2 | 60.30 | 30.15 | 0.5168 | 6.04 |
| Loading Magnitude | 2 | 589.43 | 294.72 | 0.0430* | 59.04 |
| Connection Type X Loading Magnitude | 4 | 88.75 | 22.19 | 0.6972 | 8.89 |
| Clinical Situation X Loading Magnitude | 2 | 113.72 | 56.87 | 0.3312 | 11.39 |

DISCUSSION

The present FEA was carried out to evaluate the biomechanical environment of immediately placed and loaded implants. Morse-taper, internal hex and external hex connections were compared. It was demonstrated that the implant-abutment connection design did not significantly influence the bone strain and the implant displacement of immediately placed implants. On the other hand, the Morse-taper connection presented superior abutment stability and the least stress concentration in the abutment screw. In the immediate implant placement protocol, sufficient initial intraosseous stability and a safe biomechanical environment, which avoids overloading, are the most relevant parameters on implant survival. Adverse forces over the implant-supported prostheses could not only cause abutment screw loosening and mechanical failures,¹⁷⁻²¹ but could also impair osseointegration.^{6,7,9,10}

The immediately placed implant simulations showed slightly higher values of bone strain for the Morse-taper connection. On the contrary, the internal hex and external hex implants presented the lowest strain levels. These findings are in agreement with results previously reported by Palomar et al.,⁴⁰ in a FE study of an immediately loaded implant. Comparing rigid and resilient implant-abutment connections they found greater stress values in bone for the rigid ones. A resilient component in the connection was shown to absorb some of the load, which resulted in a smaller stress in bone for this kind of implant.⁴⁰ The connection type, however, had the lowest percentage contribution on the values of the peak EQV strain in the bone for immediately placed implants and was not statistically significant. The loading magnitude and the critical clinical situation of immediately placed implants were the major contributing factors for the bone strain in this protocol. Also Hansson²³ observed that when the implant-abutment connection was positioned 2mm coronally from the bone level, the effects of different connections were the same. In the present study similar tendencies were observed in immediately placed implant simulations, probably because of the initial bone defect at the marginal region. This bone gap positioned the implant-abutment connections far from the bone.

On the other hand, the statistical analysis showed a significant contribution of the interaction between the connection type and the clinical situation on the EQV strain in the bone. It seems that the influence of the connection became higher by changing the clinical situation from immediately placed to osseointegrated. In osseointegrated models the repair of bone alveolar defect and a glued bone to implant interface were assumed. In this way, the particular stress/strain distribution observed in each implant-abutment connection will

result in different stress/strain patterns in the bone, mainly when bone reaches levels close to the implant crest.²³ The results of the current FEA for the osseointegrated model are in accordance with the findings of Hansson.²³ Using FEA, Hansson²³ showed that a conical implant-abutment interface at the level of the bone crest decreases the peak bone-implant interfacial stress as compared to the flat top interface. For the conical implant-abutment interface this peak interfacial shear stress was located at some depth in the marginal bone. For the flat top implant-abutment interface, the shear stress was located at the top marginal bone.^{22,23} In the present study, the shear stress assessed in a path in the marginal buccal bone region also showed the same trend. Comparing external and internal hex connections, a smaller amount of shear stress occurred at the cervical area for the internal configurations. This can be explained by the difference in surface area between connections. The conical interface of the Morse-taper, as well as the lateral wall of the internal hex abutment, helped to dissipate the forces to the fixture.⁵²

Another interesting observation is the fact that some strain was encountered at the outside of the ridge for immediately placed implant simulations. Analogous results were observed by Cehreli et al.⁵³ in a cadaver model. The authors argued that minimal load was transferred to the labial marginal bone due to the absence of direct contact with the implant, because of the site-specific three-dimensional shape of the bone defect. However, in the real clinical situation, once an implant is immediately placed, the coagulum and thereafter the initial connective tissue in the bone defect could transfer functional load and stimulate the bone that is not contacting the implant.^{54,55}

One can speculate whether such stimulus could avoid disuse atrophy of the marginal bone.^{3,56}

In the present FEA, to facilitate the visualization of the strain state in bone, the scale was set to range between 100-4,000 $\mu\epsilon$. Frost⁴³ considered 4,000 μ strain as a possible threshold for pathological bone overload. Also Duyck et al.,⁶ by FEA based on CT-images, estimated, the value associated with overload-induced resorption as 4,200 $\mu\epsilon$. Nevertheless, although the peak of bone strain exceeded 4000 $\mu\epsilon$ for all implant connections in our immediately placed implant simulations, this does not necessarily imply a bone overloading and implant loss. Rather than only strain amplitude, also loading frequency and number of loading cycles are parameters capable to greatly influence the cortical bone adaptive response.⁴⁴⁻⁴⁸ Furthermore, the loading applied in the present study was static and bone responds to dynamic rather than to static loads.^{6,49-51} In this way, it must be clear that the modeling of bone adaptive processes was not one of the aims in the current FEA.

In addition, the peaks of strain appeared locally in a minor part of the marginal bone for 50N and 100N loading magnitudes (figure 4 D-F), where indeed some localized bone resorption is likely to occur.^{6,43} This statement is also corroborated by the strain values along paths in bone for 50N loading at 250 μ m from the implant surface. The graphs showed peaks of strain lower than 1200 $\mu\epsilon$, independently of implant connection, bone region and clinical situation. The present study focused only on the relative influence of implant connection type on bone strain values.

In essence, one of the most critical elements for an uneventful bone tissue formation around an immediately loaded implant is a stiff bone-implant

interface, allowing low implant micromovement in bone.^{16,39} In the present study, all three connection types showed similar values of displacement ranging between 5 and 25 μm , for the immediately placed simulations. Though important differences exist regarding, for example, the implant designs, the clinical situations, and the loading magnitudes and directions, the results presented in the current study are in line with other FEAs of immediately loaded implants. Huang et al.²⁸ reported a maximum sliding distance of 12.5 μm between threaded implants and bone, for a 100N force over an immediately loaded maxillary implant. Comparing resilient and rigid abutments by a FEA of immediately loaded implants in a mandibular premolar region, Polamar et al.⁴⁰ found maximum vertical implant displacements of 12.67 and 12.47 μm , respectively. This difference in implant displacement is qualitatively similar to the one found in this study for internal hex (11.1 μm) and external hex (11.7 μm). However, as shown in the statistical analysis, the connection type did not significantly influence the bone to implant relative displacement.

The current FEA showed that the connection type has a significant contribution to the EQV stress in the abutment screw and to the abutment gap. In these parameters, Morse-taper implant presented a considerably lower EQV stress in the abutment screw and lower abutment gap values, in both simulated clinical situations. Internal hex presented the intermediate values and the external hex the highest connection instability. This observation corroborates data presented by Merz et al.,²⁰ who stated that a tapered connection is mechanically more stable than the butt-joint configurations. Also Khraisat et al.,⁴¹ using repeated loading, observed a significantly better fatigue strength for a tapered joint design, compared to an external hex connection. The reduced

stress in the abutment screw and reduced gap observed for the Morse-taper in the present study was probably provided by its superior joint stability.⁴³

The same factor could also be used to explain the differences in stress distribution among the three implant-abutment connections. Basically, the Morse-taper and the butt-joint configurations have quite different functional behavior. In a taper connection, the loading is resisted mainly by the taper interface. It prevents the abutment from tilting off, allowing stable retention of position by frictional forces.²⁰ Differently, an external hex configuration determines the rotational position but there is no form or positive locking. In this way, the lateral loading is absorbed mainly by the abutment screw.²⁰ On the other hand, in an internal hex connection, the lateral wall of the abutment also helps to dissipate the lateral forces and protects the abutment screw from excessive stress. Substantially lower EQV stresses were observed in the internal hex abutment screw in the current FEA, compared with external hex. Also the bone to implant interface condition and the clinical situation have a significant contribution to abutment stability. Slightly higher abutment stability and less EQV stress in the abutment screw were seen for the osseointegrated situation.

The intricate implant designs and their relationship with the supporting tissues and prosthetic restoration prevent the use of simple formulas to evaluate the effect of external loading on the internal stresses/strains and displacements. In this way, the FE method can offer some information unavailable from clinical or experimental studies.³⁰ In addition, numerical simulations permit the evaluation of possible explanations for in vivo and clinical findings, and also suggest directions for further investigations. Nevertheless, the results obtained

in the present FEA should be interpreted with some care. It was not possible in this study to answer the question as to whether bone overload does actually occur in immediately placed implants. The answer to that question is indeed patient-specific, and requires a patient-specific finite element model that incorporates the patient specific bone anatomy, bone density distribution, implant position and in vivo measured implant loads.⁵⁷ On the other hand, the statistical analysis on the FEA results allowed the assessment of the real relative effects of each investigated factor on the mechanical response of the bone and implant components in various clinical situations. The relevance of efforts to develop implant designs capable of providing a safe biomechanical environment, especially for the newer protocols of implant usage, is not disputed. However, varying the implant-abutment connection type was not able to significantly improve the biomechanical environment in the immediately placed implant protocol.

CONCLUSION

Within the limitation of this FE analysis it can be concluded:

1. Different implant-abutment connection types do not significantly influence the biomechanical environment of immediately placed implants.
2. Loading magnitude and the critical clinical situation of immediately placed implants itself are the main factors affecting the equivalent bone strain and implant displacement.

3. The Morse-taper connection provided the best abutment stability and the lowest von Mises stress concentration in the abutment screw, compared to internal hex and external hex connections.
4. The effect of the various connection types on bone stress/strain may be higher for osseointegrated implants.

ACKNOWLEDGEMENTS

The authors thank the Neodent® implant system for providing the implant CAD models. Dr. S. Fieuws from the Leuven Biostatistics and Statistical Bioinformatics Centre (L-BioStat) is acknowledged for the factorial design optimization and ANOVA analyses. Roberto Pessoa gratefully thanks the grants and scholarships from: FAPESP (Research Support Foundation of São Paulo State), CAPES (Committee for Postgraduate Courses in Higher Education) and CNPq (National Council for Scientific and Technological Development). Siegfried Jaecques gratefully acknowledges funding from the K.U.Leuven research fund (project OT/06/58). The CT-based FEM methods are based on research funded by the EU Framework Programme 5 Quality of Life project QLK6-CT-2002-02442 IMLOAD.

REFERENCES:

1. Gapski R, Wang HL, Mascarenhas P, Lang NP. Critical review of immediate implant loading. *Clin Oral Implants Res* 2003; 14:515–527.

2. Ioannidou E, Doufexi A. Does loading time affect implant survival? A meta-analysis of 1,266 implants. *J Periodontol* 2005; 8:1252-8.
3. Esposito M, Grusovin MG, Willings M, Coulthard P, Worthington HV. Interventions for replacing missing teeth: different times for loading dental implants. *Cochrane Database Syst Rev* 2007; 2: CD003878.
4. Schwartz-Arad D, Chaushu G. The ways and wherefores of immediate placement of implants into fresh extraction sites: A literature review. *J Periodontol* 1997; 68:915-923.
5. Esposito MA, Koukouloupoulou A, Coulthard P, Worthington HV. Interventions for replacing missing teeth: dental implants in fresh extraction sockets (immediate, immediate-delayed and delayed implants). *Cochrane Database Syst Rev* 2006; 4: CD005968.
6. Duyck J, Ronald HJ, Van Oosterwyck H, Naert I, Vander Sloten J, Ellingsen JE. The influence of static and dynamic loading on marginal bone reactions around osseointegrated implants: an animal experimental study. *Clin Oral Implants Res* 2001; 12: 207-218.
7. Hoshaw SJ, Brunski JB, Cochran GVB. Mechanical loading of Brånemark implants affects interfacial bone modeling and remodeling. *Int J Oral Maxillofac Implants* 1994; 9: 345–360.
8. Misch CE, Suzuki JB, Misch-Dietsh FM, Bidez MW. A positive correlation between occlusal trauma and peri-implant bone loss: literature support. *Implant Dent* 2005; 14: 108-16.
9. Isidor F. Loss of osseointegration caused by occlusal load of oral implants. A clinical and radiographic study in monkeys. *Clin Oral Implants Res* 1996; 7:143–152.

10. Isidor F. Histological evaluation of periimplant bone at implants subjected to occlusal overload or plaque accumulation. *Clin Oral Implants Res* 1997; 8:1–9.
11. Bengazi F, Wennstrom J, Lekholm U. Recession of the soft tissue margin at oral implants. A 2-year longitudinal prospective study. *Clin Oral Implants Res* 1996; 7: 303–310.
12. Tarnow DP, Magner AW, Fletcher P. The effect of the distance from the contact point to the crest of bone on the presence or absence of the interproximal papilla. *J Periodontol* 1992; 63: 995-996.
13. Søballe K, Brockstedt-Rasmussen H, Hansen ES, Bünger C. Hydroxyapatite coating modifies implant membrane formation. Controlled micromotion studied in dogs. *Acta Orthop Scand* 1992; 63:128–140.
14. Brunski JB. Biomechanical factors affecting the bone-dental implant interface. *Clin Mater* 1992; 10: 153–201.
15. Brunski JB. Avoid pitfalls of overloading and micromotion of intraosseous implants. *Dent Implantol Update* 1993; 4: 77–81.
16. Geris L, Andreykiv A, Van Oosterwyck H, Vander Sloten J, van Keulen F, Duyck J, Naert I. Numerical simulation of tissue differentiation around loaded titanium implants in a bone chamber. *J Biomech* 2004; 37: 763–769.
17. Ekefeld A, Carlsson GE, Borjesson G. Clinical evaluation of single-tooth restorations supported by osseointegrated implants: A retrospective study. *Int J Oral Maxillofac Implants* 1994; 9: 179-183.
18. Levine RA, Clem DS, Wilson Jr TG, Higginbottom F, Saunders SL. A multicenter retrospective analysis of the ITI implant system used for single-

- tooth replacements: results of loading for 2 or more years. *Int J Oral Maxillofac Implants* 1999; 14: 516–520.
19. Schwarz MS. Mechanical complications of dental implants. *Clin Oral Implants Res* 2000; 1:156–158.
20. Merz BR, Hunenbart S, Belser UC. Mechanics of the implant-abutment connection: an 8-degree taper compared to a butt joint connection. *Int J Oral Maxillofac Implants* 2000; 15: 519–526.
21. Behneke A, Behneke N, d'Hoedt B. The longitudinal clinical effectiveness of ITI solid-screw implants in partially edentulous patients: a 5-year follow-up report. *Int J Oral Maxillofac Implants* 2000; 15: 633–645.
22. Hansson S. A conical implant–abutment interface at the level of the marginal bone improves the distribution of stresses in the supporting bone. *Clin Oral Implants Res* 2003; 14:286–293.
23. Hansson S. Implant–abutment interface: biomechanical study of flat top versus conical. *Clin Implant Dent Relat Res* 2000; 2: 33–41.
24. Puchades-Roman L, Palmer RM, Palmer PJ, Howe LC, Ide M, Wilson RF. A clinical, radiographic, and microbiologic comparison of Astra Tech and Brånemark single tooth implants. *Clin Implant Dent Relat Res* 2000; 2: 78–84.
25. Palmer RM, Palmer PJ, Smith BJ. A 5-year prospective study of Astra single tooth implants. *Clin Oral Implants Res* 2000; 11: 179–182.
26. Astrand P, Engquist B, Dahlgren S, Kerstin E, Feldmann H. Astra Tech and Branemark system implants: a 5-year prospective study of marginal bone reactions. *Clin Oral Implants Res* 2004; 15: 413–420.

27. Quirynen M, Van Assche N, Botticelli D, Berglundh T. How does the timing of implant placement to extraction affect outcome? *Int J Oral Maxillofac Implants* 2007; 22(Suppl):203-23.
28. Huang HL, Hsu JT, Fuh LJ, Tu MG, Ko CC, Shen YW. Bone stress and interfacial sliding analysis of implant designs on an immediately loaded maxillary implant: A non-linear finite element study. *J Dent* 2008; 36: 409 – 417.
29. Jaecques SVN, Van Oosterwyck H, Muraru L, Van Cleynenbreugel T, De Smet E, Wevers M, Naert I, Vander Sloten J. Individualised, micro CT-based finite element modelling as a tool for biomechanical analysis related to tissue engineering of bone. *Biomaterials* 2004; 25: 1683–1696.
30. Geng JP, Tan KB, Liu GR. Application of finite element analysis in implant dentistry: a review of the literature. *J Prosthet Dent* 2001; 85:585-98.
31. Mellal A, Wiskott HWA, Botsis J, Scherrer SS, Belser UC. Stimulating effect of implant loading on surrounding bone. Comparison of three numerical models and validation by in vivo data. *Clin Oral Implants Res* 2004; 15: 239–248.
32. Steinemann SG, Mäusli PA, Szmukler-Moncler S, Semlitzsch M, Pohler O, Hintermann HE, Perren SM. Betatitanium alloy for surgical implants. In: Froes FH, Caplan I, ed. *Titanium '92. Science and Technology*. The Minerals, Metals & Materials Society, 1993:2689–2696.
33. Morneburg TR, Proschel PA. Measurement of masticatory forces and implant loads: a methodologic clinical study. *Int J Prosthodont* 2002; 15: 20–27.

34. Fontijn-Tekamp FA, Slagter AP, van't Hof MA, et al. Bite forces with mandibular implant-retained overdentures. *J Dent Res* 1998, 77: 1832–1839.
35. Duyck J, Van Oosterwyck H, Vander Sloten J, De Cooman M, Puers R, Naert I. Magnitude and distribution of occlusal forces on oral implants supporting fixed prostheses: An in vivo study. *Clin Oral Implants Res* 2000; 11: 465–475.
36. Dar FH, Meakina JR, Aspden RM. Statistical methods in finite element analysis. *J Biomech* 2002; 35: 1155–1161.
37. Frost HM. Bone 'mass' and the 'mechanostat': a proposal. *Anat Rec* 1987; 219: 1–9.
38. Kano SC, Binon PP, Curtis DA. A Classification System to Measure the Implant-Abutment Microgap. *Int J Oral Maxillofac Implants* 2007; 22: 879–885.
39. Vandamme K, Naert I, Geris L, Vander Sloten J, Puers R, Duyck J. The effect of micromotion on the tissue response around immediately loaded roughened titanium implants in the rabbit. *Eur J Oral Sci* 2007; 115: 21–29.
40. del Palomar AP, Arruga A, Cegoñino J, Doblaré M. A finite element comparison between the mechanical behaviour of rigid and resilient oral implants with respect to immediate loading. *Comput Methods Biomech Biomed Eng* 2005; 8: 45-57.
41. Khraisat A, Stegaroiu R, Nomura S, Miyakawa O. Fatigue resistance of two implant/abutment joint designs. *J Prosthet Dent* 2002; 88:604–610.

42. Sutter F, Weber HP, Sorenson J, Belser U. The new restorative concept of the ITI dental implant system: Design and engineering. *Int J Periodontics Restorative Dent* 1993; 13: 409–431.
43. Frost HM. Perspectives: bone's mechanical usage windows. *Bone Miner* 1992; 19: 257–271.
44. De Smet E, Jaecques SVN, Jansen JJ, Walboomers F, Vander Sloten J, Naert IE. Effect of constant strain rate, composed by varying amplitude and frequency, of early loading on peri-implant bone (re)modelling. *J Clin Periodontol* 2007; 34: 618–624.
45. Forwood MR, Turner CH. The response of rat tibiae to incremental bouts of mechanical loading: a quantum concept for bone formation. *Bone* 1994; 15: 603–609.
46. Hsieh YF, Turner CH. Effects of loading frequency on mechanically induced bone formation. *J Bone Miner Res* 2001; 16: 918–924.
47. Robling AG, Hinant FM, Burr DB, Turner CH. Improved bone structure and strength after long-term mechanical loading is greatest if loading is separated into short bouts. *J Bone Miner Res* 2002; 17: 1545–1554.
48. Rubin CT, McLeod KJ. Promotion of bony ingrowth by frequency-specific, low-amplitude mechanical strain. *Clin Orthop Relat Res* 1984; 298: 165–174.
49. Lanyon LE, Rubin CT. Static vs dynamic loads as an influence on bone remodelling. *J Biomech* 1984; 17: 897–905.
50. Robling AG, Duijvelaar KM, Geevers JV, Ohashi N, Turner CH. Modulation of appositional and longitudinal bone growth the rat ulna by applied static and dynamic force. *Bone* 2001; 29: 105–113.

51. Turner CH. Three rules for bone adaptation to mechanical stimuli. *Bone* 1998; 23:399–407.
52. Maeda Y, Satoh T, Sogo M. In vitro differences of stress concentrations for internal and external hex implant–abutment connections: a short communication. *J Oral Rehabil* 2006; 33: 75–78.
53. Cehreli MC, Akkocaoglu M, Comert A, Tekdemir I, Akca K. Human ex vivo bone tissue strains around natural teeth vs. immediate oral implants. *Clin Oral Implants Res* 2005; 16: 540–548.
54. Claes LE, Heigele CA, Neidlinger-Wilke C, Kaspar D, Seidl W, Margevicius KJ, Augat P. Effects of mechanical factors on the fracture healing process. *Clin Orthop Relat Res* 1998; 355: 132–147.
55. Berglundh T, Abrahamsson I, Lang NP, Lindhe J. De novo alveolar bone formation adjacent to endosseous implants. *Clin Oral Implants Res* 2003; 14: 251–262.
56. Botticelli D, Berglundh T, Lindhe J. Hard-tissue alterations following immediate implant placement in extraction sites. *J Clin Periodontol* 2004; 31: 820–828.
57. Van Oosterwyck H, Duyck J, Vander Sloten J, Van der Perre G, De Cooman M, Puers R, Naert I. Patient-dependent FE modeling as a tool for biomechanical optimization of oral reconstruction. In: Middleton J, Jones ML, Shrive NG, Pande GN, ed. *Computer Methods in Biomechanics and Biomedical Engineering*. Amsterdam: Gordon and Breach Science Publishers, 2001; 3: 559–564.

5 CAPÍTULO 3

Este capítulo é constituído pelo artigo que avalia a influência da configuração em platform-switching nos diferentes protocolos de instalação e carregamento dos implantes:

Pessoa RS, Vaz LG, Marcantonio Jr E, Vander Sloten J, Duyck J, Jaecques SVN. Biomechanical evaluation of platform switching in different implant protocols – CT based 3D finite element analysis. Int J Oral Maxillofac Implants 2009; accepted for publication.

Biomechanical evaluation of platform switching in different implant protocols – CT based 3D finite element analysis

Roberto S. Pessoa, DDS, MS

Department of Diagnostic and Surgery, Division of Periodontics, São Paulo State University - UNESP, School of Dentistry at Araraquara, Brazil

Address:

UNESP - Faculdade de Odontologia
Departamento de Diagnóstico e Cirurgia
Rua Humaitá, 1680, Sala 218 - Cep: 14802-550
Araraquara, São Paulo – Brasil
Mobile: (55 34) 8845-6569
Fax: (55 16) 3301-6406
rspessoa@uol.com.br

Luis Geraldo Vaz, MS, PhD

Department of Dental Materials and Prosthesis, Division of Dental Materials, São Paulo State University - UNESP, School of Dentistry at Araraquara, Brazil

Elcio Marcantonio Júnior, DDS, MS, PhD

Department of Diagnostic and Surgery, Division of Periodontics, São Paulo State University - UNESP, School of Dentistry at Araraquara, Brazil

Jos Vander Sloten, MS, PhD

Division of Biomechanics and Engineering Design, K.U. Leuven, Leuven, Belgium

Joke Duyck, DDS, PhD

Department of Dentistry, Oral Pathology and Maxillo-Facial Surgery, BIOMAT Research Cluster, K.U. Leuven, Leuven, Belgium

Siegfried V. N. Jaecques, MS, PhD

Department of Dentistry, Oral Pathology and Maxillo-Facial Surgery, BIOMAT Research Cluster, K.U. Leuven, Leuven, Belgium

Running title: Influence of platform switching on the biomechanical behavior of implants.

Biomechanical evaluation of platform switching in different implant protocols – CT based 3D finite element analysis

ABSTRACT

Purpose: To evaluate the influence of the platform-switching on the biomechanical environment of implants in different protocols. **Materials and Methods:** A CT-based finite element model of an upper central incisor extraction socket was constructed containing a conical 13 mm external hex implant, with a 4.3 mm diameter shoulder. A 4.3 mm and a 3.8 mm diameter abutment models were then imported and aligned to the implant. The 4.3 mm abutment edge matched perfectly the edge of the implant shoulder, while the 3.8 mm abutment assumed a platform switching configuration. The immediately placed, immediately loaded and osseointegrated (i.e. conventional delayed loaded) protocols were simulated. An ANOVA was used to interpret the data for peak equivalent strain (EQV strain) in the bone, bone to implant relative displacement, peak Von Mises stress (EQV stress) in the abutment screw, and abutment gap. **Results:** Comparing the different abutment diameters in the same clinical situation, the differences in the values of the assessed results were minor. In addition, no statistically significant influence of the abutment diameter was seen on any of the evaluated biomechanical parameters, excepted for the bone to implant displacement, though in rather low percentage. Nevertheless, a slightly higher EQV stress in the abutment screw was seen in all cases for the 3.8 diameter abutment, although it was not statistically significant. **Conclusion:** Within the limitation of this finite element analysis it can be concluded that a circumferential horizontal mismatch of 0.5 mm does not have an important contribution on the biomechanical environment of implants. Also there seems to be no significant biomechanical drawback to the design rationale of reducing the abutment diameter to move the implant-abutment gap area away from the implant-bone interface.

Keywords: platform switching, immediate implant loading, immediate implant placement, finite element analysis.

INTRODUCTION

The replacement of lost teeth by dental implants has become a predictable treatment. Consequently, as implant osseointegration is more frequently achieved, higher emphasis is being placed on the esthetic outcomes of implant therapy.^{1,2} In order to have an implant-supported restoration in harmony and symmetry with the crown form of the adjacent natural teeth, as well as with that of the contra-lateral tooth, the position of the soft tissue margin at the facial aspect of the implant-supported crown is a primary concern. It will dictate the clinical crown length and cervical form of the implant-supported crown. In addition, the degree of interdental papillae fill is of particular interest, since its location and stability is another important criterion on the determination of esthetic results of the implant treatment.² Otherwise, the bone supporting level constitutes the base for the supra-crestal soft tissue. Consequently, periimplant bone loss may negatively influence the soft tissue topography, leading to recession or absence of papillae.^{3,4} Thus, periimplant crestal bone remodeling after implant exposure to the oral environment has been given increasing attention.

Several studies have been undertaken to explain such changes in crestal bone height. Some authors have attributed bone loss to the generation of a biologic width adjacent to the implant.^{5,6} Besides, many authors have demonstrated that the implant-abutment microgap of two stage implants is associated with bacterial contamination that determines the formation of the peri-implant chronic inflammatory infiltrate, and, consequently, the crestal bone resorption.⁶⁻⁹ Additionally, biomechanical aspects of the marginal bone

resorption have also been investigated.¹⁰⁻¹⁴ Duyck et al.,¹² in an experiment in rabbits' tibia, proved that the stress/strain concentration, as well as the bone to implant relative displacement, caused by an excessive dynamic loading, are capable to induce the marginal bone loss around well osseintegrated implants, without the presence of oral biofilm. Moreover, some characteristics of implant neck design were recognized to influence the periimplant bone remodeling.^{15,16}

In this way, considering the importance of the bone crest height preservation for the final esthetic outcomes of implant treatment, the usage of a smaller-diameter healing and prosthetic components on wider-diameter implants was introduced in the clinical practice, in an attempt to reduce or eliminate the periimplant bone loss.^{17,18} The Lazzara & Porter hypothesis as the biological rationale behind the so called "platform switching" concept is that the horizontally inward repositioning of the implant-abutment interface may expose more implant surface to which the connective tissue can attach and increase the distance between the implant-abutment microgap to the crestal bone, shifting the inflammatory cell infiltrate inward, therefore reducing bone resorption.¹⁸ The authors radiographically observed that many platform-switched restored implants exhibited reduced or no vertical loss in crestal bone height. In the same way, Guirado et al.¹⁹ reported a mean of 0.7 mm bone loss for a new implant design which incorporated the platform switching concept. Also, Capiello et al.,²⁰ in a prospective clinical study, showed a significantly lower bone loss for the platform-switched implants (mean, 0.95 ± 0.32 mm) compared with implants restored with a matching-diameter abutment (mean, 1.67 ± 0.37 mm), 12 months after loading. As a consequence, platform switching has been indicated as a suitable treatment modality for the

maintenance of peri-implant soft and hard tissue, not only for two-stage osseointegrated implants, but also in immediately loaded and immediately placed implant protocols.¹⁹⁻²¹ Furthermore, a biomechanical motivation for the usage of a narrow abutment in osseointegrated implants was proposed by Maeda and colleagues.²² The authors conclude, from a finite element analysis (FEA), that the platform switching configuration shifts the stress concentration away from the periimplant marginal bone, thus decreasing its bone-resorptive effect. However, such conclusion was based on a rather simplified finite element model. The authors themselves suggested that further FE studies are still necessary in order to evaluate the consequence on platform switched implants to the implant-abutment-bone complex.²² In addition, to our knowledge no studies were published yet on the effects of platform switching on the biomechanical environment of either immediately loaded or immediately placed implant protocols.

Therefore, the purpose of the current study is to evaluate the influence of platform switching on the strain in peri-implant bone, on the stress in the abutment screw and on the stability of implants and abutments in the immediately placed, immediately loaded and osseointegrated (i.e. conventional delayed loaded) implant protocols.

MATERIALS AND METHODS

The computer tomography (CT) based 3D solid model of an upper central incisor extraction socket was constructed by thresholding within an image-processing software (Mimics 9.11, Materialise, Haasrode, Belgium). The CT

images were taken from a dry maxilla, provided by the Department of Anatomy of the Faculty of Odontology at Araraquara (São Paulo State University, Brazil), by a Picker UltraZ CT scanner (Picker International Inc., Cleveland, Ohio, USA) with a gantry tilt of 0°, at 120 kV acceleration voltage and 1mA current. The data set consisted of contiguous slices with respect to the Z-axis and had a voxel size of 0.391 x 0.391 x 1.000 mm.

The CAD (computer-aided design) solid models of a conical 13 mm external hex implant, with a 4.3 mm diameter shoulder, abutments and abutment screw were provided by an implant producer (Neodent, Curitiba, Brazil). The implant model was imported in Mimics (Materialise, Haasrode, Belgium) and positioned 1 mm deep inside the extraction socket, in a central position, to a palatal direction.²³

After placing the implant in its proper position, the abutment screw model was imported and aligned to the implant. The threads of the abutment screw were edited in order to match perfectly the internal threads of the implant, improving the contact status in that region. No simplifications were made regarding its spiral characteristic. A 4.3 mm and a 3.8 mm abutment solid models, both with 10 mm height, were then imported and aligned to the implant and abutment screw, following the instructions from the implant producer. The 4.3 mm abutment edge matched perfectly the edge of the implant shoulder, while the 3.8 mm abutment assumed a platform switching configuration. The implant insertion hole in the extraction socket solid model was obtained by a Boolean subtraction.

Bone, implant, abutments and abutment screw models were meshed separately in MSC.Patran 2005r2 (MSC.Software, Gouda, The Netherlands)

(figure 1). The finite element models had the same bone, implant and abutment screw meshes and interfaces, for both abutment diameters.

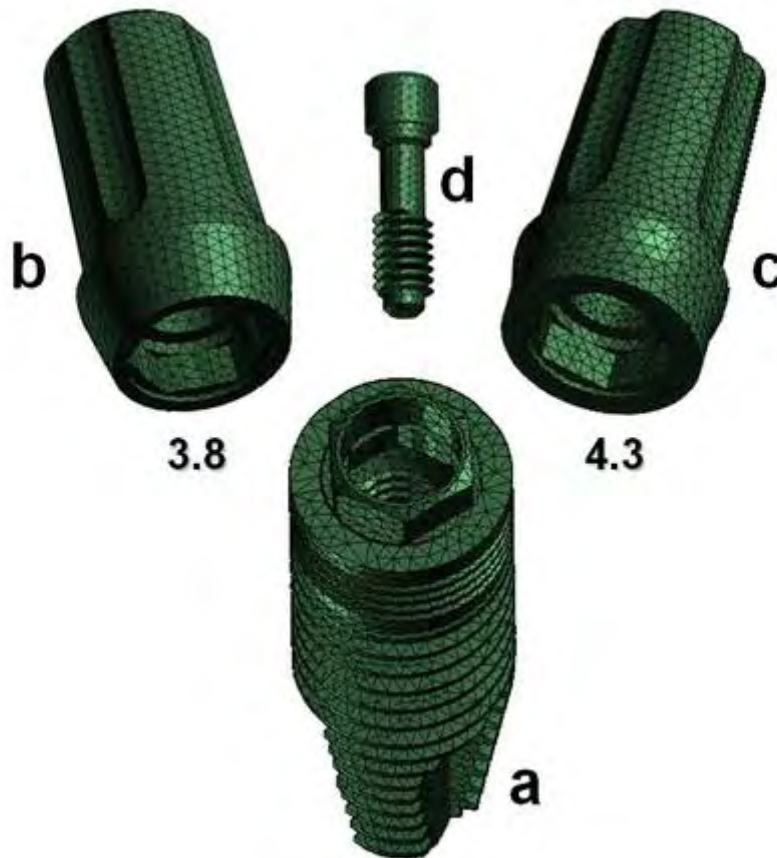


Figure 1: Three dimensional finite element models of (a) a conical 4.3 mm-diameter implant, (b) a 3.8mm-diameter abutment, (c) a 4.3 mm-diameter abutment and (d) an abutment screw.

In addition, a convergence study was accomplished in the bone mesh, to verify the influence of element size on the obtained results. The convergence was assumed to be achieved when the peak of von Mises stress (EQV stress) at the bone-implant edge did not vary more than 5%.²⁴ The number of elements did not exceed 150000, which would lead to unacceptable computational costs

with current hardware. Based on those criteria, 0.75 mm was found to be the optimal global element size.²⁵ Nevertheless, the smallest elements in the constructed tetrahedral meshes were about 50 μm in size. The different levels of mesh refinement were used for feature recognizing (i.e. threads).

The elastic properties of the bone mesh were assigned based on the grey values in the CT images.²⁶ By this procedure, the elements contained in cortical and trabecular bone tissue could be discriminated. The values of the Young's modulus and Poisson ratio for the materials used in the present study are summarized in table 1.²⁷

Table 1: Mechanical properties of bone, implant and prosthetic materials.

| Properties | Materials | | |
|---|------------------|----------------------|------------------------|
| | Titanium | Cortical Bone | Trabecular Bone |
| Young's modulus (E) – [MPa] | 110000 | 13700 | 1370 |
| Poisson ratio (ν) – [-] | 0.33 | 0.30 | 0.30 |

Frictional contact elements were used to simulate the bone to implant interface in the immediately placed and immediately loaded implant models, as well as the implant system component interfaces in contact, with a frictional coefficient μ of 0.3 and 0.5, respectively.^{24,28} In frictional contact interfaces, minor displacements without interpenetration between the model elements are allowed, providing a more realistic representation of the immediately loaded situations. In addition, in immediate loading models, the socket healing was simulated by modeling a hard tissue bridge at the alveolar ridge region.

Otherwise, for the implant osseointegration models, besides the socket healing modeling, the bone to implant interfaces were assumed to be glued.

Forces of 50N, 100N and 200N were applied on the top of the abutment central region, in a palato-buccal direction, with 40 degrees of inclination in relation to the alveolus longitudinal axis.^{29,30} Models were fully constrained in all directions at the nodes on mesial and distal borders.

A total of 18 models were accomplished by varying the abutment diameter (i.e. 3.8 and 4.3 mm), the clinical situation (i.e. immediately placed, immediately loaded and osseointegrated) and the loading magnitude (i.e. 50, 100 and 200 N). The analysis and post-processing were performed for each model by means of the MSC.MARC/Mentat 2005r3 software (MSC.Software, Gouda, NL). A general linear model Analysis of Variance (ANOVA, SAS/STAT statistical software, version 9.1, SAS Institute, Cary, NC, USA) was used to interpret the data for peak equivalent strain (EQV strain) in the bone, bone to implant relative displacement, peak Von Mises stress (EQV stress) in the abutment screw, and abutment gap.³¹

RESULTS

The data for EQV strain in the bone, bone to implant relative displacement, EQV stress in the abutment screw and abutment gap are presented in Table 2, for both the 3.8 and 4.3 diameter abutments for all the models. The ANOVA results on the relative contribution of the abutment diameter, clinical situation,

loading magnitude and their interactions on the evaluated parameters are shown in Tables 3-6.

The loading magnitude has a significantly high percentage contribution, regardless of the assessed result. The EQV strain in the bone and bone to implant displacement were also significantly influenced by the clinical situation (i.e. bone to implant interface condition and the presence of the extraction socket gap). In this respect, the immediately placed protocol showed the highest EQV strain in the bone and implant displacement, followed by the immediately loaded models. The osseointegrated models presented the lowest strain levels in the bone.

Comparing the different abutment diameters in the same clinical situation, the differences in the values of the assessed results were minor. In addition, no statistically significant influence of the abutment diameter was seen on any of the evaluated biomechanical parameters, excepted for the bone to implant displacement, though in rather low percentage. Nevertheless, a slightly higher EQV stress in the abutment screw was seen in all cases for the 3.8 diameter abutment. In addition, the largest influence of the abutment diameter was seen on the peak EQV stress in the abutment screw, although it was not statistically significant. The diameter of the abutment also does not significantly influence the abutment vertical gap. It is important to emphasize that the gap observed in the present study is a result of the abutment movement due to the loading. No pre-existing implant-abutment misfit was included in the models.

Table 2: Results for the peak equivalent strain (EQV strain) in the bone, peak equivalent stress (EQV stress) in the abutment screw, bone to implant relative displacement (displac.) and abutment gap, for all simulated models.

| Abutment diameter | Clinical situations | Loading | Bone EQV strain ($\mu\epsilon$) | Bone_implant displac. (μm) | Screw EQV Stress (MPa) | Gap (μm) |
|---------------------------------|----------------------------|----------------|---|---|-------------------------------|---------------------------------------|
| 4.3 | Immediately placed | 50N | 4,013.7 | 5.5 | 124.4 | 8.0 |
| | | 100N | 5,444.6 | 11.7 | 251.9 | 15.5 |
| | | 200N | 10,209.8 | 24.0 | 465.0 | 31.2 |
| | Immediately loaded | 50N | 1,519.9 | 2.8 | 115.2 | 7.7 |
| | | 100N | 2,639.5 | 3.6 | 226.9 | 15.2 |
| | | 200N | 5,172.1 | 7.6 | 443.0 | 29.5 |
| | Osseointegrated | 50N | 1,119.0 | ----- | 112.3 | 8.2 |
| | | 100N | 2,232.8 | ----- | 224.1 | 15.5 |
| | | 200N | 4,329.9 | ----- | 418.8 | 30.1 |
| 3.8 (platform switching) | Immediately placed | 50N | 3,014.0 | 5.8 | 134.7 | 6.9 |
| | | 100N | 5,347.9 | 11.9 | 253.5 | 11.5 |
| | | 200N | 9,719.4 | 24.3 | 510.9 | 22.6 |
| | Immediately loaded | 50N | 1,447.6 | 2.8 | 125.0 | 6.9 |
| | | 100N | 2,415.7 | 3.7 | 239.4 | 11.1 |
| | | 200N | 5,331.3 | 7.7 | 472.9 | 21.9 |
| | Osseointegrated | 50N | 1,203.0 | ----- | 197.6 | 6.0 |
| | | 100N | 2,662.6 | ----- | 229.4 | 12.0 |
| | | 200N | 4,564.9 | ----- | 451.9 | 22.3 |

Table 3: Analysis of Variance for the peak equivalent strain in the bone. $P < 0.05$, * statistically significant. DF: degrees of freedom; SS: sum of squares; MS: mean square.

| Parameter | DF | SS | MS | P-Value | Contribution (%) |
|--|----|-------------|-------------|---------|------------------|
| Abutment diameter | 1 | 52801.67 | 52801.67 | 0.2398 | 0.05 |
| Clinical Situation | 2 | 47081794.95 | 23540897.47 | <.0001* | 40.01 |
| Abutment diameter X Clinical Situation | 2 | 410854.64 | 205427.32 | 0.0452* | 0.35 |
| Loading Magnitude | 2 | 63662383.41 | 31831191.70 | <.0001* | 54.11 |
| Abutment diameter X Loading Magnitude | 2 | 113422.49 | 56711.24 | 0.2445 | 0.10 |
| Clinical Situation X Loading Magnitude | 4 | 6344406.86 | 1586101.72 | 0.0009* | 5.40 |

Table 4: Analysis of Variance for the relative displacement between implant and bone. $P < 0.05$, * statistically significant. DF: degrees of freedom; SS: sum of squares; MS: mean square.

| Parameter | DF | SS | MS | P-Value | Contribution (%) |
|--|----|--------|---------|---------|------------------|
| Abutment diameter | 1 | 0.08 | 0.08 | 0.0287* | 0.01 |
| Clinical Situation | 1 | 252.08 | 252.08 | <.0001* | 39.76 |
| Abutment diameter X Clinical Situation | 1 | 0.03 | 0.03 | 0.0742 | 0.005 |
| Loading Magnitude | 2 | 287.18 | 143.59 | <.0001* | 45.29 |
| Abutment diameter X Loading Magnitude | 2 | 0.0017 | 0.00083 | 0.7500 | 0.0003 |
| Clinical Situation X Loading Magnitude | 2 | 94.71 | 47.36 | <.0001* | 14.94 |

*Table 5: Analysis of Variance for the peak equivalent stress in the abutment screw. $P < 0.05$, * statistically significant. DF: degrees of freedom; SS: sum of squares; MS: mean square.*

| Parameter | DF | SS | MS | P-Value | Contribution (%) |
|--|-----------|-----------|-----------|----------------|-------------------------|
| Abutment diameter | 1 | 4.05 | 4.05 | 0.1080 | 1.09 |
| Clinical Situation | 2 | 1.59 | 0.79 | 0.4977 | 0.43 |
| Abutment diameter X Clinical Situation | 2 | 2.19 | 1.09 | 0.4032 | 0.59 |
| Loading Magnitude | 2 | 357.54 | 178.77 | 0.0001* | 95.84 |
| Abutment diameter X Loading Magnitude | 2 | 3.05 | 1.53 | 0.3079 | 0.82 |
| Clinical Situation X Loading Magnitude | 4 | 4.64 | 1.16 | 0.4261 | 1.24 |

*Table 6: Analysis of Variance for the abutment gap. $P < 0.05$, * statistically significant. DF: degrees of freedom; SS: sum of squares; MS: mean square.*

| Parameter | DF | SS | MS | P-Value | Contribution (%) |
|--|-----------|-----------|-----------|----------------|-------------------------|
| Abutment diameter | 1 | 8.96 | 8.96 | 0.6705 | 0.90 |
| Clinical Situation | 2 | 81.36 | 40.68 | 0.4584 | 8.24 |
| Abutment diameter X Clinical Situation | 2 | 78.74 | 39.37 | 0.4681 | 7.97 |
| Loading Magnitude | 2 | 633.78 | 316.89 | 0.0450* | 64.16 |
| Abutment diameter X Loading Magnitude | 2 | 17.77 | 8.88 | 0.8202 | 1.80 |
| Clinical Situation X Loading Magnitude | 4 | 167.16 | 41.79 | 0.5076 | 16.92 |

Figure 2 shows the EQV strain state in the bone, for both the 3.8 and 4.3 mm diameter abutments, in immediately placed, immediately loaded and osseointegrated protocols. The scale was set to range between 100-4000 $\mu\epsilon$.³² Strain distribution seemed to be very similar between both platform switching and matching-diameter abutment configurations, independently of the simulated protocol. Comparing the clinical situations, the strains were more concentrated in the buccal aspect of the implant-bone interface for the immediately placed and immediately loaded implant, while the strain was more evenly distributed in osseointegrated models.

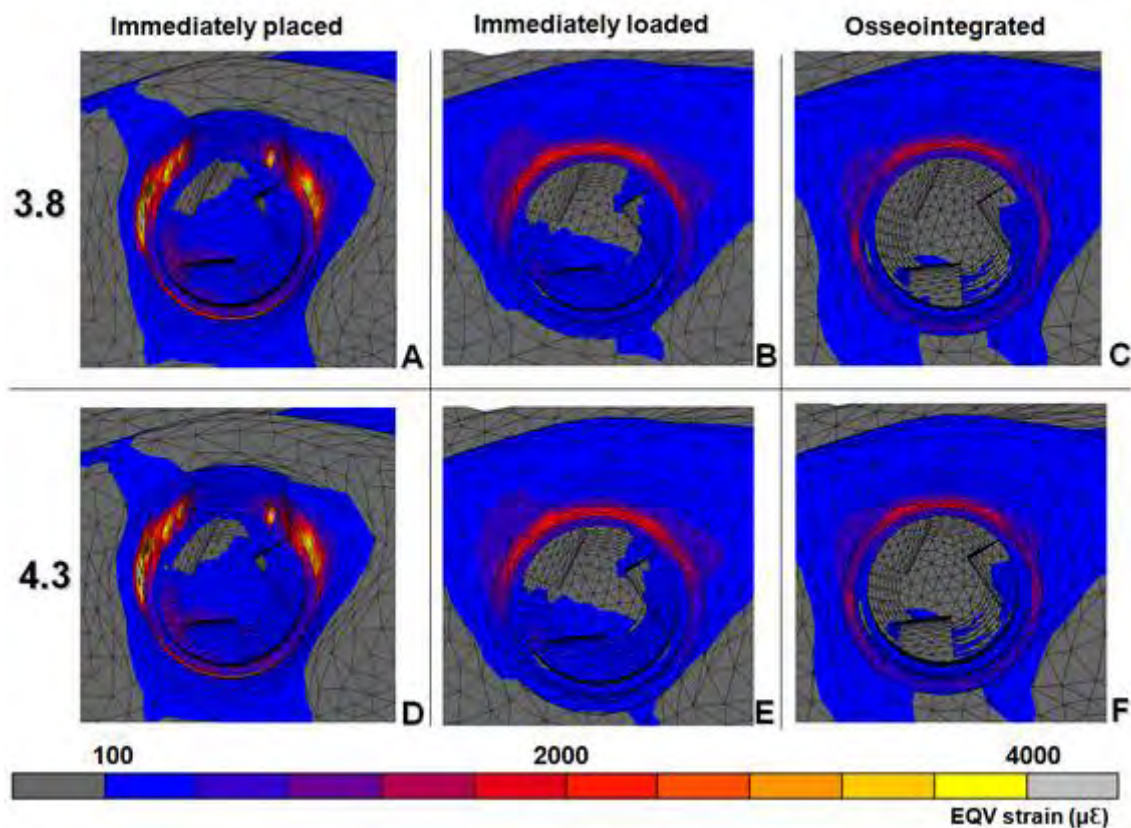


Figure 2: Occlusal view of EQV strain ($\mu\epsilon$) distribution in bone for the 3.8 mm diameter abutment (A-C) and 4.3 mm diameter abutment (D-F) 100N models.

The EQV stress on the abutment and implant surfaces is evident in figure 3. It can be noted that the 3.8 mm diameter abutment induced a higher stress concentration in the implant abutment mating area, though slightly more distant from the implant border than the 4.3 diameter abutment. In this way, a comparable stress distribution and intensity were seen on the implant neck surface for both abutment diameters.

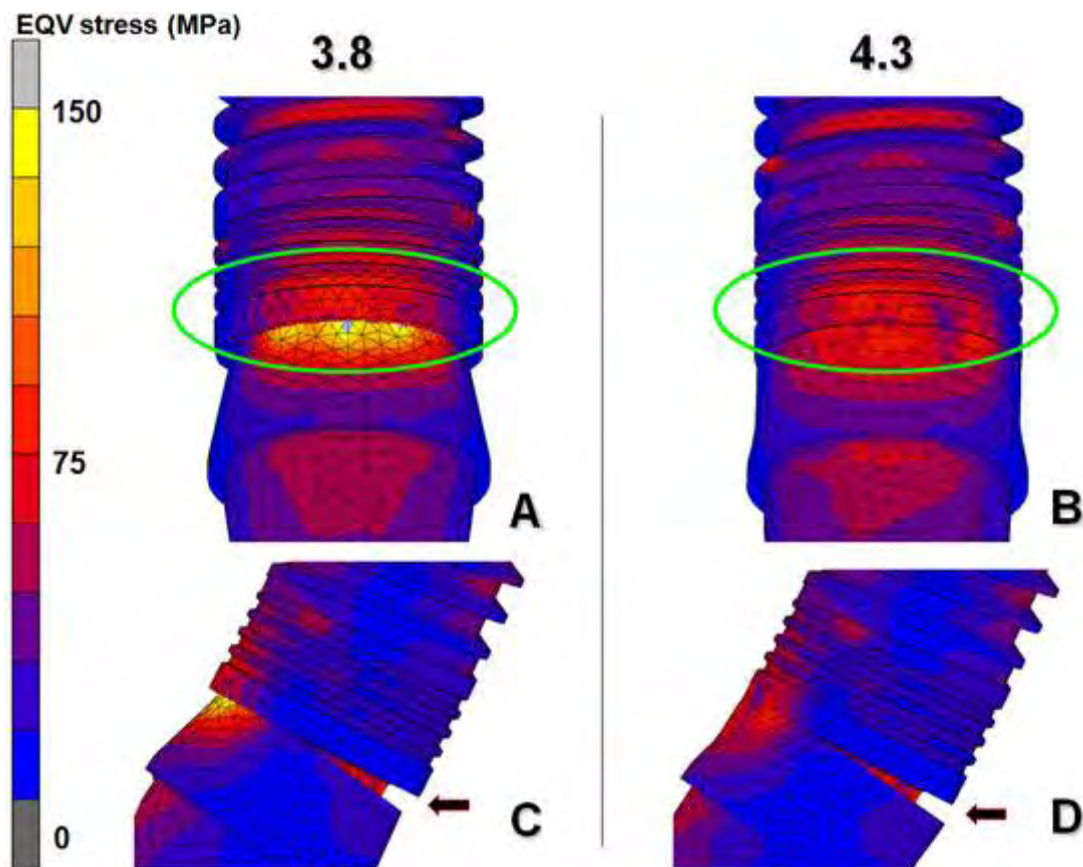


Figure 3: EQV stress (MPa) on the implant/abutment surfaces (A-B: frontal view, C-D: lateral view). The deformation is 50-fold magnified for visualization. Note the implant-abutment mating area (green ellipses) and the abutment gap due to the loading (black arrows).

The von Mises stress (EQV stress) distribution in the implant-abutment connection is shown in a bucco-palatal mesial plane in figure 4. In this plane of view, it is obvious that the stress distribution in the implant, near the implant neck surface, does not significantly differ between the 3.8 and 4.3 mm abutment diameters. The EQV stress distribution in the abutment screw was also similar for both abutment diameters, although a slightly higher stress concentration was encountered in the abutment screw of the platform switching configuration.

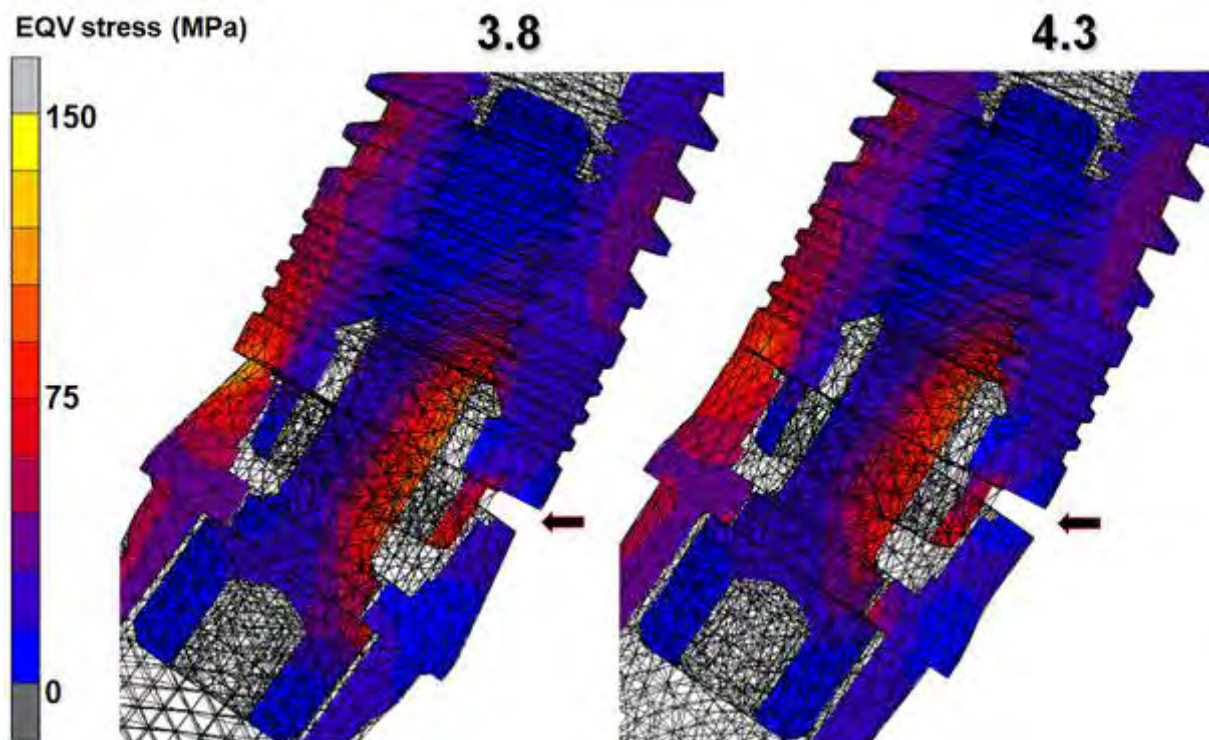


Figure 4: EQV stress (MPa) distribution inside implant connections. The deformation is 50-fold magnified for visualization. Note the abutment gap due to the loading (black arrows).

DISCUSSION

The present study focused on the biomechanical effects of a horizontal inward re-positioning of the implant–abutment interface, commonly termed platform switching, in the immediately placed, immediately loaded and osseointegrated (i.e. conventional delayed loaded) implant protocols. It was observed that, regardless of the implant protocol simulated, a circumferential horizontal mismatch of 0.5 mm does not have an important contribution on any of the assessed parameters (i.e. the strain in the bone, bone to implant displacement, stress in the abutment screw and abutment gap). From a biomechanical point of view, careful control of the functional loading and an adequate intra-osseous stability are the most important factors to the implant survival and long-term success.³³⁻³⁸

The current study evidenced a higher stress concentration in the implant-abutment mating area for the 3.8 abutment. This difference may be explained by the reduced surface area for the load transmission in the platform switching configuration. Conversely, a wider-diameter abutment results in a larger area for load dispersion and hence lower stress concentration. In the same way, Maeda et al.,³⁹ in an *in vitro* study, found a larger amount of strain at the implant cervical area in the external than in the internal hex connection. The authors argued that such difference can be explained by the difference in surface area between the connections. These findings are also in accordance with Huang et al.⁴⁰ Comparing different implant designs in a FEA, these authors demonstrated that a reduction in the implant diameter raised the stress at the surrounding bone due to a reduction of bone to implant contact areas.

On the other hand, as the distance for the stress transmission to the implant edge is larger for the platform-switching configuration, similar stress magnitudes were encountered on the implant cervical surface for both abutment diameters. Consequently, the values and distributions of EQV strain in the bone were similar for both the platform switching (3.8) and the matching-diameter (4.3) abutments, in the present FEA. In addition, even the minor variation in the strain values in the bone cannot be attributed to the differences in abutment diameter, as no significant contribution was found for it in the statistical analysis. These results are in contrast to the findings previously reported by Maeda et al.²² These authors found, in a 3D FEA model of osseointegrated implants, higher strain energy in the cortical bone surface for the matching-diameter model. However, those results were obtained in quite simplified models, not considering in detail the internal geometry of the implant-abutment connection. This geometry is recognized as a key factor associated with the pattern and magnitude of the stresses.^{25,41,42} Also the frictional non-linear contact relationship between the implant-abutment components was ignored in models of Maeda et al.²² Other published finite element studies have demonstrated that not only the level of stresses and strains, but also the stress and strain distribution are strongly affected by the interface conditions.^{24,42-45} Contact and friction have essential roles in the mechanical behavior of the implant-abutment complex and are especially necessary in the simulation of the external hex connection designs.²⁸ The contact interfaces in the finite element models transfer pressure and tangential frictional forces, but not tension, allowing the movement between the parts of the models in contact.⁴⁶ Merz et al.²⁸ demonstrated that when the loading is applied over the abutment in an external

hex configuration, there is no positive or geometric locking. In this way, under specific loading conditions, such as lateral or oblique loading, the abutment separates from the implant and tends to tilt about a small area on the implant shoulder.^{25,28} Hence, perfect bonding or connection between an implant and an abutment, as used by Maeda et al.,²² is not the actual scenario for correct simulation of an implant-abutment complex.²⁸ The 0.5 mm reduced-diameter abutment, however, does not significantly influence the implant-abutment misfit due to the loading. In the present FEA, no statistically significant difference was found for the abutment gap parameter.

Finally, in the current study, the significance of the relative effects of varying the abutment diameter on the mechanical response of the bone and implant components was assessed by a statistical analysis. The application of statistical analysis techniques to FEA results has been proven essential for the accurate evaluation of the relative contribution that each input variable (i.e. loading magnitude, clinical situation, abutment diameter) has on the results calculated in models.^{25,31,47,48} Not using such an approach may lead to an incorrect interpretation of FEA results.

Regarding the immediately loading protocols, one of the main causes that prevent implant osseointegration is an unstable bone to implant interface. A relative implant to bone displacement beyond 150 μm may induce fibrous encapsulation of the implant.^{35,44,45,49} On the other hand, Vandamme et al.,⁵⁰ in a bone chamber study, demonstrated that an implant displacement between 30 and 90 μm positively influenced osseointegration, stimulating bone formation, compared with no implant displacement. Although the direct comparison of the current FEA with the studies cited above is not possible, the highest

displacement found in the models (24.3 μm) was within the acceptable limits for an uneventful implant osseointegration. In the current study, the differences in the bone to implant relative displacement between the 3.8 and 4.3 mm abutments were negligible, as they were smaller than 0.3 μm .

The present FEA found the highest influence of varying abutment diameters on the peak EQV stress in the abutment screw. A slightly higher stress concentration was always seen for the platform-switching models. Nevertheless, these differences were not statistically significant. In an external hex configuration, the lateral loading is resisted mainly by the abutment screw.^{25,28} Only a very small amount of the stress is absorbed by the connection. In this way, a small influence of varying the abutment diameter on this parameter could indeed be expected.

The concept of platform-switching, as introduced by Lazzara & Porter,¹⁸ is based on the hypothesis that a narrower abutment can increase the distance between the implant-abutment microgap contamination and the crestal bone, thus reducing bone resorption. However, although the effects of the biological aspects (i.e. the formation of a biological width, implant-abutment gap bacterial contamination) should not be ignored, these factors alone are not sufficient to entirely explain the crestal bone remodeling. Shin et al.,¹⁵ comparing different implant neck designs in a randomized clinical study, found the greatest amount of bone loss (1.32 ± 0.27 mm) for the group with platform-switching abutment and a machined neck. The smallest amount of bone loss (0.18 ± 0.16 mm) was found for the group with matching diameter abutment and a rough-surfaced microthreaded implant neck. Hence, when planning an implant treatment to achieve an optimized functional/esthetic outcome, it is important to consider all

the possible factors that may exert an influence within the implant neck region such as, the presence of threads, surface roughness and the implant-abutment connection type.^{6,14,15,25,51} Moreover, the conclusions in some studies, in which less bone loss was observed for the platform-switching configuration, were made by comparing different implant diameters with different characteristics of implant neck designs.^{18,20} As it was actually the implant design and not only the abutment diameter that varied, it is somewhat difficult to determine which factor had the highest contribution to the observed results. In this way, the answer to the question of whether the platform-switching configuration has some beneficial influence on the periimplant bone remodeling can only be answered definitively by a randomized controlled clinical trial, in which the very same implant design should be used.

In the present study, the biomechanical effects of the platform-switching were studied by FEA. The FE method has generally been accepted as a complementary tool in dental implant biomechanics, to obtain information that is difficult to acquire from laboratory experiments or clinical studies.^{27,46} However, the assumptions made during the process of developing a finite element model, principally regarding the material properties and the interface conditions, limit the analyses of the absolute values of the stress/strain and displacement calculated in a model in which an experimental validation was not accomplished. On the other hand, the association of the FEA with a statistical analysis has been demonstrated as capable to accurately interpreting the relative influence that each of the input parameters (i.e. loading magnitude, clinical situation, abutment diameter) have on the encountered results.^{31,47,48} In this way, the present study focused only on the relative effects of a 0.5 mm

abutment mismatch. Furthermore, it must be emphasized that the modeling of bone adaptive processes was not one of the purposes in the present FEA. Although some authors considered 2,000-4,000 μ strain as a possible strain range stimulating the bone formation and beyond 4,000 μ strain as a possible threshold for pathological bone overload, also loading frequency and number of loading cycles can greatly influence the bone adaptive reaction.^{12,32,52} In addition, bone responds to dynamic rather than to static loads,¹² as they were applied in the current study.

By the current FEA, it was possible to improve the understanding of the detailed mechanical responses to a platform-switching in an external-hex connection. However, the results in the present study should be interpreted with some care. Other scenarios of platform-switching, such as, different sizes of abutment mismatch, platform-switching with a different size of implant shoulder, platform-switching in different implant-abutment connections, platform-switching in multiple implant protocols, could also affect the biomechanical environment of implants and should also be subject of investigations.

CONCLUSION

Within the limitation of this FEA, it could be demonstrated that although a better stress distribution could not be demonstrated in the platform-switching configuration, also there seems to be no significant biomechanical drawback to the design rationale of reducing the abutment diameter to move the implant-abutment gap area away from the implant-bone interface. In this way, from a

biomechanical point of view, platform switching design can be considered a valid treatment option, equivalent to conventional matching diameters designs.

ACKNOWLEDGEMENTS

The authors thank Luiza Muraru for the assistance with the FE modeling and the Neodent® implant system for providing the implant CAD models. Dr. S. Fieufs from the Leuven Biostatistics and Statistical Bioinformatics Centre (L-BioStat) is acknowledged for the factorial design optimization and ANOVA analyses. Roberto Pessoa gratefully thanks the grants and scholarships from: FAPESP (Research Support Foundation of São Paulo State) project 2006/06844-2, CAPES (Committee for Postgraduate Courses in Higher Education) and CNPq (National Council for Scientific and Technological Development). Siegfried Jaecques gratefully acknowledges funding from the K.U.Leuven research fund (project OT/06/58). The CT-based FEM methods are based on research funded by the EU Framework Programme 5 Quality of Life project QLK6-CT-2002-02442 IMLOAD.

REFERENCES

1. Chang M, Wennström JL, Ödman P, Andersson B. Implant supported single-tooth replacements compared to contralateral natural teeth. Crown and soft tissue dimensions. *Clin Oral Impl Res* 1999;10:185-194.
2. El Askary AS. Multifaceted aspects of implant esthetics: The anterior maxilla. *Implant Dent* 2001;10:182-191.

3. Bengazi F, Wennstrom J, Lekholm U. Recession of the soft tissue margin at oral implants. A 2-year longitudinal prospective study. *Clin Oral Impl Res* 1996;7:303–310.
4. Tarnow DP, Cho SC, Wallace SS. The effect of inter-implant distance on the height of inter-implant bone crest. *J Periodontol* 2000;71:546-549.
5. Berglundh T, Lindhe J. Dimension of the periimplant mucosa: Biological width revised. *J Clin Periodontol* 1996;23:971-973.
6. Hermann JS, Buser D, Schenk RK, Cochran DL. Crestal bone changes around titanium implants. A histometric evaluation of unloaded nonsubmerged and submerged implants in the canine mandible. *J Periodontol* 2000;71:1412–1424.
7. Hermann JS, Cochran DS, Nummikoski PV, Buser D, Schenk RK, Cochran DL. Crestal bone changes around titanium implants: a radiographic evaluation unloaded submerged and nonsubmerged and submerged implants in the canine mandible. *J Periodontol* 1997;68:1117-1130.
8. Hermann JS, Schoolfield JD, Nummikoski PV, Buser D, Schenk RK; Cochran DL. Crestal bone changes around titanium implants. A methodological study comparing linear radiographic versus histometric measurements. *Int J Oral Maxillofac Implants* 2001;16:475-85.
9. King GN, Hermann JS, Schoolfield JD, Buser D; Cochran DL. Influence of the size of the microgap on crestal bone levels in non-submerged dental implants: a radiographic study in the canine mandible. *J Periodontol* 2002;73,1111–1117.

10. Oh TJ, Yoon JK, Mish CE, Wang HL. The causes of early implant bone loss: Myth or science? *J Periodontol* 2002;73:322-333.
11. Tawil G. Peri-implant bone loss caused by occlusal overload: repair of the peri-implant defect following correction of the traumatic occlusion. A case report. *Int J Oral Maxillofac Implants* 2008;23:153-7.
12. Duyck J, Ronald HJ, Van Oosterwyck H, Naert I, Vander Sloten J, Ellingsen JE. The influence of static and dynamic loading on marginal bone reactions around osseointegrated implants: an animal experimental study. *Clin Oral Implants Res* 2001;12: 207-218.
13. Schwarz F, Herten M, Bieling K, Becker J. Crestal bone changes at non-submerged implants (Camlog) with different machined collar lengths. A histomorphometrical pilot study in dogs. *Int J Oral and Maxillofac Implants* 2007;(in press).
14. Zechner W, Trinkl N, Watzak G, Busenlechner D, Tepper G, Haas R, Watzek G. Radiologic follow-up of periimplant bone loss around machine-surfaced and rough-surfaced interforaminal implants in the mandible functionally loaded for 3 to 7 years. *Int J Oral Maxillofac Implants* 2004;19:216–221.
15. Shin YK, Han CH, Heo SJ, Kim S, Chun HJ. Radiographic evaluation of marginal bone level around implants with different neck designs after 1 year. *Int J Oral Maxillofac Implants* 2006;20:789-794.
16. Palmer RM, Palmer PJ, Smith BJ. A 5-year prospective study of Astra single tooth implants. *Clin Oral Implants Res* 2000;11:179–182.
17. Gardner DM. Platform switching as a means to achieving implant esthetics. *NY State Dent J* 2005;71:34-37.

18. Lazzara RJ, Porter SS. Platform switching: A new concept in implant dentistry for controlling postrestorative crestal bone levels. *Int J Periodontics Restorative Dent* 2006;26:9–17.
19. Guirado JLC, Yuguero MRS, Zamora GP, Barrio EM. Immediate Provisionalization on a New Implant Design for Esthetic Restoration and Preserving Crestal Bone. *Implant Dent* 2007;16:155–164.
20. Cappiello M, Luongo R, Di Iorion D, Bugea C, Cochotto R, Celletti R. Evaluation of peri-implant bone loss around platform-switched implants. *Int J Periodontics Restorative Dent* 2008;28:347-355.
21. Canullo L, Rasperini G. Preservation of Peri-implant Soft and Hard Tissues Using Platform Switching of Implants Placed in Immediate Extraction Sockets: A Proof-of-concept Study with 12- to 36-month Follow-up. *Int J Oral Maxillofac Implants* 2007;22:995–1000.
22. Maeda Y, Miura J, Taki I, Sogo M. Biomechanical analysis on platform switching: is there any biomechanical rationale? *Clin Oral Implants Res* 2007;18:581-4.
23. Quirynen M, Van Assche N, Botticelli D, Berglundh T. How does the timing of implant placement to extraction affect outcome? *Int J Oral Maxillofac Implants* 2007;22(Suppl):203-23.
24. Huang HL, Hsu JT, Fuh LJ, Tu MG, Ko CC, Shen YW. Bone stress and interfacial sliding analysis of implant designs on an immediately loaded maxillary implant: A non-linear finite element study. *J Dent* 2008;36:409-417.
25. Pessoa RS, Muraru L, Marcantonio Jr E, Vaz LG, Vander Sloten J, Duyck J, Jaecques S. Influence of implant connection type on the biomechanical

environment of immediately placed implants – CT-based nonlinear, 3D finite element analysis. *Clin Implant Dent Relat Res* 2009; accepted for publication.

26. Jaecques SVN, Van Oosterwyck H, Muraru L, Van Cleynenbreugel T, De Smet E, Wevers M, Naert I, Vander Sloten J. Individualised, micro CT-based finite element modelling as a tool for biomechanical analysis related to tissue engineering of bone. *Biomaterials* 2004;25:1683-1696.
27. Geng JP, Tan KB, Liu GR. Application of finite element analysis in implant dentistry: a review of the literature. *J Prosthet Dent* 2001;85:585-98.
28. Merz BR, Hunenbart S, Belser UC. Mechanics of the implant-abutment connection: an 8-degree taper compared to a butt joint connection. *Int J Oral Maxillofac Implants* 2000;15:519–526.
29. Duyck J, Van Oosterwyck H, Vander Sloten J, De Cooman M, Puers R, Naert I. Magnitude and distribution of occlusal forces on oral implants supporting fixed prostheses: an in vivo study. *Clin Oral Implant Res* 2000;11:465-475.
30. Duyck J, Van Oosterwyck H, De Cooman M, Puers R, Vander Sloten J, Naert I. Three-dimensional force measurements on oral implants: a methodological study. *J Oral Rehab* 2000;27:744-753.
31. Dar FH, Meakina JR, Aspden RM. Statistical methods in finite element analysis. *J Biomech* 2002;35:1155-1161.
32. Frost HM. Bone ‘mass’ and the ‘mechanostat’: a proposal. *Anat Rec* 1987;219:1-9.

33. Taylor TD, Agar JR, Vogiatzi T. Implant prosthodontics: Current perspective and future directions. *Int J Oral Maxillofac Implants* 2000;15:66–75.
34. Behneke A, Behneke N, d'Hoedt B. The longitudinal clinical effectiveness of ITI solid-screw implants in partially edentulous patients: a 5-year follow-up report. *Int J Oral Maxillofac Implants* 2000;15:633-645.
35. Geris L, Andreykiv A, Van Oosterwyck H, Vander Sloten J, van Keulen F, Duyck J, Naert I. Numerical simulation of tissue differentiation around loaded titanium implants in a bone chamber. *J Biomech* 2004;37:763-769.
36. Hoshaw SJ, Brunski JB, Cochran GVB. Mechanical loading of Brånemark implants affects interfacial bone modeling and remodeling. *Int J Oral Maxillofac Implants* 1994;9:345-360.
37. Isidor F. Loss of osseointegration caused by occlusal load of oral implants. A clinical and radiographic study in monkeys. *Clin Oral Implants Res* 1996;7:143-152.
38. Isidor F. Histological evaluation of periimplant bone at implants subjected to occlusal overload or plaque accumulation. *Clin Oral Implants Res* 1997;8:1-9.
39. Maeda Y, Satoh T, Sogo M. In vitro differences of stress concentrations for internal and external hex implant–abutment connections: a short communication. *J Oral Rehab* 2006;33:75–78.
40. Huang H-L, Chang C-H, Hsu J-T, Fallgatter MA, Ko C-C. Comparison of implant body designs and threads designs of dental implants: A 3-dimensional finite element analysis. *Int J Oral Maxillofac Implants* 2007;22:551-562.

41. Rieger MR, Mayberry M, Brose MO. Finite element analysis of six endosseous implants. *J Prosth Dent* 1990;63:671-676.
42. Siegele D, Soltesz U. Numerical investigations of the influence of implant shape on stress distribution in the jaw bone. *Int J Oral Maxillofac Implants* 1989;4:333-340.
43. Van Oosterwyck H, Duyck J, Vander Sloten J, Van der Perre G, De Cooman M, Lievens S, Puers R, Naert I. The influence of bone mechanical properties and implant fixation upon bone loading around oral implants. *Clin Oral Implants Res* 1998;9:407-418.
44. Brunski JB. Biomechanical factors affecting the bone-dental implant interface. *Clin Mater* 1992;10:153-201.
45. Brunski JB. In vivo response to biomechanical loading at the bone/dental-implant interface. *Adv Dent Res* 1999;13:99-119.
46. Wakabayashi N, Ona M, Suzuki T, Igarashi Y. Nonlinear finite element analyses: Advances and challenges in dental applications. *J Dent* 2008;36:463-471.
47. Lin C-L, Chang S-H, Chang W-J, Kuo Y-C. Factorial analysis of variables influencing mechanical characteristics of a single tooth implant placed in the maxilla using finite element analysis and the statistics-based Taguchi method. *Eur J Oral Sci* 2007;115:408-416.
48. Lin C-L, Wang J-C, Chang W-J. Biomechanical interactions in tooth-implant-supported fixed partial dentures with variations in the number of splinted teeth and connector type: a finite element analysis. *Clin Oral Implants Res* 2008;19:107-117. doi: 10.1111/j.1600-0501.2007.01363.x

49. Søballe K, Brockstedt-Rasmussen H, Hansen ES, Bünger C. Hydroxyapatite coating modifies implant membrane formation. Controlled micromotion studied in dogs. *Acta Orthop Scand* 1992;63:128-140.
50. Vandamme K, Naert I, Geris L, Vander Sloten J, Puers R, Duyck J. The effect of micromotion on the tissue response around immediately loaded roughened titanium implants in the rabbit. *Eur J Oral Sci* 2007;115:21-29.
51. Hermann F, Lerne H, Palti A. Factors influencing the preservation of the periimplant marginal bone. *Implant Dent* 2007;16:165-175.
52. De Smet E, Jaecques SVN, Jansen JJ, Walboomers F, Vander Sloten J, Naert IE. Effect of constant strain rate, composed by varying amplitude and frequency, of early loading on peri-implant bone (re)modelling. *J Clin Periodontol* 2007; 34: 618–624.

6 CAPÍTULO 4

Este capítulo é constituído pelo artigo que avalia a influência de diferentes designs de implantes nos protocolos de implantes imediatos, com carga imediata e osseointegrados:

Pessoa RS, Coelho PG, Muraru L, Marcantonio Jr E, Vaz LG, Vander Sloten J, Jaecques S. Influence of implant design on the biomechanical environment of immediately placed implants – CT-based nonlinear 3D finite element analysis. Clin Implant Dent Relat Res 2010; submitted for publication.

Influence of implant design on the biomechanical environment of immediately placed implants – CT-based nonlinear 3D finite element analysis

Roberto S Pessoa, DDS, MS, PhD

Department of Diagnostic and Surgery, Division of Periodontics, UNESP – São Paulo State University, Araraquara, Brazil

Address:

UNESP - Faculdade de Odontologia
Departamento de Diagnóstico e Cirurgia
Rua Humaitá, 1680, Sala 218 - Cep: 14802-550
Araraquara, São Paulo – Brasil
Fax: (55 16) 3301-6406
rp@inpes.com.br

Paulo G Coelho, DDS, MS, PhD

Department of Biomaterials and Biomimetics, New York University, New York, NY, USA

Luiza Muraru, MS, PhD

MOBILAB, Health Care and Chemistry Department University College Kempen Belgium

Elcio Marcantonio Júnior, DDS, MS, PhD

Department of Diagnostic and Surgery, Division of Periodontics, UNESP – São Paulo State University, Araraquara, Brazil

Luis Geraldo Vaz, MS, PhD

Department of Dental Materials and Prosthesis, Division of Dental Materials, UNESP – São Paulo State University, Araraquara, Brazil

Jos Vander Sloten, MS, PhD

Division of Biomechanics and Engineering Design (BMGO), K.U.Leuven, Leuven, Belgium

Siegfried V N Jaecques, MS, PhD

Leuven Medical Technology Centre (L-MTC) and Division of Biomechanics and Engineering Design (BMGO), Catholic University of Leuven (K.U.Leuven), Leuven, Belgium

Running title: Influence of implant design on the biomechanical behavior of implants.

Keywords: immediate implant loading, immediate implant placement, finite element analysis.

Influence of implant design on the biomechanical environment of immediately placed implants – CT-based nonlinear 3D finite element analysis

ABSTRACT

Purpose: To evaluate the influence of different implant designs on the biomechanical environment of immediately placed implants. **Materials and Methods:** A CT-based finite element model of an upper central incisor extraction socket was constructed containing four commercially available implant designs (SIN SW®, 3i Certain®, Nobel Replace™ and RN synOcta® ITI Standard). The diameters and heights of implants were selected to be comparable in size. All the implants have internal connection. The immediately placed, immediately loaded and osseointegrated (i.e. conventional delayed loaded) protocols were simulated. An ANOVA was used to interpret the data for peak equivalent strain (EQV strain) in the bone and bone to implant relative displacement. **Results:** The implant design has a statistically significant contribution to the strains and displacements in the immediately placed protocol. The loading magnitude (77.6%) and the clinical situation (15.0%) (i.e. the presence or absence of an extraction socket defect, the condition of the bone to implant interface) had the highest relative contribution to the results. The highest effect of varying the implant design was seen for immediately placed and immediately loaded protocols. The implant design does not considerably affect the strain values and distributions of osseointegrated implants. **Conclusion:** Within the limitations of this finite element analysis it can be concluded that implant design significantly influences the biomechanical environment of immediately placed implants. However, avoiding implant overloading and ensuring a high implant initial stability are the most important factors for the predictability of this protocol.

Keywords: platform switching, immediate implant loading, immediate implant placement, finite element analysis.

INTRODUCTION

In the conventional delayed loading implant protocol a certain period of undisturbed healing is suggested for an uneventful implant osseointegration (Brånemark et al. 1977, Adell et al. 1981, Albrektsson et al. 1986). Although this approach has been proved to be a highly predictable and successful treatment modality (Palmer et al. 2000, Berglundh et al. 2002, Wennstrom et al. 2005), the extended treatment period is an important inconvenience for certain patients for whom the prompt replacement of the lost teeth, especially in anterior regions, has a high priority. In this way, a tendency is observed towards immediate loading protocols, in which a significant reduction in time between tooth extraction and patient rehabilitation can be provided.

Despite the promising results recently reported by experimental and clinical studies for these loading protocols (De Smet et al. 2006; Duyck et al. 2007; Vandamme et al. 2008, Testori et al. 2004, Donati et al. 2008), failures can still occur and may be related to biomechanical factors. Adverse forces over the implant-supported prostheses can induce micromovements beyond 150 μm leading to the implant fiber encapsulation instead of the osseointegration (Søballe et al. 1992, Brunski 1992, 1993, Geris et al. 2004). Consequently, for healing implants it is recommended to ensure a high initial intraosseous stability and a safe biomechanical environment. Even for well osseointegrated implants, excessive loads may be the etiology for periimplant bone loss, eventually causing the implant failure (Isidor 1996, 1997, Hoshaw et al. 1994). Strains exceeding the physiological tolerance threshold of bone around the implant

(above 3000 $\mu\epsilon$) may cause microdamage accumulation and induce bone resorption (Frost 1987, Duyck et al. 2001).

Several factors are recognized to influence the implant to bone loading transmission, such as: bone quality in the insertion area, the nature of the bone-implant interface, the materials' properties of the implants and prosthesis, the surface roughness of the implant material, the occlusal condition (i.e., magnitude, direction and frequency of the loading), and the design of the implant (Bozkaya et al. 2004, De Smet et al. 2007, Vandamme et al. 2007, Pessoa et al. 2009a, Misch et al. 2005). It is, therefore, essential for the predictability of implant protocols to develop implant designs capable of providing some degree of stability, under masticatory standard loading (Hansson 1999).

In this way, attempts have been made to understand the biomechanical effect induced by different implant macro-designs (i.e., shape, presence or absence of thread, thread design) on the periimplant bone. Classic studies emphasized that bone stress distribution and magnitudes considerably vary with implant shape. Siegele and Soltesz (1989) compared cylindrical, conical, stepped, screw-shaped and hollow cylindrical implant design by means of Finite Element Analysis (FEA). The authors demonstrated that implant geometries with very small radii of curvature (conical) or discontinuities (stepped) induce higher peak stress than smoother shapes (cylindrical, screw-shaped). Holmgren et al. (1998) suggested, by applying an oblique load to implants in a FEA, that the stepped implant design exhibits a more even stress pattern than a straight cylindrical design. More recently, Huang et al. (2008) conclude by a FEA, that a tapered implant design can reduce the peak stress in cortical and trabecular

bone. They also stated that threaded implants dissipate the interfacial stresses more evenly than non-threaded implants. Moreover, threads are believed to enhance implant initial stability, enlarge implant surface area thus increasing bone to implant contact and better dissipate the interfacial stresses (Hansson & Werke 2003, Brunski 1988). Geometric parameters of threads such as depth, thickness, pitch, face angle and helix angle determine the threads function and biomechanical efficiency (Strong et al. 1998).

The influence of these implant design characteristics has been mainly investigated in the delayed loading protocol. Only a few studies can be found for the immediate loading approaches (Huang et al. 2008, Fazel et al. 2009, Ding et al. 2008). Moreover, insufficient data are available on many outcome parameters for implants immediately loaded into extraction sockets (Quirynen et al. 2007). In previous studies, we investigated the influence of implant-abutment connection type and platform-switching on the biomechanical environment of immediately placed implants (Pessoa et al. 2009 a,b). These FEA showed that although a Morse-taper connection provided the best abutment stability and the lowest von Mises stress in the abutment screw compared with the internal hex and external hex connections, different abutment connections or platform-switching do not significantly influence the bone to implant relative displacement and peak strain in periimplant bone of implants immediately loaded in extraction sockets. On the other hand, the effects of varying implant designs on immediate implant loading protocols have not been studied comprehensively.

Therefore, the objective of the present study is to evaluate the influence of different implant designs on the bone to implant relative displacement and peak strain in periimplant bone of immediately placed and loaded implants.

MATERIALS AND METHODS

A detailed description of the methods applied to obtain the individualized finite element models used in the present study can be found elsewhere (Pessoa et al. 2009 a, b). The computer tomography (CT) of an upper central incisor extraction socket, taken from a dry maxilla provided by the Department of Anatomy of the Faculty of Odontology at Araraquara (São Paulo State University, Brazil) were reconstructed in a 3D solid model by thresholding within an image-processing software (Mimics 9.11, Materialise, Haasrode, Belgium).

The implants and prosthetic components CAD (computer-aided design) solid models were obtained by reverse-engineering to resemble the commercially available Ø 4.5 x 13 mm SIN SW® (SIN Sistema de Implante, São Paulo, Brazil), Ø 4.1 x 13 mm 3i Certain® (3i, Palm Beach Gardens, USA), Ø 4.3 x 13 mm Nobel Replace™ (Nobel Biocare AB, Göteborg, Sweden), and Ø 4.1 x 12 mm RN synOcta® ITI Standard (Institut Straumann AG, Basel, Switzerland). The diameters and heights of implants were selected to be comparable in size and all the implants had internal connections. The implants were imported in Mimics (Materialise, Haasrode, Belgium) and positioned 1 mm deep inside the extraction socket, in a central position and a palatal direction (Quirynen et al. 2007). The abutment and abutment screw models were afterward aligned to the implants following the instructions from the implant producer. All the abutments had 10 mm height from the implant shoulder. The implant insertion hole in the extraction socket solid model was obtained by means of Boolean subtraction.

Bone, implant, abutments and abutment screw meshes were meshed separately in MSC.Patran 2005r2 (MSC.Software, Gouda, The Netherlands) (figure 1). No simplifications were made regarding the implant systems macro-geometry (i.e. truly spiral threads). In addition, the bone mesh was tested for convergence (Pessoa et al. 2009 a,b). The smallest elements in the constructed tetrahedral meshes were about 50 μm in size. The different levels of mesh refinement were used for feature recognizing (e.g. at the threads).

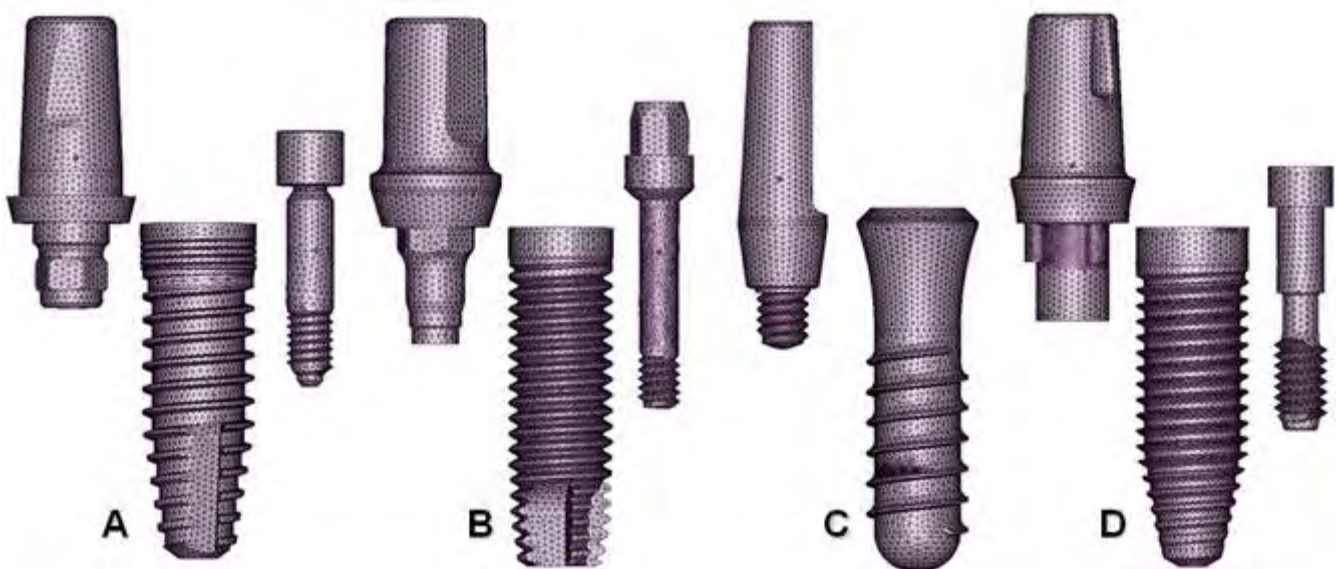


Figure 1: Implants, abutments and abutment screws meshes. A: SIN SW, B: 3i Certain, C: ITI Standard, D: Nobel Replace.

The gray values of the CT images were used to assign the material properties of the elements contained in cortical and trabecular bone (Jaecques et al. 2004). The values of the Young's modulus and Poisson ratio for the materials used in the present study are summarized in table 1 (Geng et al. 2001).

Frictional contact elements, with a frictional coefficient μ of 0.3 and 0.5 respectively were used to simulate the bone to implant interface in the immediately placed and immediately loaded implant models, as well as the implant system component interfaces in contact (Huang et al. 2008, Merz et al. 2000). In addition, the socket healing was simulated in the immediate loading and osseointegrated models by modeling a hard tissue bridge at the alveolar ridge region. Moreover, for the implant osseointegration models the bone to implant interface was assumed to be glued.

Table 1: Mechanical properties of bone, implant and prosthetic materials.

| Properties | Materials | | |
|---|------------------|----------------------|------------------------|
| | Titanium | Cortical Bone | Trabecular Bone |
| Young's modulus (E) – [MPa] | 110000 | 13700 | 1370 |
| Poisson ratio (ν) – [-] | 0.33 | 0.30 | 0.30 |

In three load cases, forces of 50N, 100N and 200N were applied with 40 degrees of inclination in relation to the alveolus longitudinal axis, in a palato-buccal direction, on the top of the abutment central region. Models were fully constrained in all directions at the nodes on the mesial and distal borders.

The FE model analysis and post-processing were accomplished by means of the MSC.MARC/Mentat 2005r3 software (MSC.Software, Gouda, NL). The results from the 36 models for the peak equivalent strain (EQV strain) in the bone and the bone to implant relative displacement were interpreted by means of a general linear model Analysis of Variance (ANOVA, SAS/STAT statistical software, version 9.1, SAS Institute, Cary, NC, USA) (Dar et al. 2002).

RESULTS

Table 2 shows the data for the EQV strain in the bone and bone to implant relative displacement for SIN, 3i, Nobel and ITI models. The different design characteristics of the implants resulted in non-negligible differences in the values of the EQV strain and bone to implant relative displacement. In general, the highest values of strains and displacements were found in the immediately placed simulations. In this clinical situation, the 3i design induced the highest EQV strain in the bone. The SIN and Nobel induced intermediate values and the ITI the lowest strains levels. On the other hand, the ITI models presented the highest relative displacements, followed by 3i and SIN. The lowest bone to implant relative displacements were seen for the Nobel models. A smaller variation in the values of EQV strain and bone to implant displacement between the implant designs was found in immediately loaded and osseointegrated simulations. For these protocols, in the strains and displacement differences between the implant designs, a tendency similar to the immediately placed models could be still be observed.

The ANOVA results on the relative importance of the implant design, clinical situation and loading magnitude on the peak EQV strain and bone-implant relative displacement can be found in tables 3 and 4, respectively. Considering all models, in a general way, the loading magnitude and the clinical situation had the highest percentage contribution to the results. Nevertheless, also the implant design presented a statistically significant influence to the EQV strain in the bone and, principally, to the bone to implant relative displacement. In tables 5 and 6, the different clinical situations were separately analyzed to

demonstrate the varying contribution of the implant design on the strains and displacements in immediately placed, immediately loaded and osseointegrated (i.e. delayed implant loading) protocols. In addition, as the differences between the implant designs is subtle compared with the range of loading (50-200N), the results of 200N loaded models were removed from the statistical analysis in these tables. The reduction in the loading range would allow for better evaluating the influence of different implant designs on these protocols. Comparing the influence of the implant design on the EQV strain for the different implant protocols, the highest contribution of the varying implant designs was seen for the immediately loaded followed by the immediately placed situations. For the osseointegrated models, 2-fold less influence of the implant design could be observed. In respect to the bone to implant relative displacement in immediately placed simulations, the contribution of the implant design was even higher than the contribution of a loading magnitude ranging between 50-100N and it is 2 times higher than the influence observed for the immediately loaded models.

Table 2: Results for the peak equivalent strain (EQV strain) in the bone and bone to implant relative displacement (displac.) for all simulated models.

| Implant Design | Clinical Situations | Loading | Bone EQV strain ($\mu\epsilon$) | Bone_implant displac. (μm) |
|----------------|---------------------|---------|-----------------------------------|---|
| SIN | Immediately placed | 50N | 2,873.3 | 7.6 |
| | | 100N | 5,982.0 | 15.3 |
| | | 200N | 10,022.2 | 30.1 |
| | Immediately loaded | 50N | 1,720.1 | 1.7 |
| | | 100N | 4,543.0 | 3.2 |
| | | 200N | 9,587.3 | 6.4 |
| | Osseointegrated | 50N | 1,329.0 | ----- |
| | | 100N | 2,978.3 | ----- |
| | | 200N | 6,010.4 | ----- |
| 3i | Immediately placed | 50N | 3,459.9 | 10.1 |
| | | 100N | 6,940.8 | 20.5 |
| | | 200N | 10,945.3 | 42.1 |
| | Immediately loaded | 50N | 1,804.5 | 1.4 |
| | | 100N | 5,163.3 | 2.8 |
| | | 200N | 7,382.2 | 5.6 |
| | Osseointegrated | 50N | 1,802.6 | ----- |
| | | 100N | 3,449.8 | ----- |
| | | 200N | 7,382.2 | ----- |
| Nobel | Immediately placed | 50N | 2,732.4 | 5.5 |
| | | 100N | 5,672.1 | 10.0 |
| | | 200N | 11,044.1 | 22.3 |
| | Immediately loaded | 50N | 1,752.9 | 1.5 |
| | | 100N | 3,260.0 | 3.1 |
| | | 200N | 6,599.4 | 6.3 |
| | Osseointegrated | 50N | 1,580.5 | ----- |
| | | 100N | 3,159.7 | ----- |
| | | 200N | 6,330.9 | ----- |
| ITI | Immediately placed | 50N | 2,582.8 | 14.5 |
| | | 100N | 5,196.5 | 29.3 |
| | | 200N | 10,659.8 | 59.5 |
| | Immediately loaded | 50N | 1,618.6 | 2.2 |
| | | 100N | 3,231.3 | 4.5 |
| | | 200N | 6,082.4 | 9.1 |
| | Osseointegrated | 50N | 1,540.5 | ----- |
| | | 100N | 3,032.9 | ----- |
| | | 200N | 6,082.4 | ----- |

*Table 3: Analysis of Variance for the peak equivalent strain in the bone. $P < 0.05$, * statistically significant. DF: degrees of freedom; SS: sum of squares; MS: mean square.*

| Parameter | DF | SS | MS | P-Value | Contribution (%) |
|--|-----------|-------------|-------------|----------------|-------------------------|
| Implant Design | 3 | 8239676.6 | 2746558.9 | 0.0143* | 2.57 |
| Clinical Situation | 2 | 48328401.0 | 24164200.5 | <.0001* | 15.07 |
| Implant Design X Clinical Situation | 6 | 4672145.9 | 778691.0 | 0.2538 | 1.46 |
| Loading Magnitude | 2 | 248902526.1 | 124451263.0 | <.0001* | 77.63 |
| Implant Design X Loading Magnitude | 6 | 2231006.5 | 371834.4 | 0.6389 | 0.70 |
| Clinical Situation X Loading Magnitude | 4 | 8246935.8 | 2061734.0 | 0.0272* | 2.57 |

*Table 4: Analysis of Variance for the relative displacement between implant and bone. $P < 0.05$, * statistically significant. DF: degrees of freedom; SS: sum of squares; MS: mean square.*

| Parameter | DF | SS | MS | P-Value | Contribution (%) |
|--|-----------|-----------|-----------|----------------|-------------------------|
| Implant Design | 3 | 458.9 | 152.9 | 0.0122* | 9.65 |
| Clinical Situation | 1 | 1998.4 | 1998.4 | <.0001* | 42.00 |
| Implant Design X Clinical Situation | 3 | 347.5 | 115.8 | 0.0233* | 7.30 |
| Loading Magnitude | 2 | 1220.4 | 610.2 | 0.0005* | 25.65 |
| Implant Design X Loading Magnitude | 6 | 135.4 | 22.6 | 0.3700 | 2.85 |
| Clinical Situation X Loading Magnitude | 2 | 597.2 | 298.6 | 0.0031* | 12.55 |

*Table 5: Analysis of Variance for the peak equivalent strain in the bone for a 50-100N loading. $P < 0.05$, * statistically significant. DF: degrees of freedom; SS: sum of squares; MS: mean square.*

| Clinical Situation | Parameter | DF | SS | MS | Contribution (%) |
|---------------------------|------------------------------------|-----------|-------------|-------------|-------------------------|
| Immediately placed | Implant Design | 3 | 1874585.7 | 624862.0 | 9.1 |
| | Loading Magnitude | 1 | 18431556.1 | 18431556.1 | 89.9 |
| | Implant Design X Loading Magnitude | 3 | 195416.0 | 65138.7 | 1.0 |
| Immediately loaded | Implant Design | 3 | 1548804.97 | 516268.32 | 11.4 |
| | Loading Magnitude | 1 | 10814737.78 | 10814737.78 | 79.5 |
| | Implant Design X Loading Magnitude | 3 | 1246488.99 | 415496.33 | 9.2 |
| Osseointegrated | Implant Design | 3 | 237829.7 | 79276.6 | 4.5 |
| | Loading Magnitude | 1 | 5069087.2 | 5069087.2 | 95.37 |
| | Implant Design X Loading Magnitude | 3 | 8207.2 | 2735.7 | 0.15 |

Table 6: Analysis of Variance for the relative displacement between implant and bone for a 50-100N loading. Saturated experimental design, no p-values reported. DF: degrees of freedom; SS: sum of squares; MS: mean square.

| Clinical Situation | Parameter | DF | SS | MS | Contribution (%) |
|---------------------------|------------------------------------|-----------|-----------|-----------|-------------------------|
| Immediately placed | Implant Design | 3 | 219.3 | 73.1 | 51.89 |
| | Loading Magnitude | 1 | 174.8 | 174.8 | 41.37 |
| | Implant Design X Loading Magnitude | 3 | 28.5 | 9.5 | 6.75 |
| Immediately loaded | Implant Design | 3 | 1.8 | 0.6 | 23.28 |
| | Loading Magnitude | 1 | 5.8 | 5.8 | 73.54 |
| | Implant Design X Loading Magnitude | 3 | 0.3 | 0.1 | 3.18 |

The strain distribution for SIN, 3i, Nobel and ITI 100N loaded models is presented in figures 2 and 3, in occlusal and buccopalatal plane views, respectively. The strain scale was set to range between 100 and 4000 $\mu\epsilon$ (Frost 1987, Duyck et al, 2001). The design characteristics of the implants resulted in comparable strain distributions independently of the clinical situation simulated. Only small differences could be noted. One common observation was that the highest strain concentration was located at the buccal aspects of the implants in immediately placed simulations, regardless of the implant design. In this clinical situation, some strain concentration could also be found in the apex of the implants, principally for the SIN and Nobel designs. The ITI implant presented the biomechanically preferably strain distribution in the immediately placed protocol, although a slightly higher volume of bone with strains above 4000 $\mu\epsilon$ was observed for this design, as well as for the 3i models. For all designs, in immediately loaded and osseointegrated simulations, the strains were mainly concentrated at the coronal region of the implants, though some high strains could also be seen along the implant body for the immediately loaded protocol. The lowest strain levels were seen for the osseointegrated models. The preferably strain distribution in this clinical situation was seen for ITI and SIN implants, followed by Nobel models. A slightly higher strain concentration was found for 3i models.

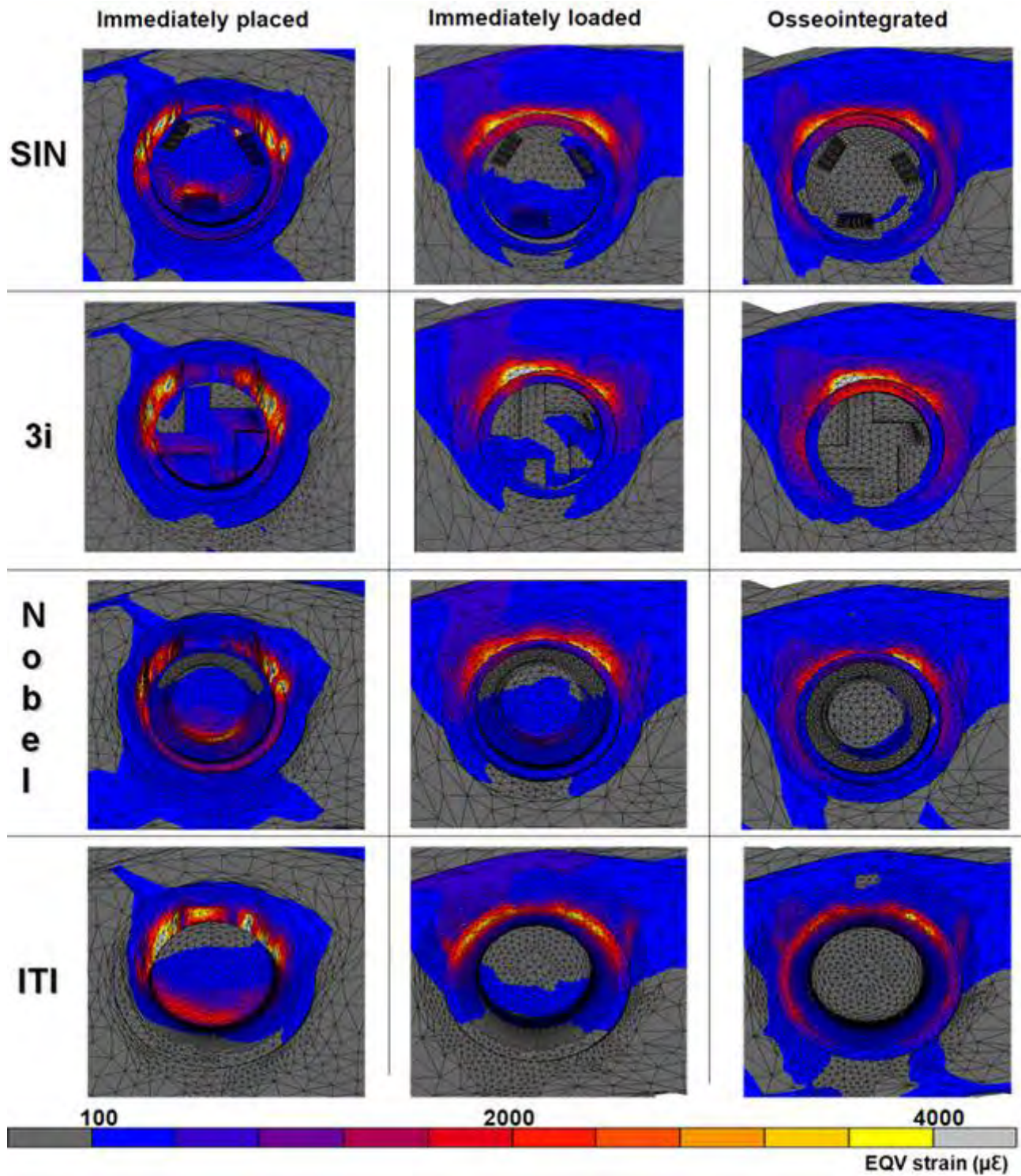


Figure 2: Occlusal view of EQV strain ($\mu\epsilon$) distribution in bone for the SIN, 3i,

Nobel and ITI implants; $F=100N$ models.

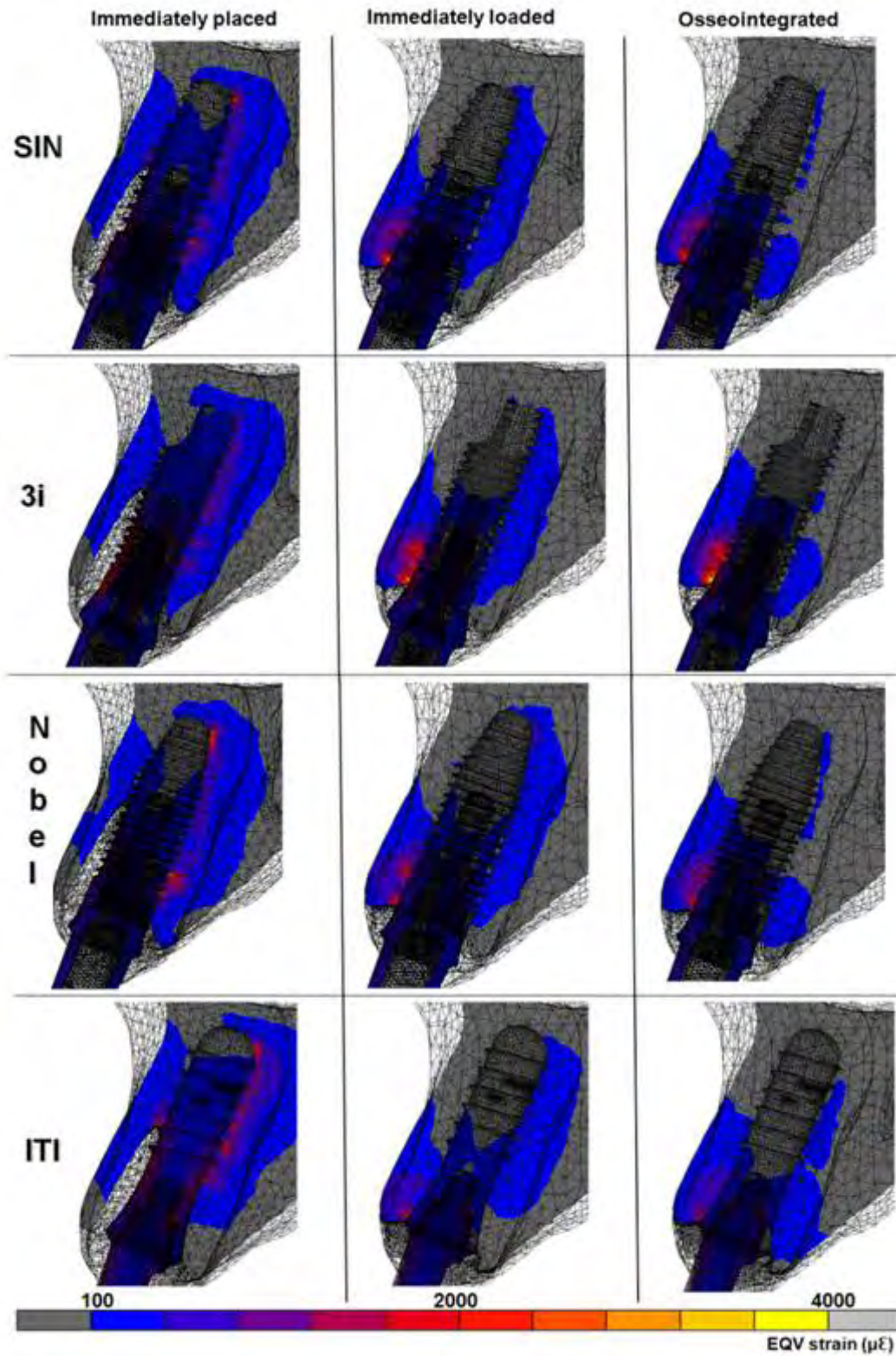


Figure 3: EQV strain ($\mu\epsilon$) distribution for the SIN, 3i, Nobel and ITI implants, $F=100N$ models, in a median buccopalatal plane.

DISCUSSION

The implant design has been suggested to affect the treatment outcomes of osseointegrated implants. However, the effects of different implant designs are still not completely understood in many immediate implant loading approaches. Quirynen et al. (2007), in a recent literature review, found insufficient data for many outcome parameters for immediately placed implants. The authors suggested a tendency toward higher implant losses, when implants are immediately loaded in fresh extraction sockets. The evaluation of the effects of implant designs on immediate implant placement was one of the research areas recommended in a Consensus Report (Quirynen et al. 2007). In fact, in a prospective clinical multicenter study, Donati et al. (2008) reported significant differences on frequency of implant loss and amount of bone loss for different implant designs immediately loaded in a single tooth replacement scenario, in anterior regions of mandible and maxilla. In this way, the present investigation was carried out to study the influence of different implant designs on the biomechanical environment of implants in immediate loading protocols. The obtained results indicated that, although the loading magnitude and the clinical situation (i.e. the presence or absence of an extraction socket defect, the condition of the bone to implant interface) are the most important contributing factor to the biomechanical environment of immediately placed and loaded implants, the implant design does have a statistically significant contribution to the strains and displacements in these protocols. Furthermore, the implant design is even more relevant to the relative bone-implant displacement (which

is a measure for implant stability) in immediately placed models than a loading magnitude ranging between 50-100N.

For immediate loading situations, the initial implant stability, allowing low micromovement in bone, is essential for an uneventful bone tissue formation on the bone-implant interface (Kenwright et al. 1991, Sz mukler-Moncler et al. 1998, Akkocaoglu et al. 2005). Vandamme et al. (2007), in a bone chamber experiment, demonstrated that an implant displacement between 30 and 90 μm stimulated the bone formation at the implant surface compared with an unloaded condition. On the other hand, micromovement beyond 150 μm can induce fibro connective tissue formation, preventing immediately loaded implant osseointegration (Søballe et al.1992, Brunski 1992, 1993, Geris et al. 2004). An additional difficulty, when considering immediate loading for immediately placed implants, is the inevitable initial bone defect at the marginal region (Nemcovsky et al. 2002, Schropp et al. 2003). This bone defect increases the crown/implant ratio and theoretically leads to higher bending moments acting upon the implant (Akkocaoglu et al. 2005).

In fact, in the current study, the highest levels of displacement were found for the immediately placed implants. Also, the highest relative contribution of the implant design was seen for the bone to implant relative displacement. In this respect, although all implants presented micromovements between 5 and 60 μm , depending on the implant design, loading magnitude and clinical situation, the ITI® Standard design presented the highest values of displacement. These results are in line with the reports by Akkocaoglu et al. (2005). The authors compared, in a cadaver model, the stability of two ITI implant designs, immediately loaded after implantation in extraction sockets. They found that the

TE® ITI implants, designed originally for immediate placement, had an enhanced stability (17%) in comparison with an ITI® Standard implant. The authors argued that the increased number of threads of the TE® implant led to more bone contact, and consequently to a higher surface area and friction along the interface, promoting decreased levels of micromovement in bone. Huang et al. (2008), in a FEA of immediately loaded implants, showed that adding threads to stepped and cylindrical designs decreased the implant sliding distance by 41% and 35%, respectively. Other authors also demonstrated that the use of threaded implants provided a more engaging interface between implant and bone and improved the implant stability (Sykaras et al. 2000, Fazel et al 2008). In this way, the smaller number of threads could also explain the current observation of higher displacement for ITI implant compared to 3i, SIN and Nobel designs. However, not only the number of the threads, but also the thread design (i.e. thread pitch, depth, and shape) determine the initial contact, surface area, stress dissipation, stability at the bone-implant interface, and thus the thread function and effectiveness (Eraslan & İnan 2009). The v-threads, such as those used in SIN and 3i implants, are generally included in the implant designs for a simpler and more efficient placement (Misch et al. 2001). On the contrary, the reverse buttress threads of the Nobel implant are optimized for withstanding pull-out loads. These threads were actually more capable to hold the implant to the palatal bone of the extraction socket, in the immediately placed simulations (Sykaras et al. 2000, Misch 2005). In the present study, comparing these implant designs, the Nobel had the lowest micromovements, followed by SIN and 3i, respectively.

In immediately placed models, a slightly higher volume of bone with strains above $4000 \mu\epsilon$ was observed for the ITI implant at the buccal aspect of the bone to implant interface, as well as for the 3i models, which presented the highest peak of EQV strain. These observations are in agreement with the Bozkaya et al. (2005) FEA which showed a larger area of bone overloading due to bending moments for the ITI system, comparing to 4 other implant systems. The authors reported that, in general, overloading occurred near the superior region of the compact bone, in compression, and was primarily caused by the normal and lateral components of the occlusal load. In this case, again the number of threads and the thread design could possibly have compromised the implant stability, which led to a higher compression of the bone to implant buccal interface in ITI and 3i immediately placed models. Tada et al. 2003, in a FEA, showed that higher displacements with large areas of high strain were found for cylindrical non-threaded implants. They also demonstrated that the presence of threads favorably influences the force transmission to bone. Likewise, Huang et al. (2008) showed, by FE simulations of immediately loaded implants, that adding threads to an implant body reduced the bone stress by 20% as compared with non-threaded models. The stress dissipation in immediately loaded protocols is dependent also on the amount of the implant surface contacting with bone during the loading.

In immediately placed situations, some strain concentration could also be found in the apex of the implants, principally for the SIN and Nobel designs. In the same way, Siegele and Soltész (1989), using a non-rigid bone to implant interface, described higher stress concentration at the apex of a cuneiform implant comparing with a cylindrical implant geometry. The authors related this

fact to the small area at the apex of the conical design. Lately, Huang et al. 2008, in a FEA, also demonstrated that root-form shape designs, such as conical and stepped implants, decrease the contact area between the implant and bone, which raised the stress at the immediately loaded implant apex as compared with the cylindrical implant. On the contrary, the round-end nature of the ITI apex decreased the magnitude and concentration of stresses in the apical region.

In the present FEA, the strains in immediately loaded and osseointegrated simulations were mainly concentrated at the coronal region of the implants. In addition, some moderate strain levels could still be found along the implant body in the immediately loaded models. Furthermore, smaller values and variations of EQV strain and bone to implant displacement were noted between the implant designs in these situations. These results were consistent with those of previous FEA studies by Ding et al. (2009) who found no statistically significant differences in stresses and strains between different implant lengths, in immediately loaded simulations. Statistically significant differences were found by the authors only for different implant diameters. The results of this simulation have shown that implant diameter was more important for improved stress distribution in immediately loaded implants than implant length. This likely results from the fact that stress distribution inside the repaired bone socket is uneven, the elements exposed to maximum stress are located around the neck. Hence, the characteristic of the cervical portion of the implants (i.e diameter, presence or absence of threads, surface roughness, connection type) may exert a higher influence on the stress distribution and values of these protocols compared to the implant body design.

Conversely, in the current investigation, the relative contribution of the implant design on the differences in EQV strains was higher for the immediately loaded implants, rather than for the immediately placed implants. This may be explained by the fact that the implant design in the present study is represented not only by the implant body design (i.e. threads design, implant shape), but also by the implant-abutment connection design. Pessoa et al. (2009a) have demonstrated by a statistical analysis of FE models, that the connection type does not have an important contribution to the strains in immediately placed implants. In this way, the 9.1% of contribution of the implant design observed in the immediately placed situation corresponds solely to the influence of the implant body design. On the other hand, the repair of bone alveolar defect will result in different stress/strain patterns in the bone for different connection designs, mainly when bone reaches levels close to the implant crest (Hansson 2000, Pessoa et al. 2009a). Thus, in addition to the contribution of the implant body design, the 11.4% of contribution of the implant design observed in the present study may be related also to the additional effect of the singular connection and crestal module designs of each implant. On the contrary, in FEA simulations by Ding et al. (2009), the implant-abutment connection was disregarded and the implant and abutment were simulated as a single unit. This procedure allowed isolating the effect of the implant body design in the immediately loaded simulations of Ding et al. (2009).

The lowest strain values were seen in the current FEA for the osseointegrated models. Huang et al. (2008) also reported a decrease of 28-63% in the values of bone stress for a bonded interface (osseintegrated implant), comparing with a contact interface with a frictional coefficient of $\mu =$

0.3 (immediately loaded implant). Besides, this result agreed with the outcome of Van Oosterwyck et al. (1998), who demonstrated that through the bonded interface the force was dissipated evenly in both the compressive site and the tension site. However, on the contact interfaces, tensions are not transferred and force only is passed through the compressive site, which resulted in excessive stresses.

In another FEA, Tada and coworkers (2003) demonstrated that, as the strain was mainly concentrated around the implant neck for osseointegrated models, the differences of length and shape in the lower part of the implant did not influence the strain levels in the upper cortical bone. The authors explained that the similar stress distribution in cortical bone was due to the comparable shape and diameter at the implant neck, which transferred the stress similarly to the surrounding bone. Likewise, 2-fold less influence of the implant design could be seen in the current FEA for osseointegrated implants, comparing to immediately placed and loaded protocols. The relatively weak influence of implant body design on osseointegrated implants may be also related to the fact that 80% to 100% of the stresses are concentrated at the crestal 40% of the implant length (Tada et al. 2003, Himmlöva et al. 2004, Pessoa et al. 2009a). On the other hand, as discussed above, the implant design in the present FEA also considered the singular characteristics of the implant connection and crestal module designs. In this way, 4.5% of implant design contribution could still be observed for the osseointegrated protocol.

In osseointegration simulations of the present study, the biomechanically preferable strain distribution was seen for ITI implants. SIN and Nobel models presented comparable strain levels, while 3i models showed a slightly higher

strain concentration. These results are in accordance with FEA by Hansson (2000) who showed that a conical implant-abutment interface, as used in the ITI design, at the level of the bone crest decreases the peak bone-implant interfacial stress as compared to the flat top interface. In a recent FEA also Pessoa et al. demonstrated the same trend. Comparing the other internal connections, the slight differences in strain values may be explained by the difference in surface area between connections. The larger the surface areas for force dissipation, the lower the strain in surrounding bone (Pessoa et al. 2009, Maeda et al. 2006).

In the present FEA, a scale ranging between 100-4000 $\mu\epsilon$ was used to display the strain state in the bone. Frost (1992) considered 4000 $\mu\epsilon$ a possible threshold for pathological bone overload, suggesting that higher strains would lead to the accumulation of micro-damage, thus leading to bone resorption. In a well designed rabbit experiment, Duyck et al. (2001) estimated, by a CT-based FEA, the strain associated with periimplant bone loss as being 4200 $\mu\epsilon$. However, it is must be clear that the present investigation focused only on the relative influence of the different implant design on the biomechanical environment of immediately placed implants, rather than the modeling of bone adaptive processes. In this way, even if some of the models presented values of strain above 4000 $\mu\epsilon$, this does not inevitably mean bone resorption and implant failure. The loading applied in the current study was static and the bone responds to dynamic loads (Lanyon & Rubin 1984, Robling et al. 2001, Turner 1998, Duyck et al. 2001). Furthermore, not only strain amplitude, but also loading frequency and number of loading cycles are parameters capable to greatly influence the cortical bone adaptive response (De Smet et al. 2007,

Forwood & Turner 1994, Hsieh & Turner 2001, Robling et al. 2002, Rubin & McLeod 1984).

In the current investigation, a FEA study was carried out to evaluate the biomechanical behavior of immediately placed implants. The numerical analysis has been demonstrated to be a reliable method to simulate the complexity of different clinical situations. However, some assumptions made in the development of the finite element models, especially concerning the material properties and the interfaces conditions, may compromise the accuracy of the absolute values calculated. In this way, it is advisable to focus on the qualitative comparison rather than on quantitative data from these analyses. Although it would be tempting to compare the results of the present study with the critical values for human bone, it is not fully justified to do so, as a rigorous experimental validation was not accomplished yet. Nevertheless, the integration of advanced engineering techniques, such as computer tomography imaging and computer-aided design systems to construct FE models with reasonable interface conditions (contact), and statistical analysis to assess model sensitivities to variations in input parameters (i.e. implant designs, loading magnitudes, clinical situations), provided relevant information on the relative influence of different implant designs to diverse implant protocols.

CONCLUSION

Within the limitations of the present study, the following can be concluded:

1. Different implant designs significantly influence the biomechanical environment of immediately placed implants;
2. The loading magnitude and the clinical situation (i.e. presence or absence of extraction socket defect, interface condition) have the greatest contribution to the variation of the equivalent strain and bone to implant displacement;
3. The highest effect of varying the implant design was seen for immediately placed and immediately loaded protocols;
4. The implant design does not considerably affect the strain values and distributions of osseointegrated implants.

ACKNOWLEDGEMENTS

The authors thank Dr. S. Fieuws from the Leuven Biostatistics and Statistical Bioinformatics Centre (L-BioStat) for the factorial design optimization and ANOVA analyses. Roberto Pessoa gratefully thanks the grants and scholarships from: FAPESP (Research Support Foundation of São Paulo State) project 2006/06844-2, CAPES (Committee for Postgraduate Courses in Higher Education) and CNPq (National Council for Scientific and Technological Development). Siegfried Jaecques gratefully acknowledges funding from the K.U.Leuven research fund (project OT/06/58). The CT-based FEM methods are based on research funded by the EU Framework Programme 5 Quality of Life project QLK6-CT-2002-02442 IMLOAD.

REFERENCES

1. Adell R, Lekholm U, Rockler B, Brånemark PI. A 15-year study of osseointegrated implants in the treatment of the edentulous jaw. *Int J Oral Surg* 1981; 10: 387–416.
2. Akkocaoglu M, Uysal S, Tekdemir I, Akca K, Cehreli MC. Implant design and intraosseous stability of immediately placed implants: a human cadaver study. *Clin Oral Implants Res* 2005; 16: 202-209.
3. Albrektsson T, Zarb G, Worthington P, Eriksson AR. The long-term efficacy of currently used dental implants: a review and proposed criteria of success. *Int J of Oral Maxillofac Implants* 1986; 1: 11–25.
4. Berglundh T, Persson L, Klinge B. A systematic review of the incidence of biological and technical complications in implant dentistry reported in prospective longitudinal studies of at least 5 years. *J Clin Periodontol* 2002; 29(Suppl 3): 197–212.
5. Bozkaya D, Muftu S, Muftu A. Evaluation of load transfer characteristics of five different implants in compact bone at different load levels by finite elements analysis. *J Prosthet Dent*; 92: 523-30, 2004.
6. Bozkaya D, Müftü S. Mechanics of the taper integrated screwed-in (TIS) abutments used in dental implants. *J Biomech* 2005; 38: 87–97.
7. Brånemark PI, Hansson BO, Adell R, Breine U, Lindstrom J, Hallen O, Ohman A. Osseointegrated implants in the treatment of the edentulous jaw. Experience from a 10-year period. *Scand J Plastic Reconstr Surg* 1977; 16(Suppl): 1–132.

8. Brunski JB. Biomaterials and biomechanics in dental implant design. *Int J Oral Maxillofac Implants* 1988; 3: 85–97.
9. Brunski JB. Biomechanical factors affecting the bone-dental implant interface. *Clin Mater* 1992; 10: 153–201.
10. Brunski JB. Avoid pitfalls of overloading and micromotion of intraosseous implants. *Dent Implantol Update* 1993; 4: 77–81.
11. Dar FH, Meakina JR, Aspden RM. Statistical methods in finite element analysis. *J Biomech* 2002; 35: 1155–1161.
12. De Smet E, Jaecques SVN, Jansen JJ, Walboomers F, Vander Sloten J, Naert IE. Effect of constant strain rate, composed by varying amplitude and frequency, of early loading on peri-implant bone (re)modelling. *J Clin Periodontol* 2007; 34: 618–624.
13. De Smet E, Jaecques SV, Wevers M, Jansen JA, Jacobs R, Vander Sloten J, Naert IE. Effect of controlled early implant loading on bone healing and bone mass in guinea pigs, as assessed by micro-CT and histology. *Eur J Oral Sci* 2006; 114: 232–242.
14. Ding X, Liao S-H, Zhu X-H, Zhang X-H, Zhang L. Effect of Diameter and Length on Stress Distribution of the Alveolar Crest around Immediate Loading Implants. *Clin Implant Dent and Related Res* DOI 10.1111/j.1708-8208.2008.00124.x
15. Donati M, La Scala V, Billi M, Di Dino B, Torrisi P, Berglundh T. Immediate functional loading of implants in single-tooth replacement: a prospective clinical multicenter study. *Clin. Oral Impl. Res* 2008, doi: 10.1111/j.1600-0501.2008.01552.x

16. Duyck J, Ronald HJ, Van Oosterwyck H, Naert I, Vander Sloten J, Ellingsen JE. The influence of static and dynamic loading on marginal bone reactions around osseointegrated implants: an animal experimental study. *Clin Oral Implants Res* 2001; 12: 207-218.
17. Duyck J, Slaets E, Sasaguri K, Vandamme K, Naert I. Effect of intermittent loading and surface roughness on peri-implant bone formation in a bone chamber model. *J Clin Periodontol* 2007; 34: 998–1006.
18. Eraslan O, Inan O. The effect of thread design on stress distribution in a solid screw implant: a 3D finite element analysis. *Clin Oral Invest* 2009; DOI 10.1007/s00784-009-0305-1.
19. Fazel A, Aalai S, Rismanchian M, Sadr-Eshkevari P. Micromotion and Stress Distribution of Immediate Loaded Implants: A Finite Element Analysis. *Clin Implant Dent Related Res* 2009; DOI 10.1111/j.1708-8208.2008.00121.x.
20. Forwood MR, Turner CH. The response of rat tibiae to incremental bouts of mechanical loading: a quantum concept for bone formation. *Bone* 1994; 15: 603–609.
21. Frost HM. Bone 'mass' and the 'mechanostat': a proposal. *Anat Rec* 1987; 219: 1-9.
22. Frost HM. Perspectives: bone's mechanical usage windows. *Bone Miner* 1992; 19: 257–271.
23. Geng JP, Tan KB, Liu GR. Application of finite element analysis in implant dentistry: a review of the literature. *J Prosthet Dent* 2001; 85: 585-98.

24. Geris L, Andreykiv A, Van Oosterwyck H, Vander Sloten J, van Keulen F, Duyck J, Naert I. Numerical simulation of tissue differentiation around loaded titanium implants in a bone chamber. *J Biomech* 2004; 37: 763–769.
25. Hansson S. The implant neck: smooth or provided with retention elements: a biomechanical approach, *Clin Oral Implants Res* 1999; 10: 394–405.
26. Hansson S. Implant–abutment interface: biomechanical study of flat top versus conical. *Clin Implant Dent Relat Res* 2000;2:33–41.
27. Hansson S, Werke M. The implant thread as a retention element in cortical bone: the effect of thread size and thread profile: a finite element study. *J Biomech* 2003; 36: 1247-58.
28. Himmlöva L, Dostalova T, Kacovsky A, Konvickova S. Influence of implant length and diameter on stress distribution: a finite element analysis. *J Prosthet Dent* 2004; 91: 20-5.
29. Holmgren EP, Seckinger RJ, Kilgren LM, Mante F. Evaluating parameters of osseointegrated dental implants using finite element analysis—A two-dimensional comparative study examining the effects of implant diameter, implant shape and load direction. *J Oral Implantol* 1998; 24: 80–88.
30. Hoshaw SJ, Brunski JB, Cochran GVB. Mechanical loading of Brånemark implants affects interfacial bone modeling and remodeling. *Int J Oral Maxillofac Implants* 1994; 9: 345–360.
31. Hsieh YF, Turner CH. Effects of loading frequency on mechanically induced bone formation. *J Bone Miner Res* 2001; 16: 918–924.

32. Huang HL, Hsu JT, Fuh LJ, Tu MG, Ko CC, Shen YW. Bone stress and interfacial sliding analysis of implant designs on an immediately loaded maxillary implant: A non-linear finite element study. *J Dent* 2008; 36: 409-417.
33. Isidor F. Loss of osseointegration caused by occlusal load of oral implants. A clinical and radiographic study in monkeys. *Clin Oral Implants Res* 1996; 7: 143–152.
34. Isidor F. Histological evaluation of periimplant bone at implants subjected to occlusal overload or plaque accumulation. *Clin Oral Implants Res* 1997; 8: 1–9.
35. Jaecques SVN, Van Oosterwyck H, Muraru L, Van Cleynenbreugel T, De Smet E, Wevers M, Naert I, Vander Sloten J. Individualised, micro CT-based finite element modelling as a tool for biomechanical analysis related to tissue engineering of bone. *Biomaterials* 2004; 25: 1683–1696.
36. Kenwright J, Richardson JB, Cunningham JL, White SH, Goodship AE, Adams MA, et al. Axial movement and tibial fractures. A controlled randomized trial of treatment. *J Bone Joint Surg Br* 1991; 73: 654–659.
37. Lanyon LE, Rubin CT. Static vs dynamic loads as an influence on bone remodelling. *J Biomech* 1984; 17: 897–905.
38. Maeda Y, Satoh T, Sogo M. In vitro differences of stress concentrations for internal and external hex implant–abutment connections: a short communication. *J Oral Rehabil* 2006; 33: 75–78.

39. Merz BR, Hunenbart S, Belser UC. Mechanics of the implant-abutment connection: an 8-degree taper compared to a butt joint connection. *Int J Oral Maxillofac Implants* 2000; 15: 519–526.
40. Misch CE, Bidez MW, Sharawy M. A bioengineered implant for a predetermined bone cellular response to loading forces. A literature review and case report. *J Periodontol* 2001; 72: 1276-86.
41. Misch CE, Suzuki JB, Misch-Dietsh FM, Bidez MW. A positive correlation between occlusal trauma and peri-implant bone loss: literature support. *Implant Dent* 2005; 14: 108-16.
42. Nemcovsky CE, Artzi Z, Moses O, Gelernter I. Healing of marginal defects at implants placed in fresh extraction sockets or after 4–6 weeks of healing. A comparative study. *Clin Oral Implants Res* 2002;13: 410–419.
43. Palmer RM, Palmer PJ, Smith BJ. A 5-year prospective study of Astra single tooth implants. *Clin Oral Implants Res* 2000; 11: 179–182.
44. Pessoa RS, Muraru L, Marcantonio Jr E, Vaz LG, Vander Sloten J, Duyck J, Jaecques S. Influence of implant connection type on the biomechanical environment of immediately placed implants – CT-based nonlinear, 3D finite element analysis. *Clin Implant Dent Relat Res* 2009 (a), DOI 10.1111/j.1708-8208.2009.00155.x.
45. Pessoa RS, Vaz LG, Marcantonio Jr E, Vander Sloten J, Duyck J, Jaecques SVN. Biomechanical evaluation of platform switching in different implant protocols – CT based 3D finite element analysis. *Int J Oral Maxillofac Implant* 2009 (b), accepted for publication.

46. Quirynen M, Van Assche N, Botticelli D, Berglundh T. How does the timing of implant placement to extraction affect outcome? *Int J Oral Maxillofac Implants* 2007; 22(Suppl): 203-23.
47. Robling AG, Duijvelaar KM, Geevers JV, Ohashi N, Turner CH. Modulation of appositional and longitudinal bone growth the rat ulna by applied static and dynamic force. *Bone* 2001; 29: 105–113.
48. Robling AG, Hinant FM, Burr DB, Turner CH. Improved bone structure and strength after long-term mechanical loading is greatest if loading is separated into short bouts. *J Bone Miner Res* 2002; 17: 1545–1554.
49. Rubin CT, McLeod KJ. Promotion of bony ingrowth by frequency-specific, low-amplitude mechanical strain. *Clin Orthop Relat Res* 1984; 298: 165–174.
50. Siegele D, Soltesz U. Numerical investigations of the influence of implant shape on stress distribution in the jaw bone. *Int J Oral Maxillofac Implants* 1989; 4: 333–340.
51. Schropp L, Kostopoulos L, Wenzel A. Bone healing following immediate versus delayed placement of titanium implants into extraction sockets: a retrospective clinical study. *Int J Oral Maxillofac Implants* 2003; 18: 189–199.
52. Sykaras R, Iacopino AM, Marker VA, Triplett RG, Woody RD. Implant materials, designs, and surface topographies: their effect on osseointegration. A literature review. *Int J Oral Maxillofac Implants* 2000; 15: 675–90.

53. Søballe K, Brockstedt-Rasmussen H, Hansen ES, Bünger C. Hydroxyapatite coating modifies implant membrane formation. Controlled micromotion studied in dogs. *Acta Orthop Scand* 1992; 63: 128–140.
54. Strong JT, Misch CE, Bidez MW, Nalluri P. Functional surface area: Thread-form parameter optimization for implant body design. *Compend Contin Educ Dent* 1998; 19(special issue):4–9.
55. Szmukler-Moncler S, Salama H, Reingewirtz Y, Dubruille JH. Timing of loading and effect of micromotion on bone-dental implant interface: review of experimental literature. *J Biomed Mater Res* 1998; 43: 192–203.
56. Tada S, Stegaroiu R, Kitamura E, Miyakawa O, Kusakari H. Influence of Implant Design and Bone Quality on Stress/Strain Distribution in Bone Around Implants: A 3-dimensional Finite Element Analysis. *Int J Oral Maxillofac Implants* 2003; 18: 357–368
57. Testori T, Meltzer A, Del Fabbro M, Zuffetti F, Troiano M, Francetti L, Weinstein RL. Immediate occlusal loading of osseotite implants in the lower edentulous jaw. A multicenter prospective study. *Clin Oral Implants Res* 2004; 15: 278–284.
58. Turner CH. Three rules for bone adaptation to mechanical stimuli. *Bone* 1998; 23:399–407.
59. Van Oosterwyck H, Duyck J, Vander Sloten J, Van der Perre G, De Cooman M, Lievens S, Puers R, Naert I. The influence of bone mechanical properties and implant fixation upon bone loading around oral implants. *Clin Oral Implants Res* 1998; 9: 407–18.

60. Vandamme K, Naert I, Geris L, Vander Sloten J, Puers R, Duyck J. Influence of controlled immediate loading and implant design on peri-implant bone formation. *J Clinical Periodontol* 2007; 34: 172–181.

61. Vandamme K, Naert I, Vander Sloten J, Puers R, Duyck J. Effect of implant surface roughness and loading on peri-implant bone formation. *J Periodontol* 2008; 79: 150–157.

62. Wennstrom JL, Ekestubbe A, Grondahl K, Karlsson S, Lindhe J. Implant-supported single-tooth restorations: a 5-year prospective study. *J Clin Periodontol* 2005; 32: 567–574.

7 DISCUSSÃO

Devido ao fato do colapso inicial da interface entre o implante e os tecidos circundantes geralmente começar na região da crista óssea, em implantes com a osseointegração consolidada,^{3,6,7} e da maioria das falhas mecânicas ocorrerem no módulo da crista do implante,²⁴⁻²⁸ esforços têm sido realizados para avaliar os efeitos de diferentes conexões protéticas sobre a distribuição e magnitude das tensões/deformações no osso e nos componentes do implante.

Simulando implantes ossointegrados, Merz e colaboradores,²⁷ compararam as tensões induzidas por cargas laterais em implantes cone-morse e hexágono externo, por métodos experimental e de elementos finitos. Estes concluíram que a interface cônica distribui as tensões de maneira mais uniforme, quando comparado com encaixes hexágono externo. Em outro estudo, utilizando FEA, Hansson²⁹ observou que a conexão cone-morse no nível do osso marginal diminuiu substancialmente o pico e otimizou a distribuição das tensões no osso de suporte. Hansson²⁹ também evidenciou que com uma interface em hexágono externo no nível da margem da mucosa periimplantar, o pico das tensões cisalhantes na interface osso-implante estava localizado no topo do osso marginal. Com uma conexão cone-morse, o pico da tensão cisalhante se encontrava em uma localização mais apical, o que poderia reduzir a reabsorção óssea marginal.^{29,30} Comparando conexões em hexágono interno e externo, uma menor concentração de tensões na região marginal foi observada para a configuração interna.²⁰ Este fato pode ser justificado pela diferença de superfície de contato entre as conexões. A interface cônica da

conexão cone-morse, bem como a parede lateral do abutment do hexágono interno, ajudam a dissipar a força que seria transmitida ao osso marginal.^{20,27}

Entretanto, apesar dos resultados de diversas pesquisas comprovarem uma influencia expressiva do tipo de conexão protética no ambiente biomecânico de implantes osseointegrados, uma contribuição não significativa do tipo de conexão protética foi observada por Pessoa et al.²⁰ nas variações de deformações EQV e deslocamentos relativos na interface osso-implante, para o protocolo de implantes imediatos com carga imediata. Neste sentido, Hansson³⁰ demonstrou que quando o módulo da crista do implante é posicionado 2 mm acima do nível do osso marginal, o efeito das diferentes conexões protéticas sobre osso é semelhante. No caso de implantes instalados em alvéolos de extração, o defeito ósseo inicial na região marginal, resultante da diferença de diâmetro entre a região cervical do dente e a plataforma do implante, posiciona o módulo da crista do implante distante do osso. Desta forma, a transmissão de tensões, singular entre as diferentes conexões protéticas, resulta em magnitudes e distribuição de deformações análogas no osso alveolar.

Por outro lado, independente do protocolo utilizado na instalação e carregamento dos implantes, o design da conexão protética é determinante nas tensões do parafuso do abutment e na desadaptação (gap) entre o implante e o abutment.^{20,27} Comparando as tensões internas de diferentes tipos de conexões protéticas, Pessoa et al.²⁰ encontraram valores de tensão no parafuso do abutment e gap significativamente menores para a conexão cone-morse. A conexão em hexágono interno apresentou valores intermediários e a

hexágono externo a maior instabilidade e tensões na região do encaixe protético.

Além disso, considerando a importância da preservação da altura da crista óssea para os resultados estéticos finais do tratamento, a utilização de componentes protéticos de menor diâmetro que a plataforma do implante foi introduzida na prática clínica, como tentativa de redução ou eliminação da perda óssea periimplantar marginal.³¹⁻³² Como sustentação biológica para a chamada “platform-switching”, Lazzara, Porter³² sugeriram que o posicionamento horizontal da interface implante-abutment mais distante do osso exporia maior área da superfície do implante, no qual o tecido conjuntivo poderia aderir, e afastaria da crista óssea a contaminação bacteriana do gap, desta forma reduzindo a tendência à reabsorção óssea periimplantar marginal. Os autores³² observaram radiograficamente que muitos implantes restaurados com abutments em platform-switching exibiram uma perda óssea na crista marginal reduzida ou ausente. Da mesma forma, Guirado et al.³³ reportaram uma perda óssea marginal média de 0,7 mm para um novo design de implante que incorporava o conceito de platform switching. Também Capiello et al.,³⁴ em um estudo prospectivo, mostraram uma perda óssea significativamente menor para implantes com platform-switching (média, $0,95 \pm 0,32$ mm), comparados com implantes restaurados com abutments do mesmo diâmetro da plataforma do implante (média, $1,67 \pm 0,37$ mm), após 12 meses de função.

Como consequência, a platform-switching tem sido indicada como uma modalidade de tratamento válida na manutenção dos tecidos periimplantares moles e duros, não apenas para implantes de dois estágios, como também nos protocolos de implantes imediatos com carga

imediate.^{33,34,35} Além disso, uma motivação biomecânica para o uso de abutments mais estreitos foi proposta por Maeda e colaboradores.³⁶ Os autores concluíram, por meio de FEA, que o design em platform-switching afastava a concentração de tensões da margem óssea periimplantar, reduzindo seu efeito na reabsorção óssea marginal. Entretanto os resultados apresentados por Maeda et al.³⁶ foram baseados em modelos em elementos finitos muito simplificados que não consideraram a geometria interna da conexão protética. Esta geometria é reconhecida como um fator chave associado com os padrões e magnitudes das tensões.^{20,27} Mais ainda, a relação de contato não-linear entre o implante, abutment e parafuso do abutment, permitindo a movimentação entre as partes do modelo, foi ignorada nas análises de Maeda et al.³⁶ Outros estudos têm demonstrado que não apenas os níveis, mas também a distribuição das tensões e deformações são fortemente afetados pelas condições de interface.³⁷⁻³⁸

Por outro lado, comparando por meio de FEA a utilização de abutments de 4,3 e 3,8 mm em implante com plataforma de 4,3 mm, Pessoa et al.²¹ evidenciaram uma maior concentração de tensões na área da conexão para o abutment de 3,8 mm (platform-switching). Esta diferença pode ser explicada pela redução da área de superfície para a transmissão da carga na configuração platform-switching. Ao contrário, um abutment mais largo resulta em uma maior área para a dissipação das cargas e, desta forma, em uma menor concentração de tensões.

Entretanto, como a distância para a transmissão das tensões para a borda do implante é maior na configuração platform-switching, tensões similares foram encontradas por Pessoa et al.²¹ na superfície cervical do

implante para ambos os diâmetros dos abutments. Conseqüentemente, os valores e distribuição das deformações no osso foram similares para ambos o platform-switching (3,8 mm) e o abutment coincidente (4,3 mm) com o diâmetro da plataforma do implante, independentemente da situação clínica simulada.²¹ Da mesma forma, uma diferença insignificante no deslocamento relativo entre o implante e osso foi relatada para os abutments de 3,8 e 4,3 mm, nos protocolos com carga imediata.²¹ A maior influencia na variação dos diâmetros dos abutments foi observada nas tensões no parafuso do abutment. Uma concentração de tensões no parafuso um pouco maior foi encontrada nos modelos com platform-switching.²¹

Neste sentido, apesar de existir uma plausibilidade biológica para o conceito do platform-switching, baseado na hipótese de que um abutment com o diâmetro menor que a plataforma do implante aumentaria a superfície do implante para formação da distância biológica e a distância entre a possível contaminação presente no gap do abutment e a crista óssea, apenas estes fatores não são suficientes para explicar inteiramente a remodelação óssea no módulo da crista do implante. Shin e colaboradores,³⁹ comparando diferentes designs de módulo da crista de implantes em um ensaio clínico randomizado, encontrou uma maior perda óssea para implantes com a configuração platform-switching ($1,32 \pm 0,27$ mm) e um módulo da crista liso. As menores perdas ósseas ($0,18 \pm 0,16$ mm) foram encontradas para o grupo com o abutment coincidente com a plataforma do implante e um módulo da crista com tratamento de superfície e com micro-roscas. Desta maneira, quando planejar um tratamento de implante para atingir um resultado estético/funcional otimizado, é essencial considerar todos os possíveis fatores que podem

exercer uma influência na região do módulo da crista do implante, como por exemplo, a presença de micro-roscas, de tratamento de superfície e o tipo de conexão protética.^{20,39-40}

Mais ainda, as conclusões em alguns estudos,^{32,33} nos quais menos perda óssea foi observada para a configuração em platform-switching, foram feitas comparando diferentes diâmetros de implantes, com diferentes características de módulo da crista. Como na verdade foi o design do implante e não apenas o diâmetro do abutment que variou, é difícil determinar qual fator teve a maior contribuição para os resultados observados.

De fato, o design do implante tem sido indicado como um fator capaz de influenciar o resultado do tratamento de implantes osseointegrados. Em um estudo clínico prospectivo, Donati et al.⁴¹ (2008) reportaram diferenças significantes na frequência de perda de implantes e na quantidade de reabsorção óssea para diferentes designs de implantes instalados em alvéolos de extração na região anterior de mandíbula e maxila. Entretanto, o efeito de diferentes designs de implantes é menos entendido em protocolos com carga imediata.²³

Em uma recente FEA, Pessoa et al.²² (2010) compararam quatro diferentes designs de implantes disponíveis comercialmente (\varnothing 4,5 x 13 mm SIN SW® [SIN Sistema de Implante, São Paulo, Brasil], \varnothing 4,1 x 13 mm 3i Certain® [3i, Palm Beach Gardens, USA], \varnothing 4,3 x 13 mm Nobel Replace™ [Nobel Biocare AB, Göteborg, Sweden], e \varnothing 4,1 x 12 mm RN synOcta® ITI Standard [Institut Straumann AG, Basel, Switzerland]), nos protocolos de implantes imediatos, com carga imediata e com carga tardia. Os autores²² reportaram uma contribuição significativa do design dos implantes nas

diferenças de valores de deslocamentos relativos, nas simulações de implantes imediatos com carga imediata. Neste sentido, apesar de todos os implantes apresentarem micro-movimentos entre 5 e 60 μm , dependendo do design, magnitude da carga e situação clínica, o ITI® Standard apresentou os maiores valores de deslocamento. Estes resultados estão alinhados com relatos feitos por Akkocaoglu et al.¹³ (2005). Os autores compararam, em um modelo de cadáver, a estabilidade de dois designs de implantes ITI instalados em alvéolos de extração. Eles encontraram que os implantes ITI TE®, originalmente projetados para protocolos imediatos, tiveram uma maior estabilidade (17%) em comparação com o implante ITI® Standard. Os autores argumentaram que o número aumentado de roscas do implante TE® levou a um maior contato osso-implante, e conseqüentemente, a maiores áreas de superfície e atrito, resultando em uma diminuição da tendência à micro-movimentação do implante.

Huang et al.,⁴² (2008) em uma FEA de implantes com carga imediata, demonstraram que a inclusão de roscas em implantes lisos diminuía de 35 a 40% o deslocamento do implante. Outros autores também evidenciaram que a utilização de implantes com roscas promovem maior interface de contato osso-implante, otimizando a estabilidade do implante.⁴³⁻⁴⁴ Desta maneira, o menor número de roscas pode também explicar as observações de maiores deslocamentos para o implante ITI, comparados com os designs da 3i, SIN e Nobel²². Entretanto, não apenas o número de roscas, mas também o design das roscas (i.e. forma, passo, profundidade) determina o contato inicial, área de superfície, dissipação das tensões, estabilidade na interface osso-implante, e desta maneira, a função e eficiência da rosca.⁴⁵ As

roscas em V, como as usadas nos implantes SIN e 3i, são geralmente incluídas para promover uma inserção mais simples e eficiente do implante no osso.⁴⁶ Ao contrário, as roscas em apoio invertido, como as usadas no implante Nobel, são empregadas para resistir a forças de tração. Este design de roscas é realmente mais eficiente para estabilizar o implante ao osso palatino de alvéolos de extração, em casos de implantes imediatos.^{4,43} No estudo realizado por Pessoa et al.²² (2010), os implantes da Nobel tiveram os menores deslocamentos relativos osso-implante, seguidos pelos implantes da SIN e 3i, respectivamente.

No mesmo estudo, Pessoa et al.²² (2010) observaram, nos modelos de implantes imediatos, um maior volume de osso com deformações acima de 4000 $\mu\epsilon$ (tendência à reabsorção óssea) para os modelos do design ITI, bem como para os 3i, os quais apresentaram os maiores picos de deformação, para um carregamento de 100N. Estas observações estão de acordo com uma FEA realizada por Bozkaya et al.⁴⁷ (2004) a qual demonstrou uma maior área de osso com sobrecarga devido ao momento fletor para o sistema ITI, comparando com 4 outros sistemas de implantes. Os autores reportaram que, em geral, a sobrecarga ocorria em compressão, perto da região superior do osso compacto, e era causa pelos componentes laterais da carga. Neste caso, mais uma vez o número e o design das roscas podem possivelmente ter comprometido a estabilidade do implante, o que levou a maiores compressões do osso na face vestibular do osso, nas simulações de implantes imediatos dos designs da ITI e 3i.²² Tada et al.,⁴⁸ (2003) em outra FEA, observaram maiores deslocamentos e áreas com alta deformações em implantes cilíndricos sem roscas. Eles também demonstraram que a presença de roscas influenciava

favoravelmente a transmissão de forças para o osso. De forma análoga, Huang et al.⁴² (2008) mostraram, por meio de FEA de implantes com carga imediata, que a adição de roscas ao corpo de implantes reduziu em 20% as tensões no osso, quando comparadas com implantes sem roscas. Além dos deslocamentos entre o osso e o implante, também a dissipação das tensões nos protocolos de implantes com carga imediata, é dependente da quantidade de superfície em contato com o osso durante aplicação da carga.

No entanto, é importante enfatizar que alguns dos designs de implantes nos estudos acima podem não ter sido projetados pelos fabricantes especificamente para o protocolo no qual foram avaliados. Sendo assim, em alguns casos, as comparações do desempenho entre estes implantes podem se mostrar inadequadas. Além disso, mesmo que alguns modelos tenham apresentado deformações acima de 4000 $\mu\epsilon$, isto não significa necessariamente a reabsorção óssea e falha do implante. A carga aplicada nestes estudos foi estática e o osso responde a cargas dinâmicas.³ Mais ainda, não apenas a amplitude da deformação, mas também a frequência da carga são fatores capazes de influenciar a resposta adaptativa do osso cortical.⁴⁹ Finalmente, quando um implante é instalado cirurgicamente nos ossos maxilares, este é mecanicamente rosqueado em uma perfuração de menor diâmetro. Grande quantidade de tensões ocorrerá devido ao torque aplicado neste processo. Esta condição pode ter grande impacto na estabilidade do implante, assim como em todo o ambiente biomecânico de implantes com carga imediata. Entretanto, este fenômeno tem sido negligenciado nas análises em elementos finitos apresentadas, e deverá ser tema de estudos futuros.

8 CONCLUSÃO

Um entendimento aprofundado da Biomecânica dos implantes dentais, nos diversos protocolos de instalação e carregamento, pode dar suporte para a otimização dos designs dos implantes em função dos parâmetros benéficos ao osso periimplantar, desta forma diminuindo os riscos de falhas. Neste sentido, dentro dos limites do presente estudo, pode-se concluir que, apesar de o design da conexão protética ser determinante nas tensões do parafuso do abutment e no gap entre o abutment e o implante, este não foi capaz de afetar as deformações no osso e deslocamentos de implantes instalados em alvéolos de extração. Por outro lado, o design dos implantes influencia significativamente o ambiente biomecânico de implantes imediatos.

9 REFERENCIAS*

1. Gapski R, Wang HL, Mascarenhas P, Lang NP. Critical review of immediate implant loading. *Clin Oral Implants Res.* 2003; 14: 515–27.
2. Esposito MA, Koukoulopoulou A, Coulthard P, Worthington HV. Interventions for replacing missing teeth: dental implants in fresh extraction sockets (immediate, immediate-delayed and delayed implants). *Cochrane Database Syst Rev.* 2006; 4: CD005968.
3. Duyck J, Ronald HJ, Van Oosterwyck H, Naert I, Vander Sloten J, Ellingsen JE. The influence of static a dynamic loading on marginal bone reactions around osseointegrated implants: an animal experimental study. *Clin Oral Implants Res.* 2001; 12: 207-18.
4. Misch CE, Suzuki JB, Misch-Dietsh FM, Bidez MW. A positive correlation between occlusal trauma and peri-implant bone loss: literature support. *Implant Dent.* 2005; 14: 108-16.
5. Frost HM. Perspectives: bone's mechanical usage windows. *Bone Miner.* 1992; 19: 257–71.
6. Isidor F. Loss of osseointegration caused by occlusal load of oral implants. A clinical and radiographic study in monkeys. *Clin Oral Implants Res.* 1996; 7:143–52.
7. Isidor F. Histological evaluation of periimplant bone at implants subjected to occlusal overload or plaque accumulation. *Clin Oral Implants Res.* 1997; 8: 1–9.

* De acordo com o estilo Vancouver. Disponível no site:
<http://www.nlm.nih.gov/bsd/uniform-requirements.html>

8. Søballe K, Brockstedt-Rasmussen H, Hansen ES, Bünger C. Hydroxyapatite coating modifies implant membrane formation. Controlled micromotion studied in dogs. *Acta Orthop Scand*. 1992; 63:128–40.
9. Brunski JB. Biomechanical factors affecting the bone-dental implant interface. *Clin Mater*. 1992; 10: 153–201.
10. Geris L, Andreykiv A, Van Oosterwyck H, Vander Sloten J, van Keulen F, Duyck J, Naert I. Numerical simulation of tissue differentiation around loaded titanium implants in a bone chamber. *J Biomech*. 2004; 37: 763–9.
11. Berglundh T, Abrahamsson I, Lang NP, Lindhe J. De novo alveolar bone formation adjacent to endosseous implants. *Clin Oral Implants Res*. 2003; 14: 251–62.
12. Nemcovsky CE, Artzi Z, Moses O, Gelernter I. Healing of marginal defects at implants placed in fresh extraction sockets or after 4–6 weeks of healing. A comparative study. *Clin Oral Implants Res*. 2002; 13: 410–9.
13. Akkocaoglu M, Uysal S, Tekdemir I, Akca K, Cehreli MC. Implant design and intraosseous stability of immediately placed implants: a human cadaver study. *Clin Oral Implants Res*. 2005;16: 202-9.
14. Zienkiewicz OC, Taylor RL. *The Finite Element Method*. 4th ed. New York: McGraw-Hill; 1989, vol 1- 2.
15. Geng JP, Tan KB, Liu GR. Application of finite element analysis in implant dentistry: a review of the literature. *J Prosthet Dent* .2001; 85: 585-98.
16. Van Staden RC, Guan H, Loo YC. Application of the finite element method in dental implant research. *Comput Methods Biomech Biomed Engin*. 2006; 9: 257-70.

17. Lin C-L, Chang S-H, Chang W-J, Kuo Y-C. Factorial analysis of variables influencing mechanical characteristics of a single tooth implant placed in the maxilla using finite element analysis and the statistics-based Taguchi method. *Eur J Oral Sci.* 2007; 115: 408–16.
18. Lin C-L, Wang J-C, Chang W-J. Biomechanical interactions in tooth–implant-supported fixed partial dentures with variations in the number of splinted teeth and connector type: a finite element analysis. *Clin Oral Impl Res.* 2008;19: 107–17.
19. Ding X, Liao S-H, Zhu X-H, Zhang X-H, Zhang L. Effect of Diameter and Length on Stress Distribution of the Alveolar Crest around Immediate Loading Implants. *Clin Implant Dent Relat Res* 2008; 11:279-87 [Epub 2008 Sep9].
20. Pessoa RS, Muraru L, Marcantonio Jr E, Vaz LG, Vander Sloten J, Duyck J. et al. Influence of implant connection type on the biomechanical environment of immediately placed implants – CT-based nonlinear, 3D finite element analysis. *Clin Implant Dent Relat Res* 2009; May 7 [Epub ahead of print].
21. Pessoa RS, Vaz LG, Marcantonio Jr E, Vander Sloten J, Duyck J, Jacques SVN. Biomechanical evaluation of platform switching in different implant protocols – CT based 3D finite element analysis. *Int J Oral Maxillofac Implants* 2009 (b); accepted for publication.
22. Pessoa RS, Coelho PG, Muraru L, Marcantonio Jr E, Vaz LG, Vander Sloten J, Jacques S. Influence of implant design on the biomechanical environment of immediately placed implants – CT-based nonlinear 3D finite element analysis. *Int J Oral Maxillofac Implants* 2010; submitted for publication.

23. Quirynen M, Van Assche N, Botticelli D, Berglundh T. How does the timing of implant placement to extraction affect outcome? *Int J Oral Maxillofac Implants* 2007; 22 Suppl : 203-23.
24. Ekefeld A, Carlsson GE, Borjesson G. Clinical evaluation of single-tooth restorations supported by osseointegrated implants: A retrospective study. *Int J Oral Maxillofac Implants*. 1994; 9: 179-83.
25. Levine RA, Clem DS, Wilson Jr TG, Higginbottom F, Saunders SL. A multicenter retrospective analysis of the ITI implant system used for single-tooth replacements: results of loading for 2 or more years. *Int J Oral Maxillofac Implants*. 1999;14: 516–20.
26. Schwarz MS. Mechanical complications of dental implants. *Clin Oral Implants Res*. 2000; 1: 156–58.
27. Merz BR, Hunenbart S, Belser UC. Mechanics of the implant-abutment connection: an 8-degree taper compared to a butt joint connection. *Int J Oral Maxillofac Implants*. 2000; 15: 519–26.
28. Behneke A, Behneke N, d’Hoedt B. The longitudinal clinical effectiveness of ITI solid-screw implants in partially edentulous patients: a 5-year follow-up report. *Int J Oral Maxillofac Implants*. 2000; 15: 633–45.
29. Hansson S. A conical implant–abutment interface at the level of the marginal bone improves the distribution of stresses in the supporting bone. *Clin Oral Implants Res*. 2003; 14: 286–93.
30. Hansson S. Implant–abutment interface: biomechanical study of flat top versus conical. *Clin Implant Dent Relat Res*. 2000; 2: 33–41.
31. Gardner DM. Platform switching as a means to achieving implant esthetics. *NY State Dent J*. 2005; 71: 34-7.

32. Lazzara RJ, Porter SS. Platform switching: A new concept in implant dentistry for controlling postrestorative crestal bone levels. *Int J Periodontics Restorative Dent.* 2006; 26: 9–17.
33. Guirado JLC, Yuguero MRS, Zamora GP, Barrio EM. Immediate Provisionalization on a New Implant Design for Esthetic Restoration and Preserving Crestal Bone. *Implant Dent.* 2007;16: 155–64.
34. Cappiello M, Luongo R, Di Iorion D, Bugea C, Cochotto R, Celletti R. Evaluation of peri-implant bone loss around platform-switched implants. *Int J Periodontics Restorative Dent.* 2008; 28: 347-55.
35. Canullo L, Rasperini G. Preservation of Peri-implant Soft and Hard Tissues Using Platform Switching of Implants Placed in Immediate Extraction Sockets: A Proof-of-concept Study with 12- to 36-month Follow-up. *Int J Oral Maxillofac Implants.* 2007; 22: 995–1000.
36. Maeda Y, Miura J, Taki I, Sogo M. Biomechanical analysis on platform switching: is there any biomechanical rationale? *Clin Oral Implants Res.* 2007; 18: 581-4.
37. Van Oosterwyck H, Duyck J, Vander Sloten J, Van der Perre G, De Cooman M, Lievens S, Puers R, Naert I. The influence of bone mechanical properties and implant fixation upon bone loading around oral implants. *Clin Oral Implants Res.* 1998; 9: 407-18.
38. Brunski JB. Biomechanical factors affecting the bone-dental implant interface. *Clin Mater.* 1992; 10: 153-201.
39. Shin YK, Han CH, Heo SJ, Kim S, Chun HJ. Radiographic evaluation of marginal bone level around implants with different neck designs after 1 year. *Int J Oral Maxillofac Implants.* 2006; 20: 789-94.

40. Zechner W, Trinkl N, Watzak G, Busenlechner D, Tepper G, Haas R, Watzek G. Radiologic follow-up of periimplant bone loss around machine-surfaced and rough-surfaced interforaminal implants in the mandible functionally loaded for 3 to 7 years. *Int J Oral Maxillofac Implants*. 2004;19: 216–21.
41. Donati M, La Scala V, Billi M, Di Dino B, Torrisi P, Berglundh T. Immediate functional loading of implants in single-tooth replacement: a prospective clinical multicenter study. *Clin. Oral Impl Res*. 2008; 19: 740-8 [Epub 2008 May 2007].
42. Huang HL, Hsu JT, Fuh LJ, Tu MG, Ko CC, Shen YW. Bone stress and interfacial sliding analysis of implant designs on an immediately loaded maxillary implant: A non-linear finite element study. *J Dent*. 2008; 36: 409–17.
43. Sykaras R, Iacopino AM, Marker VA, Triplett RG, Woody RD. Implant materials, designs, and surface topographies: their effect on osseointegration. A literature review. *The International Journal of Oral and Maxillofacial Implants*. 2000; 15: 675–90.
44. Fazel A, Aalai S, Rismanchian M, Sadr-Eshkevari P. Micromotion and Stress Distribution of Immediate Loaded Implants: A Finite Element Analysis. *Clin Implant Dent Related Res* 2009; 11: 267-71 [Epub 2008 Sep 9].
45. Eraslan O, İnan O. The effect of thread design on stress distribution in a solid screw implant: a 3D finite element analysis. *Clin Oral Investig*. 2009; jun 20 [Epub ahead of print].
46. Misch CE, Bidez MW, Sharawy M. A bioengineered implant for a predetermined bone cellular response to loading forces. A literature review and case report. *J Periodontol*. 2001; 72: 1276-86.

47. Bozkaya D, Muftu S, Muftu A. Evaluation of load transfer characteristics of five different implants in compact bone at different load levels by finite elements analysis. *J Prosthet Dent.* 2004; 92: 523-30.
48. Tada S, Stegaroiu R, Kitamura E, Miyakawa O, Kusakari H. Influence of Implant Design and Bone Quality on Stress/Strain Distribution in Bone Around Implants: A 3-dimensional Finite Element Analysis. *Int J Oral Maxillofac Implants* 2003; 18: 357–68.
49. De Smet E, Jaecques SVN, Jansen JJ, Walboomers F, Vander Sloten J, Naert IE. Effect of constant strain rate, composed by varying amplitude and frequency, of early loading on peri-implant bone (re)modelling. *J Clin Periodontol.* 2007; 34: 618–24.

Autorizo a reprodução deste trabalho.
(Direitos de publicação reservados ao autor)

Araraquara, 25 de março de 2010.

ROBERTO SALES E PESSOA